TRANSIENT MOISTURE CHARACTERISTICS OF SPRUCE PLYWOOD

A Thesis Submitted to the College of

Graduate Studies and Research

in Partial Fulfillment of the Requirements

for the Degree of

Master of Science

in the Department of Mechanical Engineering

University of Saskatchewan

Saskatoon

By

Olalekan Fatai Osanyintola

PERMISSION TO USE

In presenting this thesis in partial fulfilment of the requirements for a Postgraduate degree from the University of Saskatchewan, I agree that the Libraries of this University may make it freely available for inspection. I further agree that permission for copying of this thesis in any manner, in whole or in part, for scholarly purposes may be granted by the professor or professors who supervised my thesis work or, in their absence, by the Head of the Department or the Dean of the College in which my thesis work was done. It is understood that any copying or publication or use of this thesis or parts thereof for financial gain shall not be allowed without my written permission. It is also understood that due recognition shall be given to me and to the University of Saskatchewan in any scholarly use which may be made of any material in my thesis.

Requests for permission to copy or to make other use of material in this thesis in whole or part should be addressed to:

Head of the Department of Mechanical Engineering

University of Saskatchewan

Saskatoon, Saskatchewan, S7N 5A9

ABSTRACT

In this thesis, the moisture characteristics of spruce plywood are studied experimentally and numerically with special attention given to moisture storage and release as the indoor humidity changes diurnally. This is referred to as the moisture buffering capacity. Two test facilities (a glass jar facility and a transient moisture transfer facility) are used to measure the moisture accumulation and temperature and relative humidity profiles within spruce plywood. These measured data are used to determine the moisture buffering capacity of spruce plywood and validate a one-dimensional transient numerical model that can be used to calculate the transient heat and moisture transfer in spruce plywood. There is good agreement between the measured and simulated results over the range of test variables investigated.

This validated numerical model is used to investigate the effect of initial conditions, boundary conditions, thickness and humidity step change on the moisture buffering capacity. In addition, sensitivity studies are performed to investigate the effect of variations in material properties used in the numerical model. The properties that are considered in these sensitivity studies are the sorption isotherm, effective thermal conductivity, heat of sorption and effective diffusion coefficient. These studies show that the sorption isotherm has the greatest effect on the moisture buffering capacity, as well as the temperature and relative humidity profiles within spruce plywood. For example, a ± 10% change in sorption isotherm has a ± 7%, ± 6% and ± 10% effect on the moisture buffering capacity, and the relative temperature and relative humidity change, respectively.

This thesis also verifies the moisture diffusivity property for spruce plywood, which was developed by Olutimayin and Simonson (2005) to account for moisture storage in cellulose insulation for a single step change in humidity. It was found that for spruce plywood, the moisture penetration depth may be over predicted by an order of magnitude when moisture storage is neglected using a transient analytic solution which does not include moisture storage.

AKNOWLEDGEMENTS

I give special thanks to God almighty for His mercies to complete this thesis. I want to sincerely thank my supervisor, Professor Carey J. Simonson for his support, guidance, expertise, patience, and most especially for his wealth of knowledge. Many thanks to my committee members (Professor R. W. Besant and Professor David Sumner) for their input in making this thesis a success. Also many thanks to Mr. Chris James and Mr. Dave Deutscher for their technical support with my experiment and their willingness to help at all times.

My appreciation goes to my fiancée, Vicki Strain, and my family for their continuous support, understanding, prayer and love without which it would have been impossible to complete my master's. Finally, I want to say thank you to my friends and colleagues in the department for their help and care.

DEDICATION

I dedicate this work to my fiancée, Vicki Strain, my parents, Alhaji and Alhaja Ganiyu Osanyintola, my brothers, Sulaimon, Luqman and Lateef Osanyintola, my sister, Mrs Faosat Oyeti and her lovely family.

TABLE OF CONTENTS

Page

LIST OF TABLES

Page

LIST OF FIGURES

Page

NOMENCLATURE

ACRONYMS

ASHRAE	American Society of Heating, Refrigerating and Air-conditioning Engineers
ASTM	American Society for Testing and Materials
DAS	Data Acquisition System
FSP	Fibre Saturation Point
HVAC	Heating, Ventilating, and Air Conditioning
IAQ	Indoor Air Quality
ISO	International Standard Organization
MBC	Moisture Buffering Capacity
MBV	Moisture Buffering Value
PAQ	Perceived Air Quality
RH	Relative Humidity
TMT	Transient Moisture Transfer

ENGLISH SYMBOLS

A	Surface area of the plywood in contact with the ambient air and exposed to convective moisture transfer [m^2]
A_{kj}	Interface area between phases k and j [m^2]
ach	Air change per hour [1/h]
C_d	Discharge Coefficient

C_m	Moisture storage coefficient
C_p	Specific heat capacity at constant pressure [J/(kg·K)]
D	Diameter of the circular supply air duct [m]
D_a	Binary diffusion coefficient for water vapour in air [m^2/s]
D_{eff}	Effective vapour diffusion coefficient [m^2/s]
D_h	Hydraulic diameter [m]
d	Particle size and thickness of the specimen used in calculating the water vapour permeability. Also, the diameter across the orifice plate [m]
G	Rate of mass transfer through the specimen [kg/s]
h_a	Convective heat transfer coefficient [W/(m^2·K)]
h_{ad}	Heat of phase change [J/kg]
h_{fg}	Latent heat of vapourization [J/kg]
h_m	Convective mass transfer coefficient [m/s]
k	Thermal conductivity [W/(m·K)]
k_{eff}	Effective thermal conductivity [W/(m·K)]
L	Effective thickness of specimen defined as the distance between the surface exposed to ambient air and the impermeable plane in the test specimen. Also, the thickness of the plywood specimen used for the thermal conductivity tests [m]
MBC	Moisture buffering capacity defined as a measure of the mass of moisture that a material can absorb and desorb during a specified humidity cycle per unit exposed surface area [g/m^2]

MBV	Moisture buffering value is the amount of moisture uptake or release by a material normalized by the size of the relative humidity change [g/(m^2·% RH)]
m	Mass of the test specimen [g]
$\dot{m}$	Phase change rate per unit volume [kg/(m^3·s)]
$\dot{m}_a$	Mass flow rate of air [kg/s]
m_{final}	Mass of the test specimen measured at the end of an adsorption/desorption phase [g]
m_o	Mass of dry plywood specimen [kg]
m_{start}	Mass of the test specimen when the adsorption or desorption phase started [g]
Nu	Nusselt Number
n_{kj}	Normal unit vector for the interface between phases k and j
P	Pressure [Pa]
q''	Heat flux [W/m^2]
R	Ideal gas constant [J/(kg·K)]
Re	Reynolds number of air flow over the specimen
RH	Relative humidity [%]
RH_{mean}	Average of the high and low ambient air relative humidity used in a moisture buffering capacity test cycle [%]
S	Multiplication constant used to modify the properties in the sensitivity studies
T	Temperature [^{o}C]

t	Time [s]
u	Mass of moisture adsorbed per kg of dry spruce plywood [kg/kg]
V	Volume [m^3]
W	Humidity ratio [kg/kg]
X_{mm}	Thickness of the air gap between the spruce plywood and the air above it in the TMT facility [m]
x	Distance from the top of plywood specimen [m]

GREEK SYMBOLS

α	Thermal diffusivity [m^2/s]
α_m	Moisture diffusivity [m^2/s]
$\alpha_{m,eff}$	Effective moisture diffusivity [m^2/s]
β	Ratio of orifice plate diameter to the diameter of the duct
δ	Water vapour permeability [kg/(m·s·Pa)]
δ_m	Vapour boundary layer thickness [m]
ΔM	Change in mass per unit exposed surface area since the beginning of the test as defined in equation (4.1) [g/m^2]
Δm	Mass of moisture accumulation/loss in the plywood specimen per exposed surface area during a given adsorption/desorption phase as defined in equation (4.2) [g/m^2]
Δm_{ave}	Average of the moisture accumulated during a given adsorption phase of a given cycle (Δm_{ads}) and the moisture loss during the desorption phase of the same cycle (Δm_{des}) per exposed surface area (see equation (4.4)) [g/m^2]

Δm_{diff}	Percentage difference between the average moisture accumulated/loss (Δm_{ave}) for a given cycle and the average moisture accumulated/loss at steady state (Δm_{ss}) (see equation (4.5)) [%]
Δm_{ss}	Mass of moisture accumulation/loss during an adsorption/desorption cycle per exposed surface area when the plywood has reached quasi-steady state (i.e., equation (4.3)). It is also the value that Δm_{ave} will approach when the same adsorption and desorption cycle is repeated indefinitely [g/m^2]
ΔP	Pressure difference [Pa]
Δp_v	Water vapour pressure difference across the specimen [Pa]
ΔRH	Daily RH variation [%]
ΔT	Temperature difference [^{o}C]
ε	Volume fraction
ϕ	Relative humidity in fraction
ϕ_1	First ambient relative humidity that the plywood specimen is placed in during the test (in fraction)
λ	Expansibility factor for the airflow through an orifice plate
ρ	Density [kg/m^3]
ρ_o	Dry density of the plywood specimen [kg/m^3]
ψ	A general transport variable

SUBSCRIPTS

ads	Adsorption phase
a	Dry air

des	Desorption phase
eff	Effective porous media property
f	Fluid
g	Gas phase (air and water vapour)
i	Initial value
j	Phase in a porous medium
k	Phase in a porous medium
ℓ	Adsorbed phase
s	Solid
v	Vapour
vsat	Saturated vapour property
∞	Ambient or free stream property

OTHERS

$\langle\,\rangle$	Local volume averaged variable
$\langle\,\rangle^k$	Intrinsic phase averaged variable
$\langle\langle\,\rangle\rangle$	Double volume averaged variable

CHAPTER 1

INTRODUCTION

In recent times, there has been increasing interest to reduce the energy consumption and greenhouse gas emissions associated with the use of mechanical (active) heating, ventilating and air-conditioning (HVAC) systems in buildings. In view of this, researchers are investigating the use of passive systems to assist or even eliminate some aspects of these active systems. One important task of HVAC systems is to moderate indoor relative humidity (RH) in buildings because indoor humidity affects warm respiratory comfort (Toftum et al., 1998a), skin humidity (Toftum et al., 1998b) and perceived indoor air quality (Fang et al., 1998). Also, moisture in buildings has been shown to affect sensible and latent conduction loads (Mendes et al., 2003) and may cause deteriorations in buildings (Lucas et al., 2002). In addition, conservation researchers have shown that a wide variety of artefacts displayed in museums require specific indoor conditions to minimize their deterioration (Yu et al., 2001).

Due to the importance of indoor humidity, researchers have studied the use of hygroscopic materials to moderate indoor humidity levels. Hygroscopic materials can be considered a passive system because they function without external energy input. Research has shown that hygroscopic materials are able to moderate the indoor humidity levels and thus improve the thermal comfort and air quality in buildings, while still

providing low energy consumption (Hameury, 2005; Simonson, 2005). The impact of hygroscopic materials depends on many factors: the amount and type of materials in a given room, the outdoor climate, the outdoor ventilation rate and the moisture production rate. The ability of materials to damp (or buffer) diurnal changes in indoor humidity depends on their thickness, vapour permeability and moisture storage capacity, which vary significantly for different building materials. Since there is no test standard that can be used to compare the ability of various materials to buffer indoor humidity changes (Rode et al., 2004, 2005), one of the aims of the research in this thesis is to support such standard development. This research will be conducted using spruce plywood as the example hygroscopic material.

1.1 Plywood and its Manufacture

Plywood is a common building material that gains or releases moisture and heat as the outdoor and indoor conditions change. Plywood is generally produced in panels. It is mostly used in the construction industry where its ability to withstand large racking forces that may be imposed on a structure (e.g. by an earthquake) makes it ideal for bracing walls. Plywood can be made from different wood species, such as spruce, oak, pine and poplar. Spruce plywood that was produced in Finland will be used in this thesis. The plywood manufacturing process has three stages: (i) veneer manufacture; (ii) clipping, drying and upgrading; and (iii) panel lay-up, pressing and finishing (Figure 1.1). Plywood panels are made from rotary peeled softwood veneers of 2-6 mm thickness. Rotary peeling involves rotating a log about its central axis against a knife lying parallel to the grain. The log is mounted in a set of chucks that hold it in place and provide torque. As the log is turned, a thin sheet of veneer is peeled off as a long

continuous ribbon. A veneer with a uniform thickness and smooth finish is important, as is maintaining a continuous sheet. The peeled veneers are clipped to size and then dried in a high temperature kiln to improve strength and to reduce the potential of fungi decay.

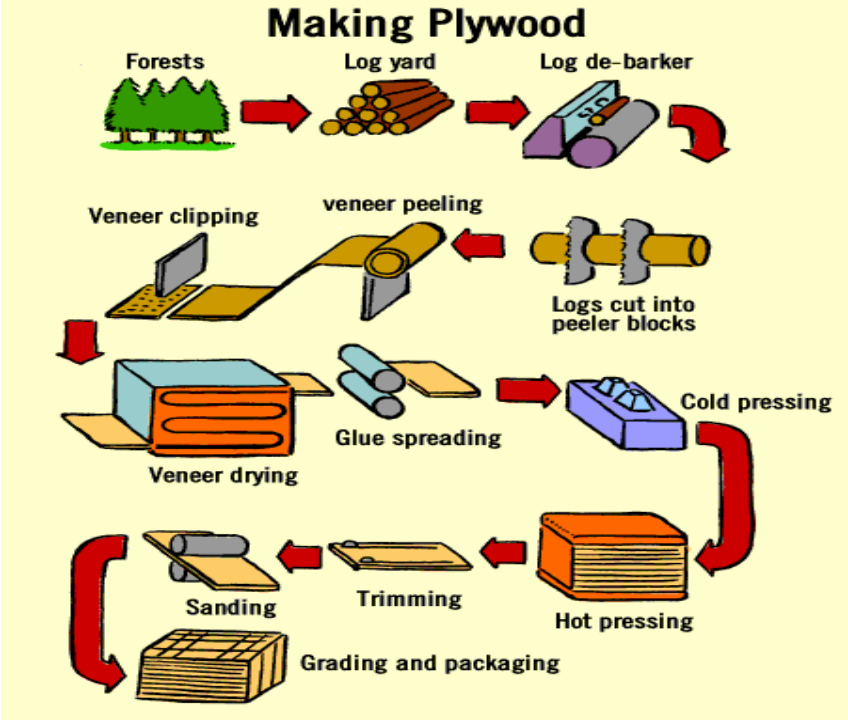

Figure 1.1. Picture of the manufacturing process of plywood showing the step-by-step process from the log stage to the packaging stage (New Zealand Forest Insight, 2004).

Plywood panels are created by gluing veneers together, layer by layer, using glue and the natural strength of the wood's grain helps to create rigid, strong wooden panels. The grains of alternate layers are arranged at right angles. Expansion or contraction within the plane of the board of one veneer is restricted by the wood fibres in the adjacent veneer. The resulting panel has similar strength and shrinkage properties in the directions parallel to the plane of the board and the large dimensional and strength variations that occur across the grain in solid wood are eliminated. Plywood products are

produced to be able to withstand extreme weather conditions by using phenolic formaldehyde resin in the gluing process. After the panels are glued, they are cold pressed as well as hot pressed to control the thickness of the panels. At this stage, the panels are trimmed and ready to be graded and packaged (New Zealand Forest Insight, 2004).

All wood products contain moisture, from saturated fresh cut logs to the fairly dry wooden indoor structures and furniture. Moisture in wood is stored as either bound water or free water. Bound water is held within cell walls by bonding forces between hydrogen molecules of water and hydroxyl molecules of the wood cellulose. Free water is contained in the cell lumens/cavities and is held by surface tension. A microscopic view of wood is shown in Figure 1.2.

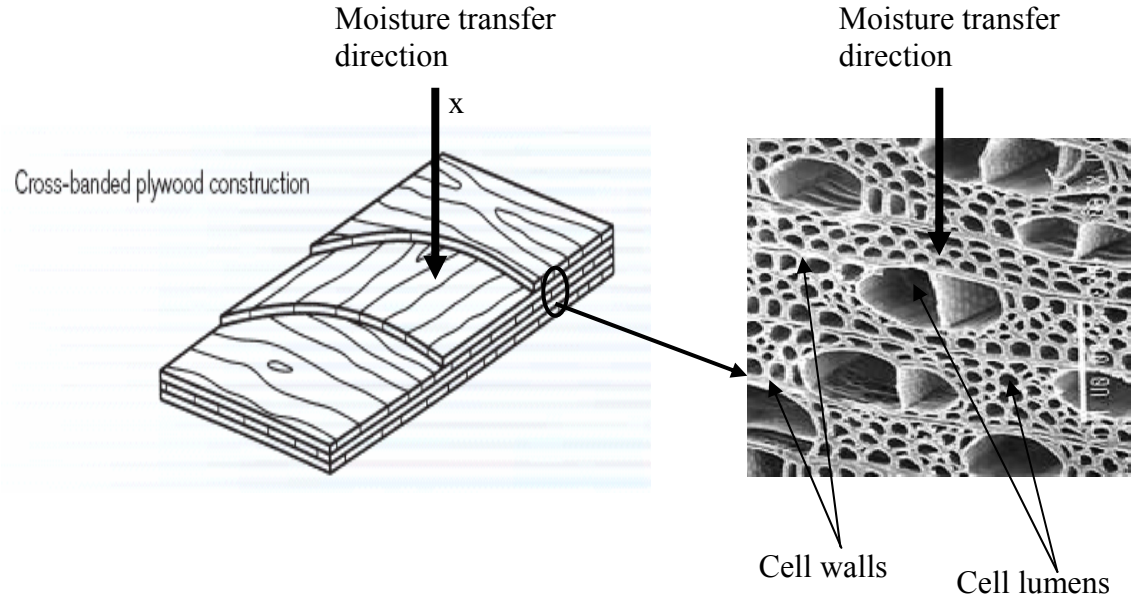

Figure 1.2. Picture of spruce plywood showing the cross-banded construction and the moisture transfer direction, Scanning electron microscope picture of spruce heartwood showing the cell walls and the cell lumens as well as the main direction of moisture transfer for plywood (Gardner, 2004).

It should be noted that since plywood veneers are made by rotating the log and peeling a thin veneer from the log, moisture transfer in the veneer in the direction of the thin dimensions is equivalent to moisture transfer in the radial direction of the log. When these veneers are assembled and used in buildings and furniture, the moisture transfer through the exposed surface and into the plywood is equivalent to moisture transfer in the radial direction of the original log. Therefore, the direction of moisture transfer considered in this thesis is across the cell walls and lumens (in the radial direction of the original log) as shown in Figure 1.2. Because of the rotary peeled veneers, plywood will have more uniform moisture transfer characteristics than raw timber for example, which will have moisture transfer in directions that are both radial and tangential to the wood grains.

1.2 Literature Review

When calculating the energy consumption, temperature and relative humidity in a building, it is important to know the dynamic temperature and moisture content distributions in the porous building envelope. Therefore, many researchers have investigated heat and moisture transfer in building materials and envelopes using both experimental and numerical studies.

The heat and moisture analysis of building materials and envelopes has been actively researched in northern Europe and North America for over a decade. Researches have used numerical models (Salonvaara and Karagiozis, 1994; Mendes et al., 1999 and 2002; Geving, 2000; and Mukhopadhyaya et al., 2003) as well as laboratory and field experiments (TenWolde, 1987; Cunningham, 1990; Padfield, 1998; Rode et al., 2001;

Kunzel et al., 2005) to analyze heat and moisture transfer in building materials. The effect of moisture on the durability and thermal performance of building envelopes has also been investigated. The studies cited above are only a few of the studies on the heat and moisture transfer in building materials in general, however, the literature review in this thesis will focus specifically on heat and moisture studies in wood materials, the interactions between indoor air and hygroscopic materials and moisture storage in building materials.

1.2.1 Heat and Moisture Transfer in Wood Materials

Plumb et al. (1985) developed a model to investigate heat and mass transport in softwood during drying. The model includes both capillary and diffusive moisture transport during wood drying, as well as heat transfer. Due to the regular packing pattern of wood cells, a mechanistic model of the wood structure was utilized to identify capillary porous properties – permeability and capillary pressure. This was useful to determine the properties that are not available in the literature and difficult to measure. The model predicted reasonably well the drying rates and moisture distributions in wood, when compared with experimental data. However, since the model is dependent on the accuracy of the permeability data, it was discovered that an error in the permeability data will translate to a poor representation of the drying rates.

Tong (1986) also studied the moisture transport in wood. He considered the transport of moisture in wood below the fibre saturation point (FSP). FSP is the moisture content at which the cell walls are saturated, and there is no free water in the cell lumens and intercellular spaces (see Figure 1.2). Shrinkage and swelling occurs when moisture changes occur below the FSP. The FSP for wood varies by species, but an average value

is generally taken to be about 28% by mass. Species with high extractive capacity (e.g., redwood) would have a lower FSP than the average wood FSP. Moisture conditions above the FSP are seldom researched in building applications and are not of great interest for building research.

Avramidis et al. (1992) evaluated a model that predicts heat and moisture transfer in the hygroscopic range of wood by comparing with transient non-isothermal diffusion experimental data. The one-dimensional model was developed according to the principles of non-equilibrium thermodynamics (Prigogine, 1961; Luikov, 1966), with no free water in the pores. The water chemical potential gradient was taken as the driving force for diffusion in the model. The measured moisture content during desorption in the hygroscopic range shows very good agreement with results from the model.

Wadsö (1993), Wadsö et al. (1994) and Håkansson (1998) from Lund University in Sweden investigated the non-Fickian behaviour of wood. Håkansson described this unusual moisture transport in wood as retarded sorption, which appears as a significant time-delay in moisture content changes compared to what is expected from the Fickian theory. Historically, this effect has been explained as a surface resistance effect that gives a thickness effect in drying and wetting. Håkansson quantified it experimentally and mathematically for thin specimens. A special experimental set-up was developed to isolate and measure the retarded sorption in wood. Extensive series of sorption response measurements with different sequences of relative humidities were performed on thin, well-exposed wood samples. The results showed that the moisture content often has an intricate dependence on moisture history. Two small steps may not give the same moisture accumulation as a corresponding single larger step. The process is not linear.

The part of the sorption that is retarded (or delayed) is especially large at high relative humidities. The retarded sorption increases with decreasing temperature. However, the retarded sorptions in wood products with normal thicknesses are yet to be clarified. Also, Wadsö et al. (1994) discovered that for a model to better describe the sorption in wood cell walls, the model should describe the response to step changes in water vapour pressure and predict sorption with more than one time scale.

Salin (1996) developed a model where the normal assumption of internal local equilibrium between the vapour and bound phases is replaced by a mass transfer resistance. The non-equilibrium model was applied to one-dimensional moisture flow to establish whether the non-Fickian behavior observed in wood could be explained. However, the model was not able to explain the non-Fickian behavior or retarded sorption measured by Wadsö (1993).

Dedic (2000) studied the effect of forced convective heat and mass transfer on moisture desorption in oak wood. An experiment was designed which enables the drying process of relatively small samples to be similar to the drying process of real timber. Results from this experiment were compared to a three-dimensional model of heat and mass transfer during desorption of water from oak wood. The comparison gave satisfactory agreement over a range of drying air temperatures.

Tremblay et al. (2000) presented an experimental method to determine the convective heat and mass transfer coefficients for wood drying. Red pine sapwood samples were cut and the edges coated with silicone sealant and aluminium foil to impose water evaporation through two open surfaces. To prevent moisture flow along longitudinal

direction, neoprene gaskets were also placed at the ends of the samples. In determining the convective heat and mass transfer coefficients, the initially saturated samples were dried in a conditioning tunnel-type cabinet at constant temperature, relative humidity and air velocity. The moisture flux normal to the wood surface was determined from the drying curve generated at different drying times. Also, the water potential at the wood surface was determined from slices cut in the direction perpendicular to the moisture flux. These values were then used to determine the convective mass transfer coefficient. In addition, heat flux was determined by establishing enthalpy profiles in the direction of moisture flux at different drying times. These enthalpy profiles were calculated from the moisture content and temperature profiles. The heat flux along with the moisture flux and temperature gradients were used to determine the convective heat transfer coefficient. Tremblay et al. (2000) also gave relationships of convective mass transfer coefficient as a function of surface moisture content and air velocity. The results showed that the convective mass transfer coefficient increased with air velocity and surface moisture content.

Rode et al. (2004) investigated the effect of vapour permeability, sorption hysteresis and temperature-dependent sorption curve on the moisture capacity of a solid wood construction using a calculation model. They found that including both the adsorption and desorption isotherms in the model resulted in a smaller equilibrium moisture content compared to the case where the mean value of the adsorption and desorption isotherms was used. For temperatures above freezing, the temperature effect on the sorption curves gave a larger increase in moisture capacity for a given increase in relative humidity

when compared to a model with an isothermal sorption characteristic. Comparison of the results from the model and the experiment showed good agreement.

1.2.2 Moderating Indoor Humidity with Hygroscopic Materials

In the last decade, many researchers have investigated the possibility of using different hygroscopic materials to damp variations in indoor humidity. This section will review literature in this area of research.

Simonson et al. (2004a) presented a research which showed that moisture transfer between indoor air and hygroscopic building structures can generally improve indoor humidity conditions. The research concentrated on the numerical investigation of a bedroom in a wooden building located in four European countries (Finland, Belgium, Germany, and Italy). A similar numerical investigation was performed in a bedroom located in three Canadian cities (Saskatoon, Vancouver, and Toronto) (Simonson et al., 2004b). The results showed that moisture transfer between indoor air and the hygroscopic structure significantly reduced the peak indoor humidity. Based on correlations from the literature (Fang et al., 1998), which quantify the effect of temperature and humidity on comfort and perceived air quality (PAQ) for sedentary adults, hygroscopic structures can improve indoor comfort and air quality. In all the investigated climates using a ventilation rate of 0.5 air-change-per hour (ach), it is possible to improve the indoor conditions such that as many as 10 more people of 100 are satisfied with the thermal comfort conditions (warm respiratory comfort) at the end of occupation. Similarly, the percent dissatisfied with PAQ can be 25% lower in the morning when permeable and hygroscopic structures are applied. They also found that using hygroscopic materials in buildings will not always ensure acceptable indoor

conditions and during some weather conditions (typically less than 10% of the time) hygroscopic materials may slightly degrade the indoor conditions.

Salonvaara et al. (2004) studied the ability of building materials to control indoor air humidity. The moisture capacity and transient response of building materials were investigated using small-scale laboratory and full-scale single room tests. Moisture production and ventilation rates were set to correspond to those typical in residential buildings. The measured interior surface materials included wood, porous wood fibreboard, gypsum board with hygroscopic insulation, perforated plywood board, and, in a reference case, aluminium foil. Salonvaara et al. (2004) also performed numerical simulations to investigate the hygrothermal performance of building envelopes and to assess the impact of hygroscopic mass on indoor air humidity. The measured and numerical results show that the indoor air humidity had greater fluctuations when the building materials have no moisture capacity. It was observed that for an air change rate of 0.5 ach, which is the hygienic minimum rate according to the Finnish and German regulations, the peak humidity could be reduced from 70% to about 50% RH. These results showed the potential for building materials to moderate indoor humidity.

Samuelson (1998) investigated the hygrothermal performance of six different attics (roof spaces) under controlled conditions. An experimental roof was constructed above a flat-roofed office building and the temperature and relative humidity were measured both outside and inside the attics at different depths in the insulation and beneath the ceiling (inside the building). The measured results for the attic having mineral wool insulation were compared with results using cellulose materials. Samuelson (1998) found that the hygroscopic insulation material (cellulose material) showed better indoor humidity

moderation than non-hygroscopic insulation (mineral wool). It was also found that the greater the outdoor ventilation rate through the insulation (as a form of infiltration), the greater the differences in moisture and temperature variations in roofs with high and low ventilation rates.

Yu et al. (2001) presented an evaluation of silica gel for humidity control in display cases. They developed a model and validated the model with data from a long-term experiment that measured the relative humidity inside three moisture impervious containers, each with a volume of 3.79 litres. The aim of the experiment was to investigate the use of silica gel to moderate the indoor humidity in museums for artifacts preservation. The silica gels investigated were regular density silica gel, Artengel and Art-Sorb. The Artengel was found to have the highest moderating capacity. It was concluded that 30 kg of silica gel are required for a 1 m^3 display case to moderate RH fluctuation of about 10% over a period of one year at a leakage rate greater than 0.5 ach.

Gaur and Bansal (2002) examined the effect of combined heat and moisture transfer across building components on the indoor temperature. The periodic variation of indoor temperature of a room over a one-day period was analyzed using the simultaneous heat and moisture transfer across the building elements. It was discovered that the humidity present in the ambient air affects the room temperature and in the hygroscopic region it can alter the room temperature by 2-3^oC depending upon the direction of the temperature and moisture gradients.

Kunzel et al. (2005) studied the hygrothermal behaviour of wooden panels used as an interior lining for an experimental test room. Wooden panels with other coating

materials like aluminium foil and lime-gypsum interior plaster were compared. In this work, a numerical simulation was carried out with a hygrothermal envelope calculation model called WUFI®+ developed by Holm et al. (2003). From this simulation, it was discovered that the wooden panels have a greater humidity moderating capacity than the other materials. It was also observed that results for wood deviated from the measured results. Kunzel et al. (2005) suggested that the deviation arose because the steady state laboratory test used for determining the hygrothermal properties of wood did not completely represent the transient diffusion and adsorption characteristics of wood. This effect has been described by Håkansson (1998) as the non-Fickian behaviour of wood.

Rode et al. (2002) measured the humidity buffering effects of several building materials placed within an airtight and highly insulated test cell. The building materials studied were plasterboard, chipboard, cellular concrete, plywood, wooden panels and painted plasterboard. The test cell was subjected to a controlled humidity cycle and the weight change of the materials being tested was measured with a load cell within the test cell. Comparing the weight change of the test materials, it was found that wood panels and cellular concrete had the best performance in indoor humidity buffering. Rode at al. (2002) also compared the measured results with predictions from a detailed numerical model. They found that, except for chipboard, the indoor humidity predictions were very similar to the measured values.

1.2.3 Moisture Buffering Capacity (MBC) of Building Material

The moisture buffering capacity (MBC) of a material reflects the ability of that material to damp indoor variations in RH. It is a measure of the mass (per unit area) of moisture that a material can absorb and desorb during a specified humidity cycle. MBC could be

used as a practical way to compare the hygroscopicity of different building materials and to estimate the impact of hygroscopic materials on the indoor RH in a building. The MBC of these materials has been shown to depend on their sorption properties, therefore, materials with different sorption properties have different MBCs.

Rode et al. (2004) reviewed moisture buffering in interior spaces. It was stated that materials have a moisture buffering effect and this effect is probably positive for both indoor air and the structures. However, there has not been enough research to quantify this effect and thus more tests and demonstrations are needed to show the benefits of this practice. It was noted the need for a standard test to quantify the moisture buffering capacity of a material. This thesis will contribute to the development of such a standard.

Svennberg et al. (2004) conducted a series of experiments in a test room to show the moisture buffering capacity of various furnishing objects. During the experiments, the furniture and other furnishings in the test office were subjected to indoor humidity variations. A series of cases was studied from an empty office to a fully furnished office including basic office furniture (office desk and chair, room divider, computer shelf and rolling shelf), books, carpet, papers on the table and in the wastebasket, and a curtain. The indoor relative humidity variations in these cases were measured and the fully furnished room was found to have smaller amplitude than the empty room. This indicates a better moisture buffering capacity. Also, the study showed the importance of a standard approach to the measurement of moisture buffering capacity.

Carmeliet et al. (2002) investigated the influence of sorption hysteresis on the moisture buffering capacity of oak wood. A new hysteresis model based on the model of Mualem

(1974) was developed. Using this model and the empirical model of Pedersen (1990), the hysteresis of oak wood was analyzed. It was found that hysteresis has a limited influence on the moisture buffering capacity of wood used in buildings. This finding will be used when developing the model in this thesis.

Peuhkuri et al. (2004) investigated the moisture buffering capacity of different thermal insulation materials (glass wool, rock wool, cellular concrete, cellulose, flax and perlite). Different ways of quantifying the moisture buffering capacity of materials was presented. This included moisture accumulation capacity, available water and slope of the sorption curve. Both isothermal and non-isothermal experimental set-ups were employed to measure the moisture buffering capacity. Both sides of the material samples were exposed to the same change in the relative humidity during the isothermal test. This was aimed at studying the sorption behavior of the material on a micro scale. For the non-isothermal tests, the experimental set-up was a representative of a full-scale field experiment within which the samples were exposed to dynamic variations in the relative humidity only on the cold side. The moisture accumulation capacity of these materials was noted gravimetrically in these two experimental apparatuses. In comparing the results, it was found that the dynamic, non-isothermal method gave a smaller moisture capacity than the steady-state, isothermal method for all the materials except cellular concrete which gave the same moisture accumulation.

As seen from this literature survey, there have been much research into the study of heat and mass transfer in wood materials, but further research needs to be done to provide more data on moisture buffering capacity, which will be useful in developing a standard

test method. This forms the main objective of the present thesis as presented in the next section.

1.3 Research Objectives

The goal of this thesis is to provide numerical and experimental data that quantify the moisture buffering capacity of spruce plywood and can be used when developing a standard test method and for validating the numerical models. In order to achieve these goals, the following objectives are set for the research work.

1 Measure the material properties of spruce plywood including: (i) adsorption/desorption isotherms, (ii) density, (iii) porosity (iv) water vapour permeability and (v) thermal conductivity.

2 Measure the moisture buffering capacity of spruce plywood during transient humidity changes as part of an international round-robin exercise with four other institutions – Norwegian Building Research Institute, Norway; VTT Technical Research Centre of Finland, Finland; Lund Institute of Technology, Sweden; and Technical University of Denmark, Denmark.

3 Investigate the effect of initial conditions, boundary conditions and thickness of the plywood on the moisture buffering capacity.

4 Quantify the transient heat and moisture transfer boundary layers within spruce plywood by measuring the temperature and relative humidity profiles within the plywood during transient changes in the ambient air humidity.

5 Develop a numerical model for transient heat and moisture transfer in spruce plywood and verify this model with experimental data.

6 Apply and verify the moisture diffusivity (α_m) property developed by Olutimayin and Simonson (2005) for spruce plywood using the experimental and numerical data.

1.4 Scope of the Thesis

In this thesis, the scope of the experimental and numerical heat and moisture transfer problem will be limited to a one-dimensional problem and the boundary conditions are as shown in Figure 1.3. Spruce plywood will be exposed to humidity conditions less than 100% RH, therefore evaporation/condensation will not be considered. The temperature boundary conditions will be above 0°C, therefore freezing and melting will not be considered.

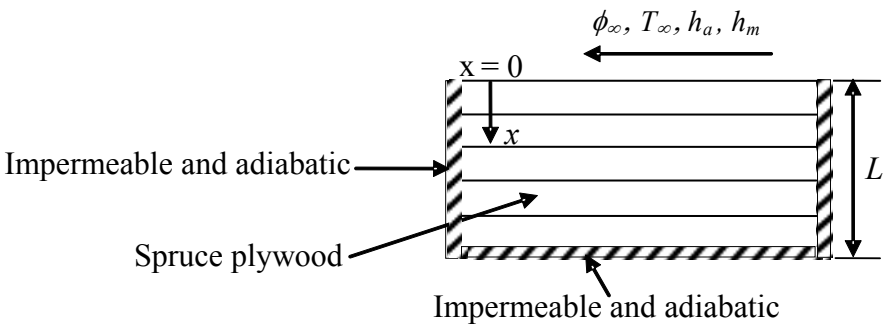

Figure 1.3. Schematic of the heat and moisture transfer problem investigated in this thesis.

1.5 Overview of the Thesis

This thesis is divided into six chapters. Chapter 2 describes the experimental test facilities, property data and instrumentation employed. In Chapter 3, a numerical model is developed and the model is validated with experimental data in Chapters 4 and 5. Chapter 4 focuses on the moisture buffering capacity tests and investigates the effect of material thickness, initial and boundary conditions and humidity step changes on the moisture buffering capacity of spruce plywood. Chapter 5 presents the measured and

simulated temperature and humidity data that quantify the thermal and moisture boundary layers within spruce plywood. It also presents the application and verification of the moisture diffusivity property (developed by Olutimayin and Simonson, 2005) for spruce plywood. A research summary, conclusions and recommendations for future work are presented in Chapter 6.

CHAPTER 2

EXPERIMENTAL FACILITIES AND PROPERTY DATA

The purpose of the experiments described in this chapter is to measure the transient moisture buffering capacity (MBC) and the temperature and relative humidity distributions within spruce plywood. The results from these measurements will be used to verify the one-dimensional numerical model of transient heat and moisture transfer in spruce plywood that will be presented in Chapter 3. Measurements of the MBC, temperature and relative humidity are performed for different boundary conditions to give a range of data to verify the numerical model. Also, some material property data are required in the numerical model and measurements of these properties are included in this chapter. This chapter focuses on the experimental facilities and procedures, the instruments used and their calibration, and the uncertainties in the measurements (the analysis of these uncertainties is presented in Appendix A).

In this thesis, the experiments are performed using two different facilities. Each of these facilities creates different convective transfer coefficients between the humid air and the plywood and thus creates different boundary conditions. This includes natural convection in sealed glass jars and fully developed, forced convection airflow (laminar and turbulent) in a small wind tunnel which will be referred to in this thesis as the transient moisture transfer (TMT) facility.

Each test facility uses different sized samples of plywood and the edges of these samples are sealed with aluminium-foil tape to eliminate lateral moisture transfer through the edges. This represents the application of plywood in practice where moisture transfer through the edge is minimal. Prior to testing, the plywood samples are conditioned using either salt solutions or ambient air in the laboratory.

Since different laboratories will use different facilities to measure MBC (Rode et al., 2005), it is important to investigate the effect that different air flow characteristics and thus different boundary conditions will have on the measured MBC. Therefore, both facilities are used to measure the MBC of spruce plywood and these data will be presented in Chapter 4. The TMT facility is also used to measure the thermal and vapour boundary layers within the spruce plywood. This is done by embedding thermocouples and humidity sensors between the layers of the plywood to monitor the temperature and humidity distribution within the plywood respectively. These tests will be done for different conditions than the MBC tests and these data will be presented in Chapter 5.

2.1 Glass Jar Facility

This facility tests a small sample of spruce plywood (60 mm x 60 mm x 9 mm) using glass jars containing still air and a thin layer (1-2 cm) of saturated salt solutions (as shown in Figure 2.1(a)). The saturated salt solutions create known relative humidities in the jar (ASTM E104, 1985). The numerical model, presented in Chapter 3, uses a convection boundary convection at $x = 0$ and an impermeable boundary condition at $x = L$. Therefore, an effective thickness (L) defined as the distance between the surface experiencing convection moisture transfer and the impermeable plane in the test

specimen is introduced and will be used throughout this thesis. It will be useful when comparing the results of the two facilities. In the glass jar facility, the effective thickness (L) for moisture penetration is 4.5 mm from each exposed side.

Prior to testing, the plywood samples are conditioned for a long time (2 months) in the laboratory and the initial moisture content of the wood is 0.028 kg/kg (dry mass basis), which corresponds to a relative humidity of about 55%. The plywood sample is then placed in a jar containing a saturated salt solution and the jars are kept in an environmental chamber maintained at 23.3 ± 0.3^{o}C during the test.

(a) (b)

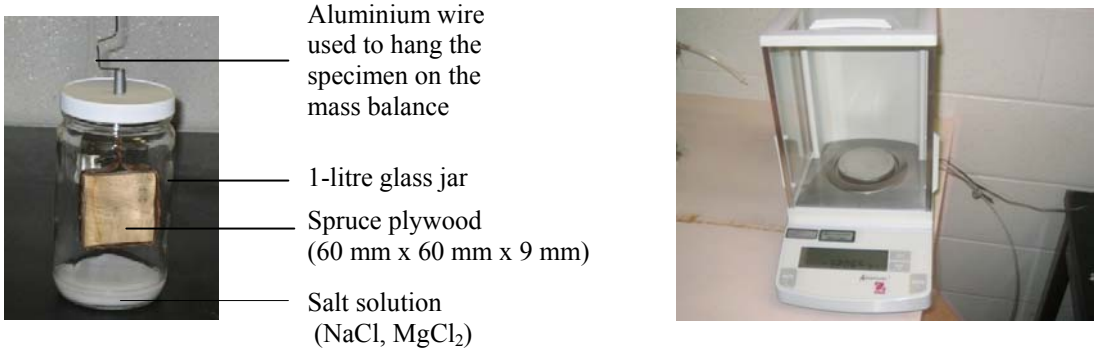

Figure 2.1. Picture showing (a) the spruce plywood in a sealed glass jar containing still air and a saturated salt solution and (b) the electronic mass balance.

The plywood is subjected to a step change in relative humidity by moving it to a jar with a different salt solution. NaCl is used to create the high humidity condition, which creates a humidity of 75.3 ± 0.1% RH at 23^{o}C according to (ASTM E104, 1985) and $MgCl_2$ is used to create the low humidity condition, which creates a humidity of 33.1 ± 0.2% RH at 23^{o}C according to (ASTM E104, 1985). To determine the actual fluctuation of humidity in the jar and if the surface area of the salt solution is adequate to

maintain a constant RH in the jar, a Vaisala temperature/humidity transmitter with uncertainty of ± 0.1°C and ± 1% RH is placed (along with the plywood) in the jar to monitor the temperature and humidity in the jar during a typical test. The transmitter is moved along with the plywood from one jar to another jar during the test and the measured temperature and humidity of the air in the jar are presented in Figure 2.2. The standard deviation of the humidity is ± 0.8% RH at both the high and low humidity condition.

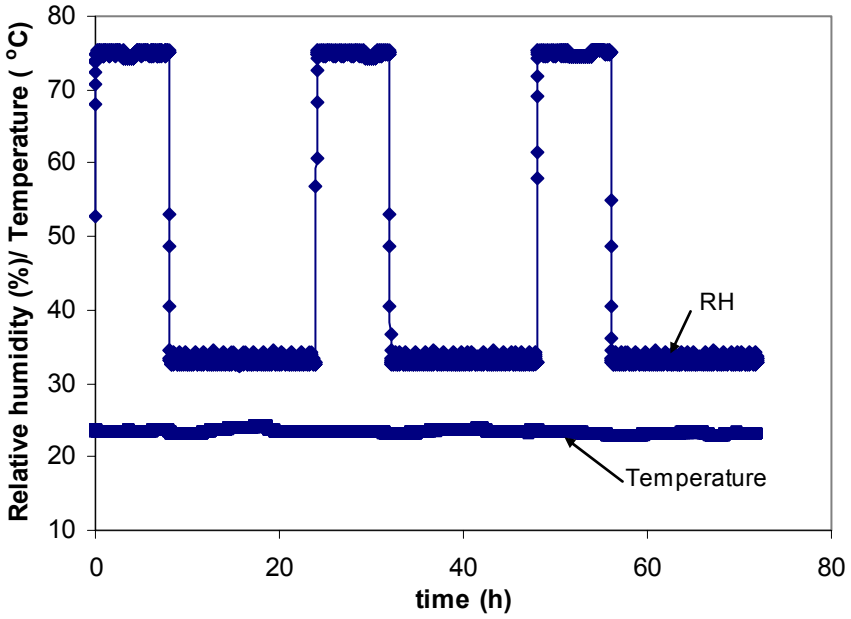

Figure 2.2. Measured relative humidity and temperature of the air in the glass jar facility during a typical test, showing the transitions from 75.2 ± 0.8% RH to 33.3 ± 0.8% RH at a constant temperature of 23.3 ± 0.3°C.

The data in Figure 2.2 are recorded every 1 minute and therefore it can be seen that it takes about 5 minutes to realize the change in humidity between 75% RH and 33% RH. As a comparative test, the temperature and humidity transmitter alone (without the plywood) is moved from one jar to another to check the transient response of the

humidity sensor. It was found that it takes the sensor less than 1 minute to reach equilibrium with the ambient air in the jar. These tests show that when plywood is first placed in a jar with a salt solution, the plywood has a minor effect on the ambient RH maintained by the salt solution. The results in Figure 2.2 also demonstrate that the surface area of the salt is adequate to change the humidity in the jar quickly.

The air inside the jar is not mixed and thus a natural convection boundary layer exists between the vertical surface of the plywood and the air in the jar. The plywood is suspended by an aluminium wire, which is also used to hang the plywood on an electronic mass balance (Figure 2.1(b)). This enables a periodic weighing of the plywood without removing the plywood from the jar. The change in mass of the plywood within the humidity cycle represents the moisture accumulated by spruce plywood. It should be noted that for this facility, only the moisture accumulation measurement, which will be used to determine the moisture buffering capacity in Chapter 4, is performed.

The electronic mass balance is manufactured by Ohaus Adventurer and has a capacity of 210 g. It is calibrated at no load with calibration masses of 100 g (which is within the balance weighing range; the maximum mass measured in this thesis is less than 100 g) and 200 g. The calibration showed that the maximum difference between the calibration masses and the balance readings is 3 mg. This gives a bias uncertainty of ± 3 mg. The precision uncertainty of the balance is ± 0.1 mg and thus the total uncertainty in the output of the balance is ± 3 mg.

2.2 Transient Moisture Transfer (TMT) Facility

A schematic of the TMT facility is given in Figure 2.3 and a picture is given in Figure 2.4. The facility is designed to create one-dimensional and transient heat and moisture transfer within a porous medium subject to convection boundary convection above. In the TMT facility, pieces of plywood (each with dimensions of 600 mm x 280 mm x 9 mm) are placed in a container made of Lexan plastic. These pieces are held together with nylon screws to reduce air gaps between the pieces (Figure 2.5).

(a)

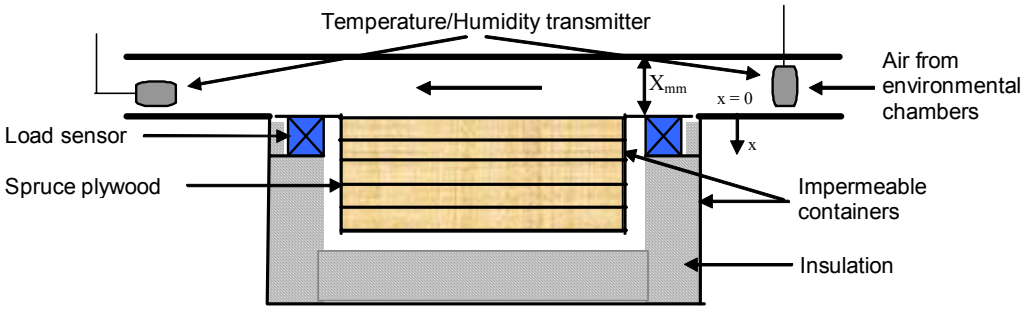

(b)

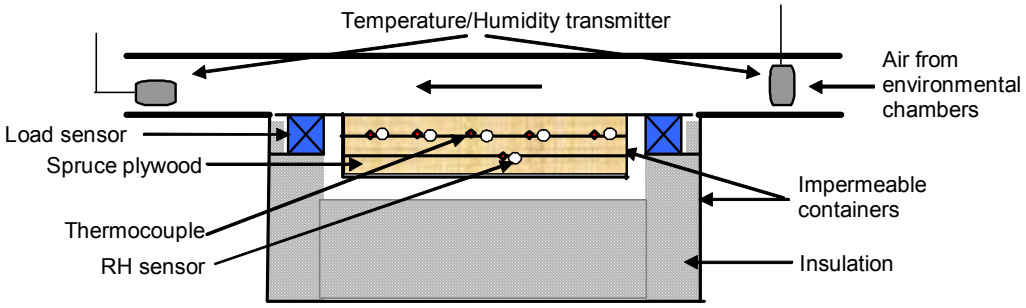

Figure 2.3. Schematic of the TMT facility showing (a) 5 pieces of spruce plywood and the temperature/humidity transmitter and (b) 3 pieces of spruce plywood with the small humidity sensors and thermocouples embedded between the layers of the three plywood samples.

The impermeable Lexan container ensures the one-dimensional moisture transport, while the insulation around the container ensures the one-dimensional heat transfer.

Since the Lexan container is impermeable to moisture transfer, the impermeable plane is at the bottom of the spruce plywood bed. Therefore, the effective thickness (L) of the sample is 45 mm in the MBC measurements where 5 pieces of plywood are tested and 27 mm in the temperature and humidity distribution measurements where 3 pieces of plywood are tested.

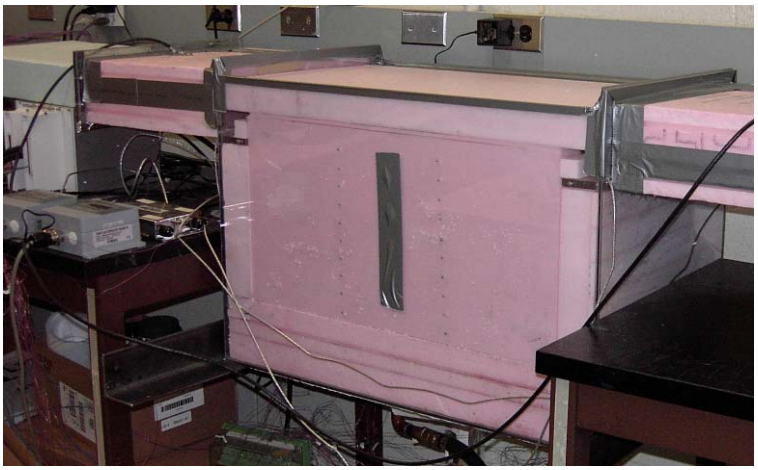

Figure 2.4. Picture of the TMT facility showing the test section and part of the flow channel.

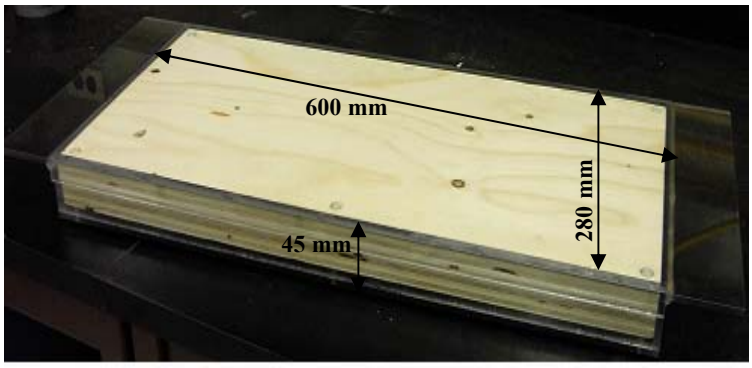

Figure 2.5. Picture showing the spruce plywood held together by nylon screws inside the Lexan container.

The temperature and humidity profile tests within spruce plywood as well as the moisture accumulation measurements are performed for various test conditions using the TMT facility. The moisture accumulation measurements will be used to determine the MBC of spruce plywood. These measurements will provide data to validate the numerical model presented in Chapter 3 and the moisture diffusivity property presented in Chapter 5. The MBC of spruce plywood is measured with 5 pieces of plywood (Figure 2.3(a)) with no sensors between the pieces, while the temperature and humidity profiles are measured with 3 pieces of plywood (Figure 2.3 (b)) with type T thermocouples and small capacitance type humidity sensors (4.27 mm by 15.66 mm by 2.03 mm) (manufactured by Honeywell) embedded between the pieces.

To fully quantify the test, the following measurements are needed: temperature, relative humidity, pressure difference and moisture accumulation. These data are recorded with a data acquisition system (DAS). The DAS comprises of a computer processing unit with two data acquisition cards: 16-bit (PCI 6052E) and 12-bit (PCI 6024E) manufactured by National Instruments. The 16-bit (PCI 6052E) card has a higher resolution and is used for measuring the temperature from the T-type thermocouples and the moisture accumulation from the gravimetric load sensors. The thermocouples and the load sensors are connected to the 16-bit card through a National Instruments SCXI 1000 chassis. The 12-bit (PCI 6024E) card has a lower resolution and is used to measure the relative humidity from the Honeywell humidity sensors and pressure difference from the differential pressure gauge. All the sensors used in the TMT facility (i.e. relative humidity sensors, gravimetric load sensors, thermocouples) are all calibrated against known standards before and after the tests. All the sensors used in the experiment show

good agreement between the pre-test and post-test calibrations. The individual measurements using these sensors are presented in the next section.

Prior to testing, the plywood samples are conditioned to a known initial condition. In the MBC tests, the plywood samples are conditioned for a long time (4 months) in the laboratory to an initial moisture content of 0.025 kg/kg, which corresponds to a relative humidity of about 48%. In the temperature and relative humidity distribution tests, the plywood samples are conditioned using a salt solution ($KC_2H_3O_2$) to equilibrium with air at 22 % RH and 23-24 ^oC.

The air flow is provided by a variable speed vacuum pump, which provides a fully developed airflow at desired temperature and relative humidity above the test specimen. The supply air is from an environmental chamber maintained at a desired temperature that can be controlled within ± 0.2^{o}C and a specified humidity that can be controlled within ± 2% RH. Figure 2.6 presents the temperature and relative humidity measured by the sensor at the inlet of the test section during a typical MBC test (75% RH for 8-hour followed by 33% RH for 16-hour at a constant temperature of 22.6^{o}C). The data in Figure 2.6 are recorded every 5 minutes for three repeated cycles and therefore it can be seen that it takes about 20 minutes to realize an increase in RH and about 30 minutes to realize a decrease in RH. From the data shown in Figure 2.6, the mean temperature of the air is 22.6^{o}C, while 95% of the temperature data are within ± 0.2^{o}C of the mean. The mean relative humidity for the adsorption and desorption periods are 75.3% RH and 33.1% RH respectively, while 95% of the relative humidity data are within ± 2% RH of the mean. These results show good control of the relative humidity and temperature of

the air in the environmental chamber. However, the change in RH is not as rapid nor is the RH control as good as that obtained in the glass jar facility (Figure 2.2).

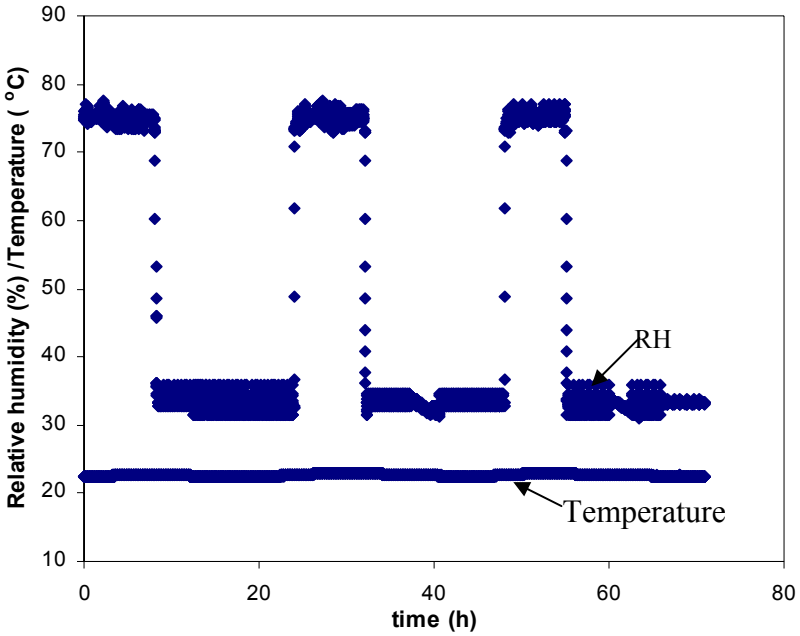

Figure 2.6. Measured relative humidity and temperature of the air entering the TMT facility during a typical MBC test, showing the transition from 75% RH to 33% RH controlled within ± 2% RH and temperature of 22.6°C controlled within ±0.2°C.

2.2.1 Temperature Measurement and Calibration

The temperature measurements that are required are the temperature of air entering and leaving the test section, the temperature distribution within the spruce plywood and the temperature of the air at the orifice plate (located downstream of the TMT facility). The temperature of air entering and leaving the test section is measured with the Vaisala HMP230 transmitter (Figure 2.7), while the other temperature profiles are measured using type-T thermocouples. The type-T thermocouples are calibrated using a temperature simulator as a transfer standard. The thermocouple wires used in the experiment are from the same roll, therefore the differences in the wire are minimized,

which decreases the uncertainty in the temperature differences. The temperature simulator has a bias uncertainty of ± 0.1°C. This calibration is over a temperature range of -40°C to 40°C and the average difference between the readings from the thermocouples and the temperature simulator is less than 0.1°C. The bias uncertainty of the thermocouples is therefore ± 0.1°C.

(a) (b)

Figure 2.7. Picture of (a) the Vaisala HMP230 transmitter and (b) the transmitter head used for measuring the temperature and humidity in the air stream above the plywood bed.

For the temperature distribution measurements within the spruce plywood, six type-T thermocouples are arranged between the pieces of plywood as shown in Figure 2.8. Five thermocouples are placed at a depth of 9 mm and a single thermocouple is placed at a depth of 18 mm.

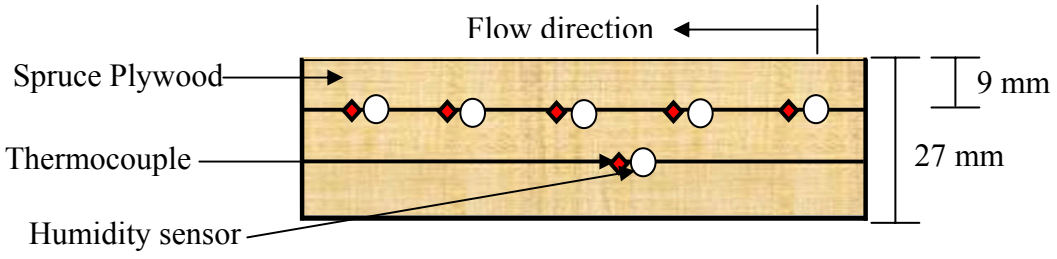

Figure 2.8. Side view of the thermocouple and humidity sensor arrangement between layers of spruce plywood.

The five thermocouples at x = 9 mm are placed at horizontal intervals of 100 mm in the flow direction as shown in Figures 2.9 and 2.10. This temperature sensor array within the spruce plywood is needed to verify the one-dimensional thermal field created by the insulation used in the TMT facility.

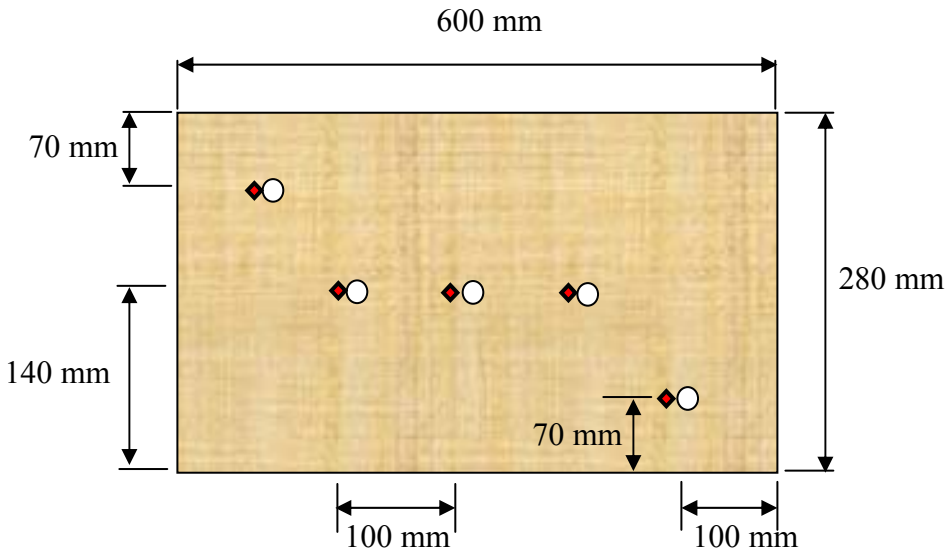

Figure 2.9. Top view of the thermocouple and humidity sensor arrangement between the layers of the spruce plywood at a depth of 9 mm.

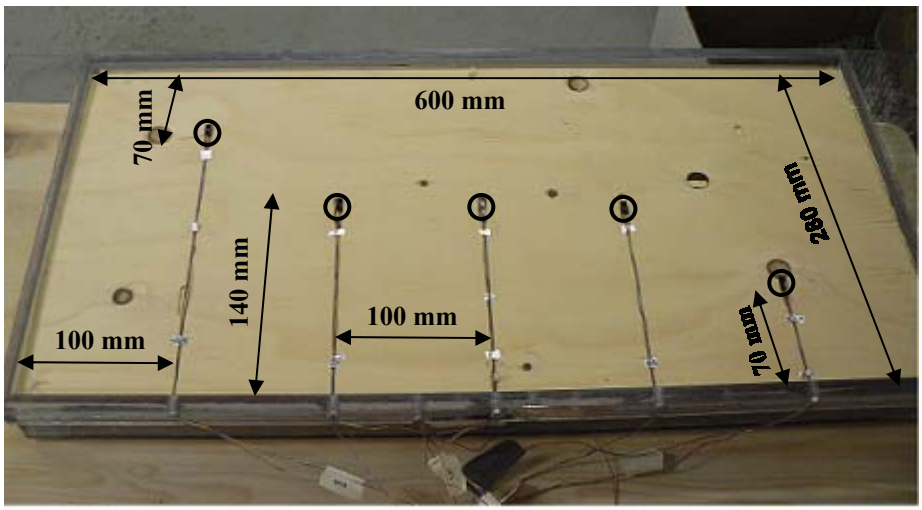

Figure 2.10. Photograph of the spruce plywood in the Lexan container showing the top view of the thermocouple and humidity sensor arrangement between the layers of the spruce plywood.

The temperature readings from the five thermocouples at a depth of 9 mm within the spruce plywood are taken after 2 days of a typical test. It is found that the maximum difference between temperature readings is less than 0.1^{o}C, which is the uncertainty in the thermocouple data and thus verifies the one-dimensional heat transfer created by the insulation.

2.2.2 Relative Humidity Measurement and Calibration

The relative humidity is measured in the airstream entering and leaving the test section as well as within the bed of spruce plywood. The relative humidity in the airstream is measured with the Vaisala (VA) HMP230 transmitter, which is the same instrument used to measure the temperature of the airstream. For the measurements of relative humidity within the spruce plywood, small capacitance-type HIH 3610 humidity sensors made by Honeywell (HW) are embedded between the layers of the spruce plywood. These sensors are 4.27 mm x 15.66 mm x 2.03 mm and are placed at the same locations as the thermocouples (as shown in Figures 2.8, 2.9 and 2.10). Five relative humidity sensors are placed at the 9 mm location to verify the one-dimensional moisture transfer created by the impermeable Lexan container of the TMT facility.

The humidity sensors relate the electrical capacitance of the sensor material, which changes with air relative humidity, to the relative humidity of the surrounding air. They are calibrated using a chilled mirror with a bias uncertainty of ± 0.5% RH as the transfer standard. The humidity sensors are calibrated in air starting at a relative humidity of 10% with an increment of 10% RH up to 90% RH. With these measurements, a calibration equation is developed for each sensor to correct the sensor readings. The

difference between the corrected relative humidity of the sensors and the relative humidity measured by the chilled mirror is presented in Figure 2.11.

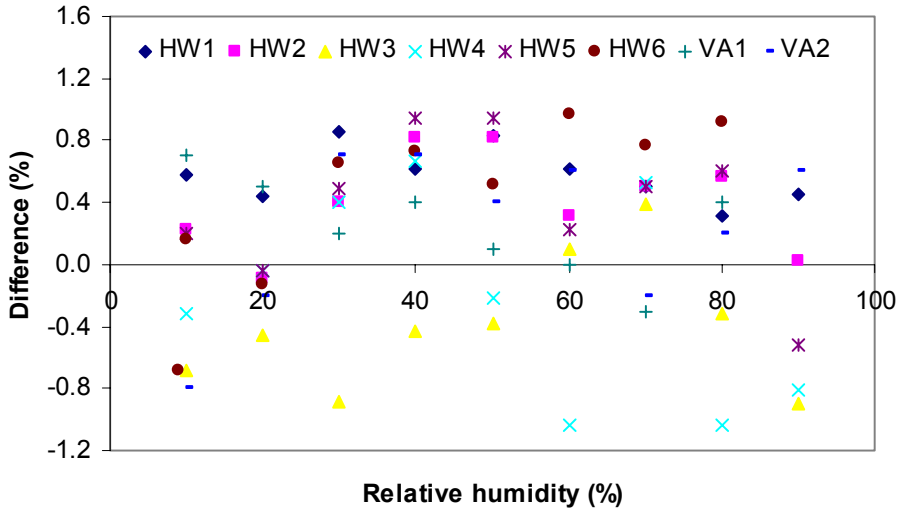

Figure 2.11. Calibration results for relative humidity sensors in air, showing the difference between the chilled mirror and the corrected sensor readings at different calibration points.

The maximum difference between corrected sensor RH and chilled mirror RH is 1% RH and the average difference is 0.5% RH. The final bias uncertainty of each humidity sensor is therefore the root-sum square of the calibration bias between the transfer standard and the corrected relative humidity and the bias uncertainty of the transfer standard. This implies that the bias uncertainty of the relative humidity sensors is ± 1.1% RH.

A second calibration test is performed in air to check the repeatability of the sensors. Figure 2.12 shows the difference obtained between two sets of readings. The maximum difference between two sets of readings is 0.9% RH, with 95% of the data within ± 0.7% RH. This indicates that the precision uncertainty of the humidity sensors is about ± 0.7%

RH. The total uncertainty of the humidity sensors is therefore ± 1.3% RH (root-sum square of the bias and the precision uncertainties). The results of the pre-test and post-test calibrations of the humidity sensors are similar to the results presented in Figure 2.12.

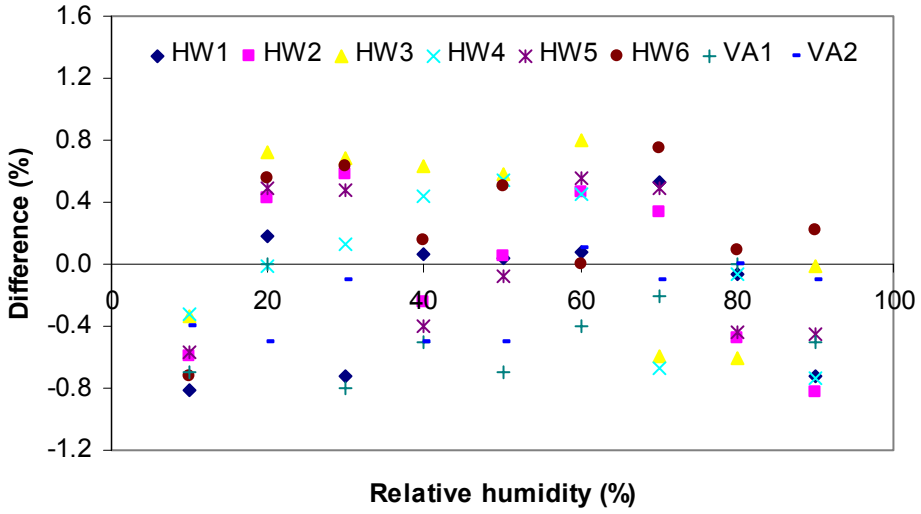

Figure 2.12. The difference between two sets of reading for the calibration of the relative humidity sensors in air.

The relative humidity readings from the five humidity sensors at a depth of 9 mm within the spruce plywood, taken after 2 days of testing are shown in Figure 2.13. The initial conditions for this test are 22% RH and 23°C and the airflow above the insulation is at 70% RH and 23°C. The results are shown for two different airflow rates (0.8 m/s and 1.6 m/s) giving Re = 2000 and Re = 4000 (in the channel above the spruce plywood). For Re = 2000, the maximum difference between relative humidity readings is 0.3% RH, while the maximum difference is 0.5% RH for Re = 4000. These differences are less than the uncertainty in the humidity sensors and thus verify the one-dimensional moisture transfer created by the impermeable Lexan container.

The Reynolds numbers (Re) are calculated thus:

$$Re = \frac{D_h U}{\nu} \quad , \tag{2.1}$$

where D_h is the hydraulic diameter of the rectangular duct, U is the average velocity of the air and υ is the kinematic viscosity of air. The hydraulic diameter of the duct is 37.5 mm and is calculated using,

$$D_h = \frac{4A}{P} \quad . \tag{2.2}$$

Where A is the cross-sectional area of the duct and P is the perimeter of the duct.

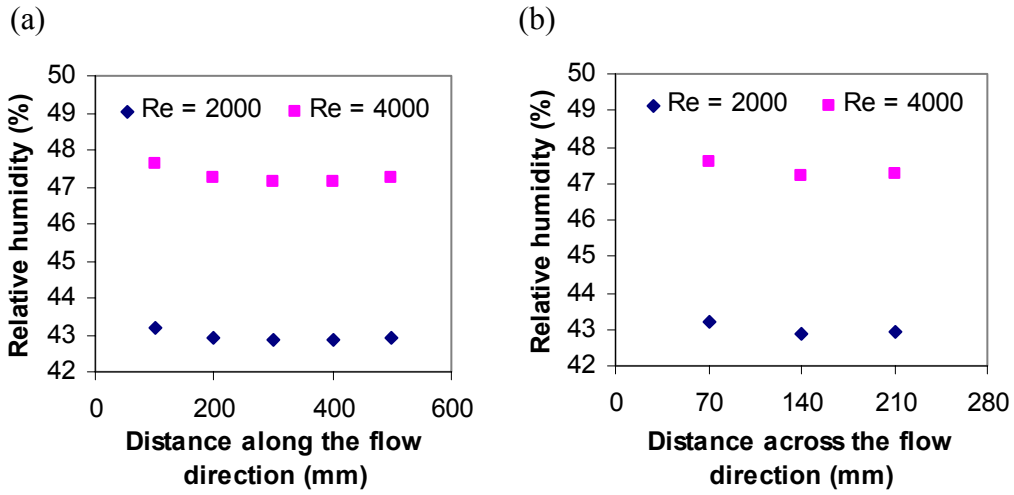

Figure 2.13. Relative humidity measurements (a) along the flow direction (b) across the flow direction at a depth of 9 mm within the spruce plywood after 2 days of testing.

2.2.3 Airflow Rate and Convection Transfer Coefficient Measurements

The airflow rate, measured according to ISO 5176-1 (1991), is required to determine the Reynolds number (Re) of the airflow above the spruce plywood. Different Re are used to create different convective heat and mass transfer coefficients at the top surface of the plywood. The airflow rate is also used to calculate the moisture accumulation in the spruce plywood together with humidity and will be presented in the next section.

The air flow rate is measured with a 30 mm tapered orifice plate embedded in a circular air duct (D = 72 mm) downstream of the test section. The pressure difference across the orifice (ΔP) is measured with a differential pressure gauge and the mass flow rate is calculated using equation (2.3). The air condition upstream of the orifice plate is referred to as point 1 in the equation.

$$\dot{m}_a = \frac{C_d}{\sqrt{1-\beta^4}} \lambda_1 \frac{\pi}{4} d^2 \sqrt{2\Delta P \rho_1}\,, \tag{2.3}$$

$$\text{where } \beta = \frac{d}{D}. \tag{2.4}$$

D is the diameter of the supply duct, d is the diameter across the orifice plate, λ_1 is the expansibility factor and C_d is the discharge coefficient. For this experiment, β = 0.42, C_d = 0.6207 and λ_1 = 0.993 (ISO 5176-1, 1991). The mass flow rate is measured with an uncertainty of ± 6%.

In this thesis, the Re numbers investigated are 1000, 2000, 4000 and 7600, which correspond to average air velocities of 0.4, 0.8, 1.6, 3.1 m/s in the channel above the plywood. The uncertainty in the Re numbers calculated from the measured air flow is ± 8% for the TMT facility. A separate test was conducted by Conrad Iskra to determine the convection mass transfer coefficients for these Re numbers. In this test, a tray of water is placed in the TMT facility and air is passed over the free surface of water. As the air with controlled Re number passes over the test section, water evaporates into the air and the mass of water in the tray decreases, which is recorded by the load sensors.

The temperature and relative humidity of the air entering and leaving the test section are measured to determine the vapour density of the air flowing above the water. The temperature of the water is also measured to determine the water vapour density at the surface of the water. From the mass readings and vapour densities, the convective mass transfer coefficient is determined. The measured convective mass coefficient is then used to determine the Sherwood number. With an assumption that the Sherwood number equals the Nusselt number, the convective heat transfer coefficient is determined. The convective heat and mass transfer coefficients determined are shown in Table 2.1 for the four Reynolds numbers investigated.

Table 2.1. Summary of the convective heat and mass transfer coefficients at different Reynolds numbers in the TMT facility.

Reynolds number (Re)	1000	2000	4000	7600
Convective heat transfer coefficient (h_a) [W/(m^2·K)]	2.5 ± 0.2	3.5 ± 0.2	8.1 ± 0.4	13.4 ± 0.7
Convective mass transfer coefficient (h_m) [10^{-3} m/s]	2.1 ± 0.2	2.9 ± 0.2	6.7 ± 0.3	11.1 ± 0.6

2.2.4 Moisture Accumulation Measurement and Calibration

Two methods are employed in the measurement of the moisture accumulated in the spruce plywood. One method uses the output of the cantilever beam type, gravimetric load sensors and the other is through calculation using the mass flow rate of air and the relative humidity of the air entering and leaving the test section.

In the first method using the load sensors, the flange of the Lexan container is free floating on four gravimetric load sensors in such a way that any change in mass during the experiment is the mass of moisture adsorbed or desorbed in the spruce plywood (Figure 2.3). The load sensors are calibrated in-situ, with the five pieces of plywood placed in the Lexan container resting on the load sensors. Calibration weights in the range of 1 g to 500 g (the maximum moisture accumulation measured in the tests in Chapter 4 and 5 is less than 100 g) with a bias uncertainty of ± 0.1 g are used to calibrate the load sensors. The calibration shows that the load sensors have a very high sensitivity and respond to changes in mass as small as 1 g. The maximum difference between the calibration weights and the load sensor readings is 2 g. The 95% uncertainty bounds for the data are also ± 2 g. Since the precision uncertainty and the transfer standard bias are negligible, the total uncertainty in the output of the load sensors is ± 2 g.

The second method involved calculating the transient change in moisture content by integrating with time the difference between the humidity ratio of the air entering and leaving the test section:

$$\Delta m(t) = \int_0 \dot{m}_a (W_{inlet} - W_{outlet}) dt \,, \tag{2.5}$$

where Δm is the moisture accumulated in the spruce plywood (positive for moisture accumulation and negative for moisture removal), $\dot{m}_a$ is the mass flow rate of the air, and W_{inlet} and W_{outlet} are the humidity ratios of the air entering and leaving the test section, respectively. The humidity ratio (W) of the air is given by,

$$W = \frac{0.62198\, \phi P_{vsat}}{P_{atm} - P_{vsat}} \,. \tag{2.6}$$

where P_{vsat} and P_{atm} are saturation vapour and atmospheric pressures respectively and ϕ is the relative humidity in fraction. The moisture accumulation measurement using the relative humidity sensors has a higher uncertainty, compared to the measurement using the load sensors, but provides a useful comparison. The uncertainty in the measurement of moisture accumulation using the relative humidity sensors is typically ± 15%.

2.3 Material Property Measurements

Although the measured material properties are not part of the main experiment, these measurements are required in the numerical model in Chapter 3. The measured properties described in this section are the sorption isotherm, porosity, effective thermal conductivity and water vapour permeability.

2.3.1 Sorption Isotherm and Dimensional Changes

Different materials hold different amount of moisture at different humidity conditions below 100% RH. The relationship between the equilibrium moisture content of a material and the relative humidity it is exposed to at a specific temperature is called the sorption isotherm. The experiment to generate the sorption isotherm is performed according to ISO 12571 (1996) using salt solutions to generate the relative humidity (ASTM E104, 1985). Three samples of spruce plywood (each of size 60 mm by 60 mm by 9 mm) are dried using a vented oven at 50^{o}C and approximately 2% RH until the change in mass between two successive measurements, with a time interval of at least 24 hours, is lower than 0.1%. After drying, the samples are wrapped in plastic to make sure that they do not pick up moisture between drying and weighing. The dried samples are allowed to cool to room temperature and weighed. The samples are then placed in the air

above the salt solution in glass jars (Figure 2.1(a)). Each of the samples is first placed in a jar with a relative humidity of 11% until equilibrium is reached. The mass is weighed, and the specimen is placed in a jar with an air relative humidity of 22%. This process is repeated with increments of about 10% RH up to 97% RH for the adsorption process. For the desorption process, the plywood sample at 97% RH is placed in a jar with a relative humidity of 75% RH until equilibrium is reached. The mass is weighed and then placed in a lower relative humidity with decrements of about 20% RH up to 11%. The moisture content (u) at a given relative humidity is calculated as,

$$u = \frac{m - m_o}{m_o}, \tag{2.7}$$

where m is the final mass of the spruce plywood specimen after equilibrium is attained between the plywood and the air in the jar at a particular relative humidity and m_o is the mass of the dry spruce plywood specimen.

The sorption and desorption curves for spruce plywood are shown in Figure 2.14. The results are averages of the 3 samples measured. The uncertainty in the mass measurement is ± 3 mg and the uncertainty in the moisture content is ± 0.0001 kg/kg, which corresponds to an uncertainty in moisture content of ± 1% at 11% RH and ± 0.1% at 97% RH. The experimental adsorption data are curve-fitted with a continuous polynomial relationship between moisture content (u) and relative humidity (ϕ) in fraction. The polynomial equation for the curve fit is given as:

$$u = \left(\frac{a + c\phi + e\phi^2}{1 + b\phi + d\phi^2 + f\phi^3} \right) S, \tag{2.8}$$

where a = 1.0147E-04, b = 0.2339, c = 0.06754, d = -2.3603, e = -0.06574, f = 1.1329. Equation (2.8) fits the measured data with r^2 = 0.999 when the sensitivity coefficient (S) equals 1. Figure 2.14 also shows that equation (2.8) fits the desorption data quite well when S = 1.1. Therefore a ± 10% change in the curve fit is representative of the maximum error between the measured data and curve fit. The effect of this ± 10% change in S will be investigated using the numerical model in Chapters 4 and 5.

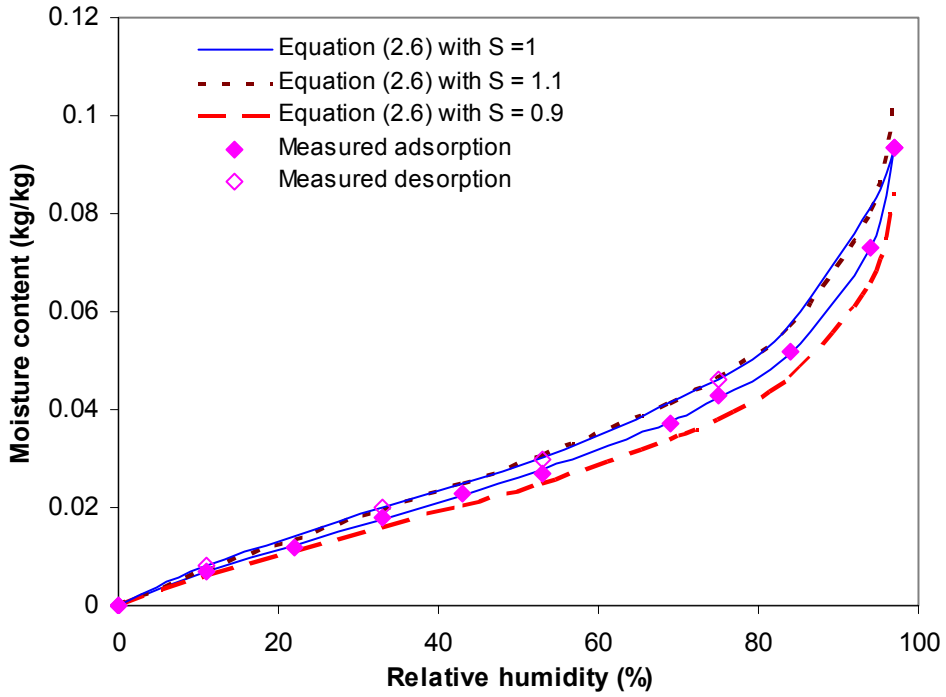

Figure 2.14. Sorption isotherm for spruce plywood showing the measured data, the curve fit and 10% changes in the curve fit used in sensitivity studies.

The dimensional changes of the spruce plywood samples with changes in relative humidity (moisture content) are monitored during the sorption isotherm test. The dimensions (length, width, thickness) of the three plywood samples are taken using a

caliper after they have reached equilibrium with each RH and the dimensional change is plotted in Figure 2.15.

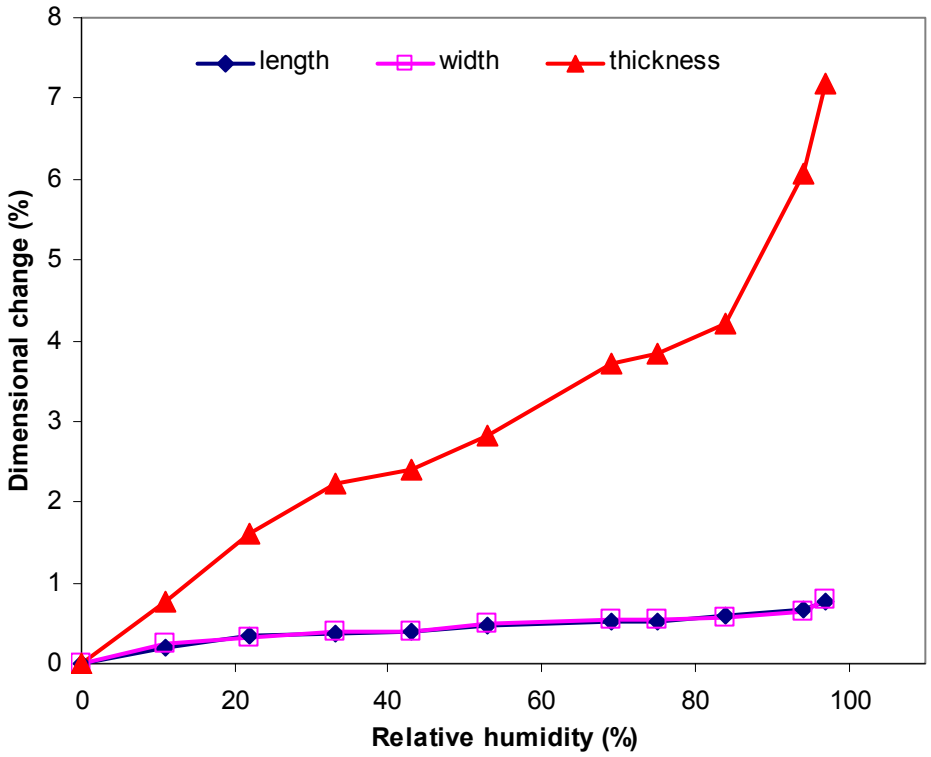

Figure 2.15. Dimensional changes (%) in the spruce plywood with changes in relative humidity.

The figure shows the average percentage difference in the dimensions of the three plywood samples as the relative humidity changes. The maximum dimensional change is less than 8% for thickness and less than 1% for the length and width. These results are similar to the experimental results obtained by Ojanen and Ahonen (2005), which showed that for a maximum humidity change of 87%, the maximum change in thickness was 6% and the changes in length and width were about 0.1%. The effect of moisture on the change of the length and width of the plywood is much lower than on the thickness,

because plywood veneers are glued together such that the grain direction in adjacent plies is at right angles to one another. Thus, the tendency to shrink and swell with moisture change is largely eliminated in the plane of the panel.

It should be noted that, although the changes in thickness of the plywood are small, this increase will tend to decrease the thickness of the air gap between the spruce plywood and the air above it in the TMT facility. In the worst case, the thickness of the air gap will change by 2%, which is expected to have a negligible effect on the convection transfer coefficients between the air and the plywood.

2.3.2 Dry Density and Porosity

The dry density (ρ_o) of the cellular material (i.e., cellulose) is practically constant at 1530 kg/m^3 for all wood species (Dinwoodie, 1981). However, wood is not comprised of 100% cell wall material because it contains air in the cell lumens. The dry density of porous wood is easily obtained by weighing the dry-mass of the spruce plywood with a certain volume. Three pieces of spruce plywood (60 mm by 60 mm by 9 mm) are dried, cooled and weighed as described in Section 2.3.1. The volume of these plywood pieces is then measured using a caliper. With the volume and the dried mass, the dry density of the plywood (ρ_o) is determined to be 445 ± 0.3 kg/m^3.

With the dry density, the volume fraction of solid material (cell walls) (ε_s) can be calculated as follows (Kellog and Wangaard, 1969):

$$\varepsilon_s = \frac{\rho_o}{1530}. \tag{2.9}$$

The void volume or porosity (ε_g) is defined in relation to the volume fraction of the cell wall material and is determined using

$$\varepsilon_g = 1 - \varepsilon_s . \tag{2.10}$$

Using a density of 445 kg/m^3 in equation (2.9), the volume fraction of the solid cell wall in plywood (ε_s) is calculated to be 0.30 and the porosity is 0.70, both with an uncertainty of ± 0.01.

2.3.3 Effective Thermal Conductivity

The effective thermal conductivity of spruce plywood is measured using a heat flow meter apparatus that measures according to ASTM standard C518 (2003). The heat flow meter apparatus consists of two isothermal plates and two heat flux meters. It establishes steady-state one-dimensional heat transfer through a test specimen between two parallel plates, which are controlled to a specified temperature, as shown in Figure 2.16.

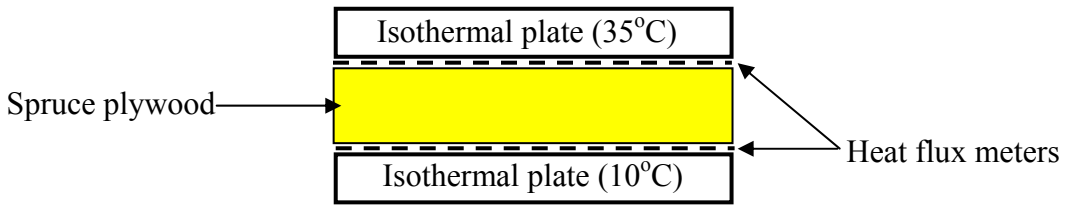

Figure 2.16. Schematic showing the heat flow meter apparatus used to measure thermal conductivity.

The thermocouples embedded in the plates, measure the temperature drop across the spruce plywood and the heat flux meters embedded in each plate measure the heat flow

through the spruce plywood. At steady state, the thermal conductivity of the spruce plywood, k_{eff} in W/(m·K) is given by,

$$k_{eff} = \frac{q'' L}{\Delta T} \tag{2.11}$$

where q'' is the heat flux rate (W/m^2), L is the thickness of the spruce plywood (m), and ΔT is the temperature difference across the spruce plywood (K).

For this experiment, a 9 mm-thick piece of spruce plywood with dimensions of 28 mm by 28 mm is used. Prior to testing, the sample is conditioned to different RH values (11%, 33%, 53% and 75% RH) using saturated salt solutions according to ASTM Standard E104 (1985) in order to quantify the change in thermal conductivity with equilibrium RH. The plywood is also dried at 50^{o}C in a vented oven so that the thermal conductivity of the dry plywood can be measured. The effective thermal conductivity is performed three times for each humidity condition and using a constant temperature drop of 25^{o}C across the specimen. The plate temperatures are of 10^{o}C and 35^{o}C, giving an average temperature of 22.5^{o}C. Figure 2.17 presents the average k_{eff} of the three measurements at each RH. Effective thermal conductivity increases with RH as expected. The maximum effective thermal conductivity over the tested range is 0.091 W/(m·K), which is 10% higher than the dry value of 0.082 W/(m·K). The uncertainty in the measured effective thermal conductivity using the heat flux meter apparatus is ± 1%. It should be noted that the thermal conductivity measurements took about 30 minutes to complete, while it took about 14 days to condition the samples to equilibrium, therefore moisture movement during the thermal conductivity test is expected to be minimal.

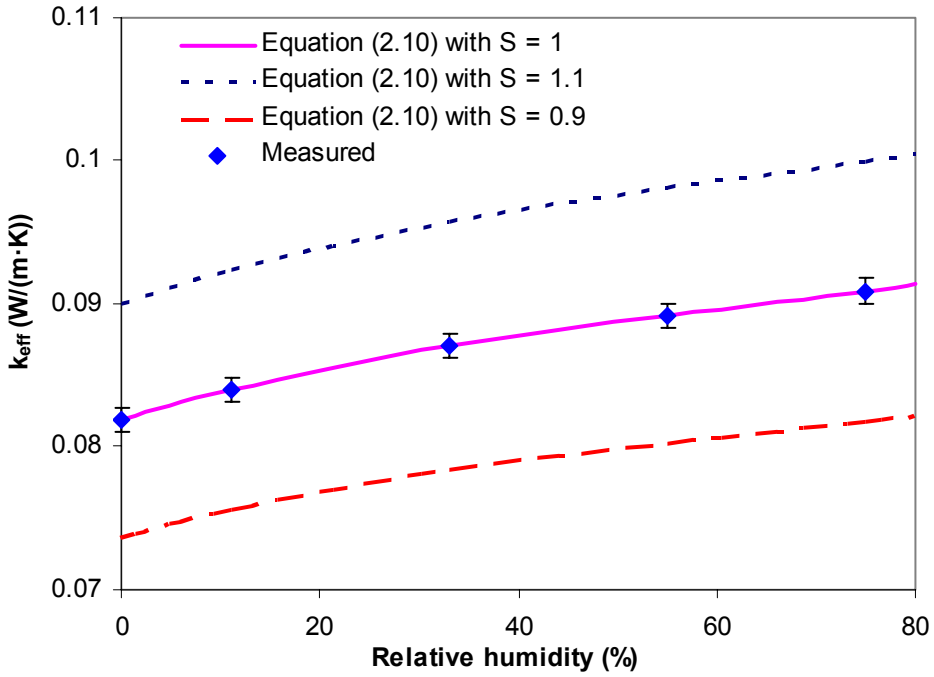

Figure 2.17. Effective thermal conductivity of spruce plywood as a function of relative showing the measured data with the 95% uncertainty bars, the curve fit and 10% changes in the curve fit used in the sensitivity studies.

The experimental data were curved-fitted with a continuous relationship that is represented by a polynomial equation given as follows:

$$k_{eff} = \left(a + b\phi + c\phi^2 + d\phi^3\right) S \,, \tag{2.12}$$

where a = 0.08185, b = 0.02212, c = -0.02313, d = 0.01291. Equation (2.12) fits the measured data very well when S = 1 as shown in Figure 2.17 (r^2 = 0.999). Figure 2.17 also shows a ± 10% change in the curve fit for the thermal conductivity, which is representative of the maximum change in k_{eff} from 0 to 75% RH. This ± 10% change is not representative of the uncertainty in $k_{eff,}$ but is chosen to be consistent with the ± 10% change used for the other properties investigated in the sensitivity studies of this thesis.

2.3.4 Water Vapour Permeability

Water vapour permeability in moisture transfer is analogous to thermal conductivity in heat transfer. It governs the rate of water vapour transmission through a porous material that has a vapour pressure difference across it. The steady-state water vapour permeability is measured using the cup method in accordance with ASTM Standard E 96 (1996). A schematic of the cup tests set-up and conditions is given in Figure 2.18 and a picture of the facility used is in Figure 2.19.

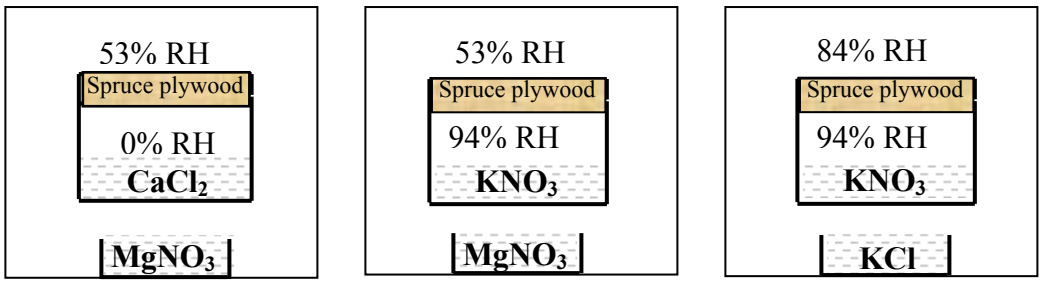

Figure 2.18. Schematic of the water vapour permeability set-up showing the cups with the salt solutions used in the cup and the chamber.

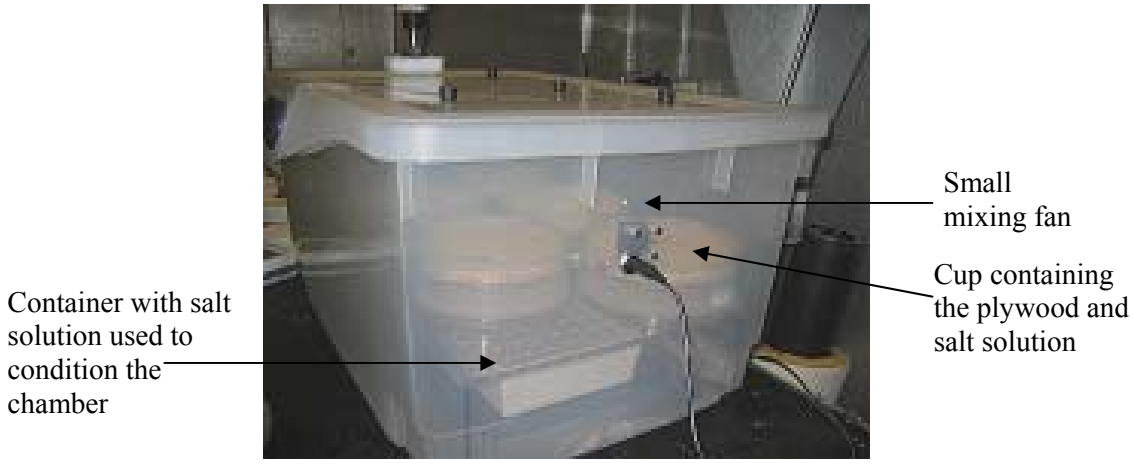

Figure 2.19. Picture of the water vapour permeability experimental set up showing the cups inside a semi-transparent plastic container (the chamber) and a small mixing fan.

The dry and wet cup are standard measurements and cover the range of humidities investigated in this thesis, but to further quantify the water vapour permeability of the plywood, an additional cup measurement is made at high humidities. The cups are placed in a chamber, which is equipped with a small fan (powered by an external motor) to gently mix the air in the chamber with a velocity of 0.06 m/s. Five pieces of circular-shaped samples of spruce plywood, each 9 mm thick and with an average diameter of 146 mm, are placed in the dry and wet cups as shown in Figures 2.18 and 2.19. The edges of the plywood in the cup are sealed with paraffin wax to avoid leakage between the cup and the plywood. In the dry cup test, $CaCl_2$ (0% RH) is used in the cup and $MgNO_3$ (53% RH) is used to condition the surrounding air. The wet cup test uses KNO_3 (94% RH) in the cup and $MgNO_3$ (53% RH) in the surrounding air, while the additional cup measurement is made using KNO_3 (94% RH) in the cup and KCl (84% RH) in the surrounding air.

Prior to testing, the plywood samples are preconditioned at 23°C and 53% RH in an environmental chamber for dry and wet cup tests and 23°C and 84% RH for the additional cup test. The cups are weighed periodically to determine the rate of mass transfer through the plywood (G), which can be converted to water vapour permeability (δ) expressed in $\mathrm{kg/(m \cdot s \cdot Pa)}$ knowing the thickness of the specimen (d) using

$$\delta = \frac{G\, d}{A\, \Delta p}. \tag{2.13}$$

where G is the rate of mass transfer through the specimen (kg/s), A is the exposed area of the test specimen (m^2) and Δp is the water vapour pressure difference across the

specimen (Pa). The value of Δp is calculated from the mean of the measured temperature and relative humidity over the course of the test. The vapour pressure on either side of the specimen is calculated using equation (2.14) and the difference between these vapour pressures gives Δp.

$$p_v = \phi \; 6.105 \; e^{\frac{17.269\theta}{237.3+\theta}} , \qquad (2.14)$$

where p_v is the water vapour pressure in Pa, θ is the temperature of the test condition in ^{o}C and ϕ is the relative humidity on one side of the specimen in %.

The results presented in Figure 2.20 show that as the average humidity condition increases, the water vapour permeability increases, enabling more moisture transport through the plywood. The uncertainty in the measured value of the water vapour permeability is ± 13%.

The measured data are curve-fitted and the relationship for water vapour permeability is given as:

$$\delta = \left[\left(a + \left(b\phi / \ell n\phi\right)\right)^{0.5}\right] S \qquad (2.15)$$

where a = -2.3573E-25, b = -8.1601E-24. Figure 2.20 also includes a ± 10% change in the curve fit for the vapour permeability, which is representative of the maximum uncertainty in the measured data.

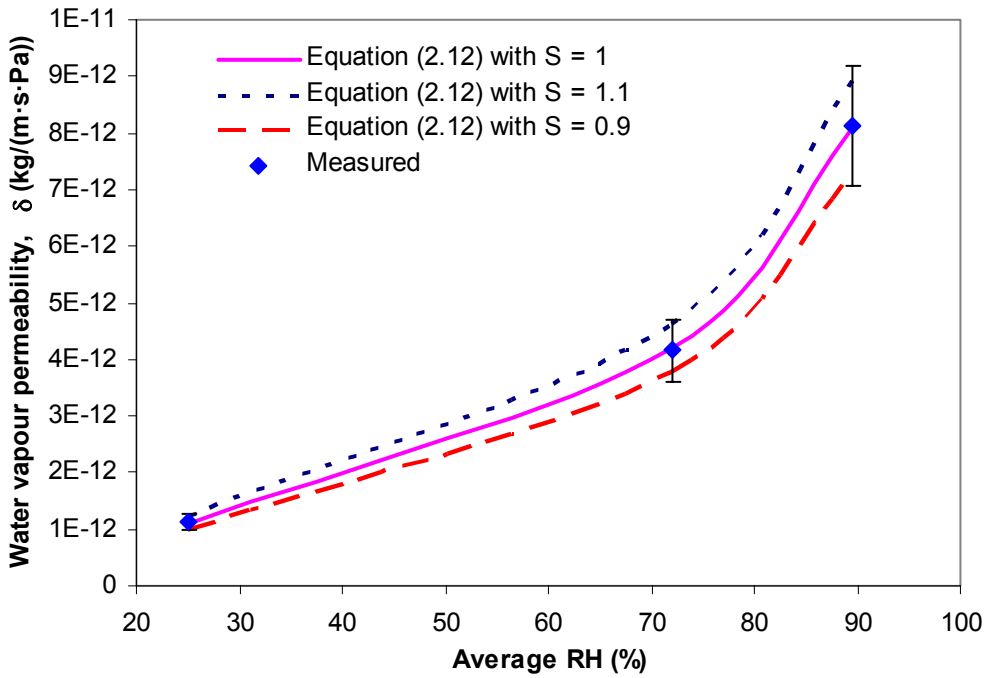

Figure 2.20. Water vapour permeability curve for spruce plywood showing the measured data with the 95% uncertainty bars, the curve fit and 10% changes in the curve fit used in sensitivity studies.

2.4 Summary

Two different test facilities are developed and presented in this chapter. Both of these facilities are able to provide well-controlled temperature and humidity boundary conditions for the hygroscopic material being tested and permit these boundary conditions to be changed rapidly. One facility (termed the glass jar facility) uses a hanging mass balance (which measures with an uncertainty of ± 3 mg) and small, sealed jars containing saturated salt solutions located in a controlled environmental chamber. The other facility (termed the transient moisture transfer (TMT) facility) is more complex and provides fully developed air flow above the hygroscopic material using a small scale wind tunnel connected to an environmental chamber. The glass jar facility provides more constant humidity conditions and is able to change these conditions more

rapidly than the TMT facility, but is limited to investigate natural convection moisture transfer and small samples. On the other hand, the air flow and convection transfer coefficients can be varied, are well controlled in the TMT facility and are known within ± 10%.

The glass jar facility is used to measure the moisture accumulation in spruce plywood, while the TMT facility measures the moisture accumulation as well as the temperature and relative humidity distribution within the plywood. The uncertainties in the mass accumulation measurements using the TMT facility are ± 2 g and ± 15%, using the load sensors and the inlet and exit humidities, respectively. The thermocouples and humidity sensors in the TMT facility measure temperature and humidity with an uncertainty of ± 0.1^{o}C and ± 1%, respectively.

CHAPTER 3

NUMERICAL MODEL

A numerical model is developed to simulate the heat and moisture processes in spruce plywood. The model solves the governing equations for the one-dimensional diffusion of heat and water vapour in a bed of spruce plywood subjected to a convective boundary condition at the top surface. This is a representative of the heat and moisture transport processes that occur in the experiments presented in Chapter 2. The numerical model, once validated using experimental results, is an excellent tool for predicting the transient response of spruce plywood and also for performing various studies that might be difficult or even impossible to do experimentally.

This chapter reviews the basic theory and assumptions made in obtaining the theoretical model of heat and moisture transfer in porous media. The governing equations, property relations (used to calculate the changes in the properties of the material due to moisture adsorption/desorption), boundary conditions and numerical solution method are all presented.

3.1 Local Volume Averaging Theory

Spruce plywood, like any wood material, is a porous material that is made up of solid cell walls and lumens (Figure 3.1). The cell walls are irregularly shaped, which makes it

extremely difficult to analytically define the boundary between each cell wall and the surrounding fluid. Therefore, solving the simultaneous heat and moisture transfer equations in both the fluid and solid phases would be impractical because it is very difficult to analytically define the solid-fluid interfacial boundary area. To overcome this problem, local averaging is performed on a representative elementary volume, which is the smallest differential volume that results in statistically meaningful local averaged properties. Increasing the size of this representative elementary volume does not change the local averaged properties. Thus, the size of the local averaged volume is the minimum volume such that the volume averaged properties will vary in a continuous manner throughout the porous medium. By averaging the governing equation of the representative elementary volume, the problem of analytically defining the boundary between the phases is avoided (Kaviany, 1991). This local volume averaging technique will be applied to the conservation of mass and energy equations in order to obtain the governing equations, which describe the diffusion process in spruce plywood.

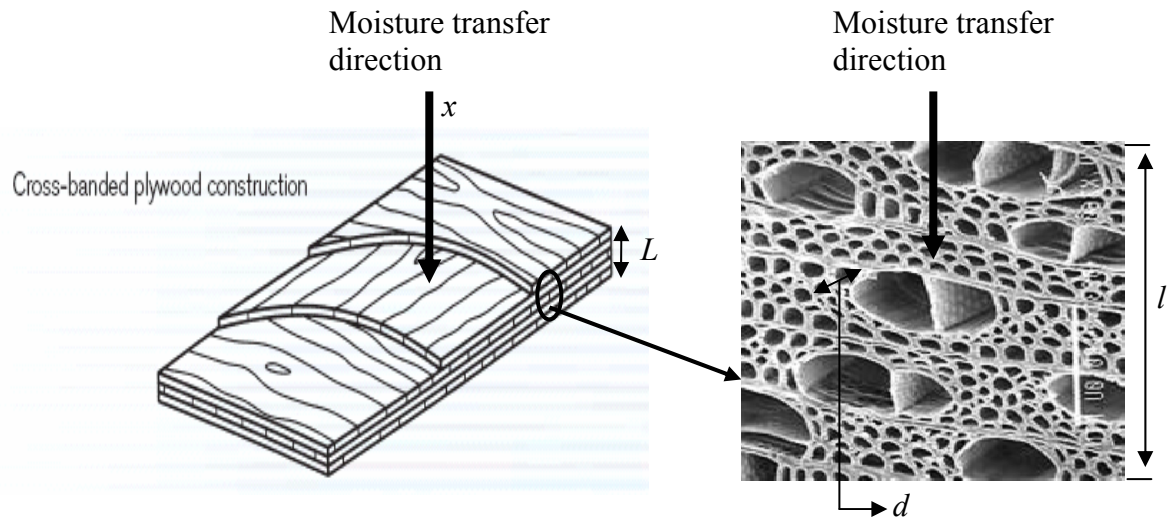

Figure 3.1. A representative elementary volume of spruce plywood showing the irregularly shaped cell walls, the lumens and the characteristic length scales.

In order for the theory of local volume averaging to be applied successfully to this problem, the three length scales must satisfy the condition as follows:

$$d < \ell << L, \tag{3.1}$$

where d is the particle size, ℓ is the length across the elementary volume and L is the length across the medium. For the spruce plywood under consideration in this thesis, the length scales (shown in Figure 3.1) are as follows: d = 50 μm, ℓ = 0.25 mm, L = 4.5 to 45 mm, which satisfies the length constraint in equation (3.1).

The assumption of local thermal equilibrium simplifies the energy equation and this assumption is valid when:

$$\Delta T_d < \Delta T_\ell << \Delta T_L . \tag{3.2}$$

This implies that the temperature difference between the solid and fluid phase is much smaller compared to the temperature difference across the elementary volume. In this thesis, the temperature scale criterion is assumed to be satisfied and the length scale criterion is satisfied for the problem investigated, therefore the local thermal equilibrium and the local volume averaging can be applied.

Therefore the transport equations which will be used in this model are the averaged equations, where the local volume average of a general variable ψ is defined as,

$$<\psi> = \frac{1}{V}\int_V \psi \, dV , \tag{3.3}$$

where $<>$ represents the local average and V is the elementary volume.

Another important averaging quantity of interest is the intrinsic phase average of any dependent variable over phase *k* defined as:

$$<\psi>^{k} = \frac{1}{V_k}\int_{V_k}\psi_k \, dV \ , \tag{3.4}$$

where k represents any of the phases.

Equations (3.3) and (3.4) imply that the phase averaged property is related to the intrinsic phase averaged property by the volume fraction of phase *k* given by:

$$\langle\phi\rangle = \varepsilon_{\mathrm{k}}\langle\phi\rangle^{\mathrm{k}}, \tag{3.5}$$

where ε_k is the volume fraction of phase *k* and is given by:

$$\varepsilon_k = \frac{V_k}{V}. \tag{3.6}$$

In order to apply local volume averaging to the energy and vapour diffusion equations, it is important to obtain the volume average of the gradient of a variable. This is given by (Kaviany, 1991):

$$\langle\nabla\psi\rangle = \nabla\langle\psi\rangle + \frac{1}{V}\int_{A_{kj}}\psi \ n_{kj} \, dA, \tag{3.7}$$

where A_{kj} is the interface area between phases k and j and n_{kj} is the unit normal vector on the interface. Application of equation (3.7) to the transport equations requires the definition of double averaging as follows:

$$\langle\langle\psi\rangle\rangle = \langle\psi\rangle. \tag{3.8}$$

The averaged heat and mass transfer equations for the medium are obtained by applying the definitions given above to the transport equations. The derivation of the governing equations for the heat and mass transport in a porous medium, which involves a significant amount of mathematical manipulations and approximations, can be found in Whitaker (1977).

3.2 Assumptions and Governing Equations

Other assumptions that reflect the experimental conditions and allow the problem to be simplified without a significant loss in accuracy are listed below.

1. The heat and moisture transfer through the spruce plywood is one-dimensional.
2. The transport process within the spruce plywood is pure diffusion of heat and water vapour.
3. Air and water vapour behave as ideal gases.
4. The only heat source in the medium is the heat of phase change resulting from the adsorption and desorption of water vapour within spruce plywood.
5. The solid and fluid states are in thermal equilibrium.
6. Knudsen diffusion is negligible and Fickian diffusion dominates.
7. The volume changes (swelling and shrinkage) with changes in humidity are negligible.

The resulting conservation equations for mass and energy are the averaged transport equations over the representative elementary volume and are listed below.

Conservation of mass

Absorbed Phase

$$\rho_{\ell} \frac{\partial \varepsilon_{\ell}}{\partial t} + \dot{m} = 0 \tag{3.9}$$

Gas Diffusion

$$\frac{\partial (\rho_v \varepsilon_g)}{\partial t} - \dot{m} = \frac{\partial}{\partial x}\left(D_{eff} \frac{\partial \rho_v}{\partial x} \right) \tag{3.10}$$

Conservation of Energy

$$\rho Cp_{eff} \frac{\partial T}{\partial t} + \dot{m} h_{ad} = \frac{\partial}{\partial x}\left(k_{eff} \frac{\partial T}{\partial x} \right) \tag{3.11}$$

These averaged transport equations are needed to solve the dependent variables of temperature (T), vapour density (ρ_v) and moisture content (u) (or volume fraction of adsorbed water (ε_l)). The other symbols are defined in the nomenclature.

The phase change rate ($\dot{m}$) can be determined from the rate of change of moisture content (u) as follows:

$$\dot{m} = -\rho_o \frac{\partial u}{\partial t}, \tag{3.12}$$

where ρ_o is the dry density of spruce plywood and u is the moisture content.

The moisture content (u) and effective thermal conductivity are calculated using the correlations developed from the experimental data in Chapter 2 (Figures 2.14 and 2.17).

They are:

$$u = \frac{a + c\phi + e\phi^2}{1 + b\phi + d\phi^2 + f\phi^3}, \tag{3.13}$$

where a = 1.0147E-04, b = 0.2339, c = 0.06754, d = -2.3603, e = -0.06574, f = 1.1329.

$$k_{eff} = a + b\phi + c\phi^2 + d\phi^3, \tag{3.14}$$

where a = 0.08185, b = 0.02212, c = -0.02313, d = 0.01291.

The vapour diffusion coefficient (D_{eff}) can be determined using

$$D_{eff} = \delta R_v T, \tag{3.15}$$

where the water vapour permeability (δ) is a function of humidity (Figure 2.21) and the relationship is:

$$\delta = \left(a + \left(b\phi / \ell n\phi\right)\right)^{0.5} \tag{3.16}$$

where a = -2.3573E-25, b = -8.1601E-24.

The equations that quantify the changes in density and specific heat capacity due to moisture adsorption result from the local volume averaging of the governing equations and are:

$$\rho = \varepsilon_s \rho_s + \varepsilon_g \rho_g + \varepsilon_l \rho_l, \text{ and} \tag{3.17}$$

$$Cp_{eff} = \frac{\varepsilon_s \rho_s Cp_s + \varepsilon_l \rho_l Cp_l + \varepsilon_g \left\{(\rho Cp)_a + (\rho Cp)_v\right\}}{\rho} \tag{3.18}$$

Other equations required in the model for closure are as follows:

The volume constraint is:

$$\varepsilon_s + \varepsilon_\ell + \varepsilon_{\mathrm{g}} = 1. \tag{3.19}$$

The thermodynamic relationships are:

$$P_v = \rho_{\mathrm{v}} R_v T, \tag{3.20}$$

$$P_g = P_a + P_v, \tag{3.21}$$

$$P_a = \rho_{\mathrm{a}} R_a T, \tag{3.22}$$

$$\rho_g = \rho_{\mathrm{a}} + \rho_{\mathrm{v}}, \tag{3.23}$$

$$\phi = \left. \frac{p_v}{P_{vsat}} \right|_T. \tag{3.24}$$

The saturation vapour pressure over liquid water is obtained from ASHRAE (2005).

$$P_{vsat} = exp\left(\frac{C_1}{T} + C_2 + C_3 T + C_4 T^2 + C_5 T^3 + C_6 \ln T \right) \tag{3.25}$$

where, C_1 = -5.6745E+03, C_2 = 1.3915, C_3 = -4.8640E-02, C_4 = 4.1765E-05, C_5 = -1.4452E-08, C_6 = 6.5460.

The material properties of spruce plywood at dry conditions are presented in Table 3.1. It should be noted that the latent heat of sorption is assumed equal to the heat of vapourization in the model. The heat of phase change is assumed constant and does not

change with moisture content. Other material properties used in the numerical model are presented in Appendix B.

Table 3.1. Properties of the dry spruce plywood.

Property	**Value for Dry Spruce Plywood**
Density (ρ_o)	445 [kg/m^3]
Effective thermal conductivity (k_{eff})	0.082 [W/(m·K)]
Effective diffusion coefficient (D_{eff})	4.10 x 10^{-7} [m^2/s]
Porosity (ε_g)	0.7
Specific heat capacity (Cp)	1880 [J/(kg·K)]
Latent heat of vapourization/sorption (h_{fg})	2.5 x 10^6 [J/kg]

3.3 Boundary and Initial Conditions

The boundary conditions for the one-dimensional heat and moisture transfer problem are convection heat and moisture transfer above the spruce plywood and an impermeable and adiabatic boundary condition below the spruce plywood. The boundary conditions for heat transfer are:

$$h_a (T|_{x=0} - T_\infty) = k_{eff} \left. \frac{\partial T}{\partial x} \right|_{x=0}, \tag{3.26}$$

where

$$h_a = \frac{k_a Nu}{D_h} \quad \text{, and} \tag{3.27}$$

$$\left.\frac{\partial T}{\partial x}\right|_{x=L} = 0. \tag{3.28}$$

The boundary conditions for moisture transfer are:

$$h_m\left(\rho_v|_{x=0} - \rho_{v,\infty}\right) = D_{eff}\left.\frac{\partial \rho_v}{\partial x}\right|_{x=0}, \tag{3.29}$$

where

$$h_m = \frac{D_a Sh}{D_h}, \text{ and} \tag{3.30}$$

$$\left.\frac{\partial \rho_v}{\partial x}\right|_{x=L} = 0. \tag{3.31}$$

The Sherwood number (*Sh*) for the different flow conditions is measured from a separate test as described previously and the Nusselt number is set equal to the Sherwood number. The initial conditions are constant temperature and relative humidity throughout the spruce plywood as determined in the experiments. The relative humidity is calculated based on the initial moisture content and the sorption isotherm.

3.4 Numerical Solution

The coupled partial differential equations are discretized using the finite-difference method with second-order accuracy for the spatial nodes and the implicit scheme for the time derivative. For the spatial nodes at the boundary, the backward or forward scheme is used for the discretization, while the central scheme is used for the central nodes. To provide a stable solution, an under-relaxed, Gauss-Seidel iteration method is used and

the solution is considered to have converged, when at any time step, the relative change in any dependent variable (T, ρ_v) is less than 10^{-6} as shown in equation (3.32). The discretized equations and the computer program to solve the equations are presented in Appendix C.

$$\left| \frac{\psi^k - \psi^{k-1}}{\psi_\infty - \psi_i} \right| < 10^{-6}. \tag{3.32}$$

After initializing all variables and properties, the rate of phase change is determined using equation (3.12) and the liquid volume fraction is then calculated from the adsorbed continuity equation (3.9). The vapour density and temperature are then calculated from the vapour and energy transport equations (3.10) and (3.11) respectively. The gas volume fraction is calculated from the volume constraint equation (3.19). Finally, the material properties are calculated using equation (3.13) to (3.19) and thermodynamic properties are calculated using equations (3.20) to (3.25) and the current dependent variables. This process is repeated until the convergence criteria are satisfied. Once the convergence criteria are satisfied, the time step is advanced and the iteration is repeated.

The numerical solution gives values for the dependent variables at discrete points in the solution domain, and this solution should be very close to the continuous solution of the partial differential equations. The choice of the grid size and time step should be such that the solution of the numerical solution is very close to the solution of the partial differential equations and this solution should be independent of the size of the grid and/or the time step. Sensitivity studies are required to determine the appropriate grid size and time step.

Figures 3.2 and 3.3 show the numerical results for the simulated relative humidity and temperature distribution in the spruce plywood for a uniform grid and time step.

(a)

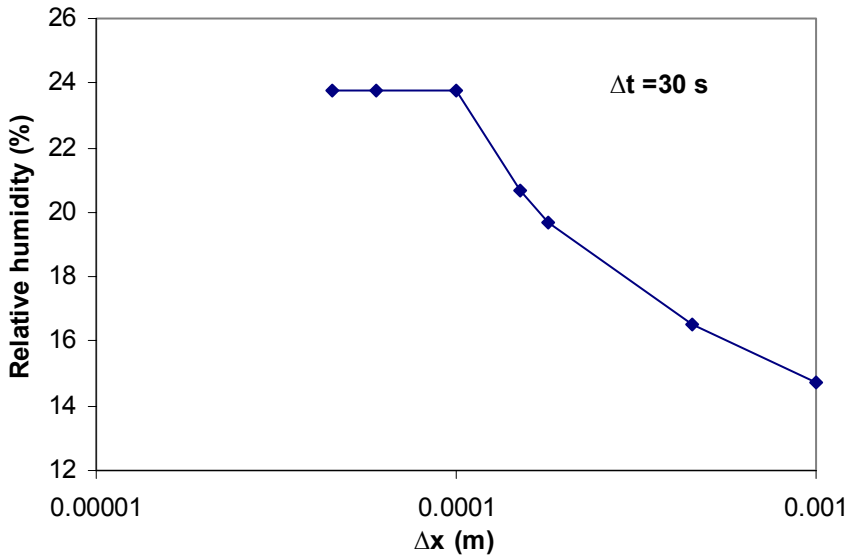

(b)

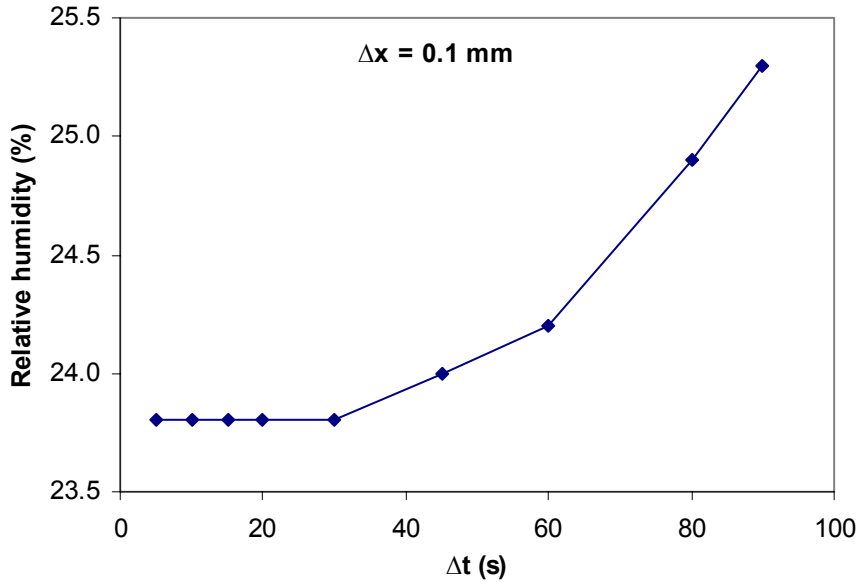

Figure 3.2. Sensitivity graph showing the effect of (a) grid size (Δx) and (b) time step (Δt) on the simulated relative humidity at a depth of x = 9 mm in the spruce plywood.

(a)

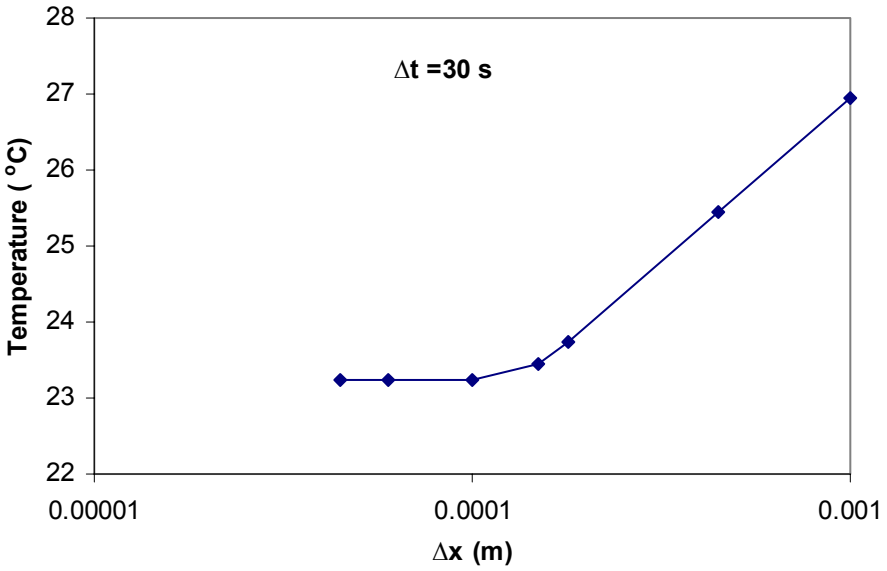

(b)

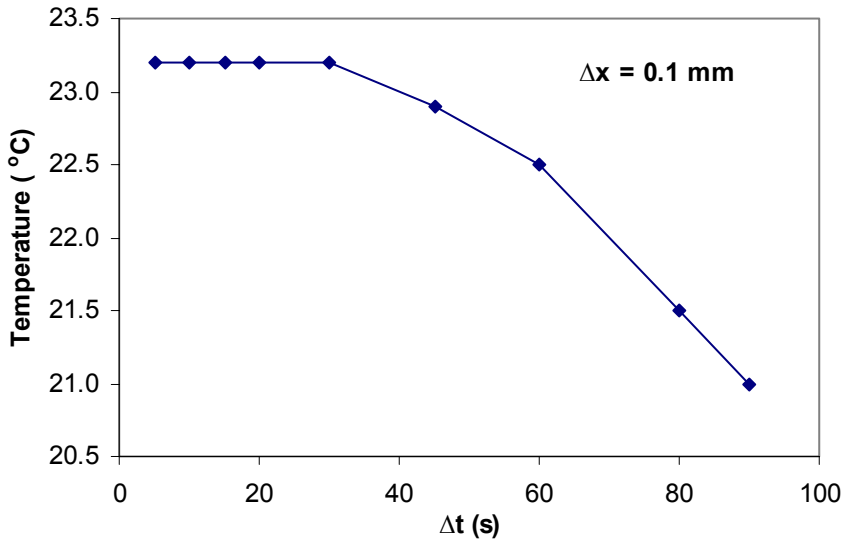

Figure 3.3. Sensitivity graph showing the effect of (a) grid size (Δx) and (b) time step (Δt) on the simulated temperature at a depth of 9 mm in the spruce plywood.

The results presented are for temperature and relative humidity at 9 mm from the top of the plywood and for 8 hours of testing. The initial conditions of the plywood are 22% RH and 23^{o}C and the boundary conditions are 70% RH, 23^{o}C and Re = 2000. The results show that a uniform grid size (Δx) of 0.1 mm and a time step (Δt) of 30 s are appropriate choices. Decreasing the grid size to 0.05 mm and the time step to 10 s changes the temperature and relative humidity by 0.01^{o}C and 0.07% RH respectively, but increases the solution time by over 450%.

Figure 3.5 shows the numerical results for the moisture accumulated per unit surface area of spruce plywood as affected by grid size and time step. The data presented are for the final cycle of three 24-hour cycles with 75% RH for 8 hours and 33% RH for 16 hours, with Re = 2000. Decreasing the grid size from 0.1 mm to 0.05 mm and the time step from 30 s to 10 s changes the moisture buffering capacity by less than 0.1%, but increases the solution time by over 5 times. A uniform grid of 0.1 mm and time step of 30 s will be used for all numerical solutions in this thesis.

(a)

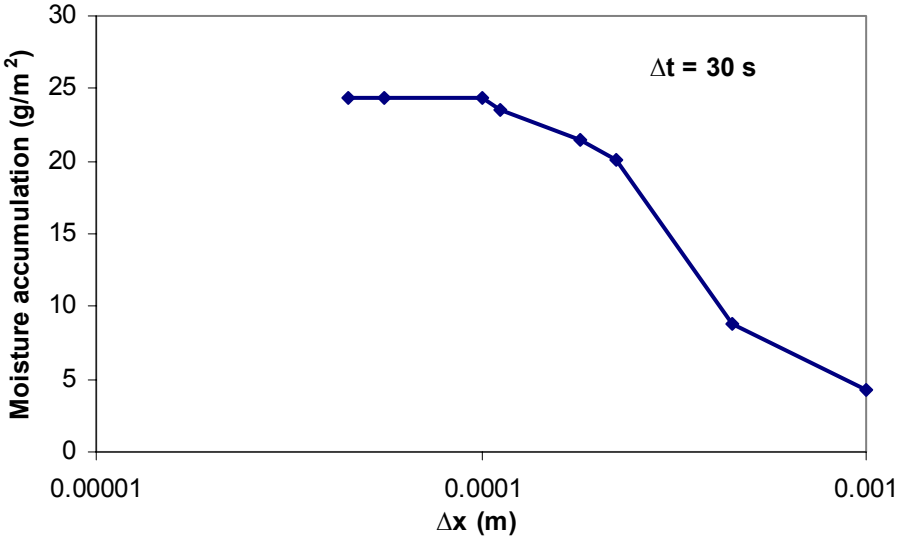

(b)

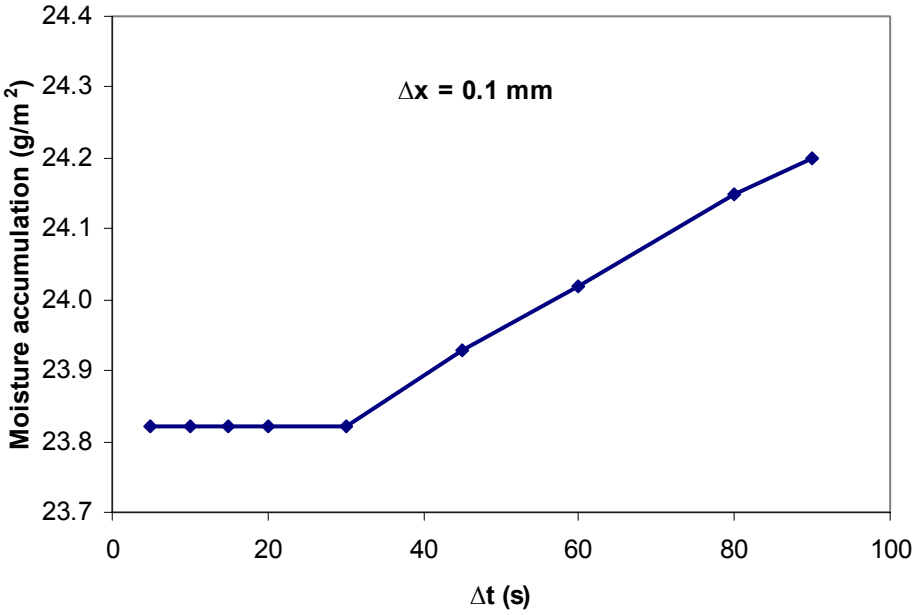

Figure 3.4. Sensitivity graph showing the effect of (a) grid size (Δx) and (b) time step (Δt) on the simulated moisture accumulated per unit surface area of the spruce plywood.

CHAPTER 4

MOISTURE BUFFERING CAPACITY RESULTS

This chapter presents experimental data (moisture accumulation within the spruce plywood) from both test facilities presented in Chapter 2. The moisture accumulation data are used to determine the moisture buffering capacity (MBC) of the spruce plywood and validate the numerical model. To verify the numerical model, experimentally determined boundary and initial conditions are used in the numerical simulation so as to obtain a direct comparison between the experiment and the numerical simulation. However, since the value of the convective transfer coefficient in the glass jar is not known, the numerical model is validated using only the experimental data from the TMT facility. Using the validated numerical model, the effect of thickness, initial and boundary conditions on the MBC of spruce plywood are investigated and presented in this chapter. These results provide guidance when designing an experiment to determine the MBC of a hygroscopic material. Sensitivity studies are also performed on the numerical model to further prove the reliability of the numerical model as well as to examine the sensitivity of the MBC of plywood to changing certain material properties in the numerical simulation.

4.1 Experimental Data and Numerical Validation

In this thesis, two different facilities (the glass jar and the TMT facilities shown in Figures 2.1(a) and 2.3) are used to measure the moisture buffering capacity (MBC) of spruce plywood. Each of these facilities creates different convective transfer coefficients between the humid air and the plywood and thus different boundary conditions. The size of the sample in the test facilities and the effective thickness (L) of the facilities are also different. The initial condition, the effective thickness, and the size of each plywood sample used in both facilities are summarized in Table 4.1. The table also presents the temperature and RH control and convective heat transfer coefficients that can be obtained in both facilities.

Table 4.1. Summary of the conditions and the plywood samples used in both facilities during the experiments.

	Glass Jar Facility	**TMT Facility**		
Size of each piece of plywood	60 mm x 60 mm x 9 mm	600 mm x 280 mm x 9 mm		
Effective thickness (L)	4.5 mm	45 mm		
Initial conditions	55% RH, 23^{o}C	48% RH, 23^{o}C		
Temperature control	23.3 ± 0.3 ^{o}C	22.6 ± 0.2 ^{o}C		
RH control	75.2 ± 0.8% RH (NaCl) 33.3 ± 0.8% RH ($MgCl_2$)	75 ± 2% RH 33 ± 2% RH		
Time for step changes to occur	5 min	20 to 30 min		
Convective heat transfer coefficient (h_a) [W/(m^2·K)]	unknown	Re=1000	Re= 2000	Re= 4000
		2.5 ± 0.2	3.5 ± 0.2	8.1 ± 0.4

It should be noted that for all the MBC data presented in this thesis, the plywood specimen is first placed in 75% RH ambient air for 8 hours after which it is exposed to 33% RH ambient air for 16 hours unless otherwise mentioned. The effect of first exposing the specimen to 33% RH ambient air followed by 75% RH ambient air will be investigated numerically.

4.1.1 Glass Jar Facility

The experimental data from the glass jar tests are presented in Figure 4.1. The figure shows the change in mass of 5 spruce plywood specimen (nominal size of 60 mm x 60 mm x 9 mm) for eight 24-hour cycles. The change in mass since the beginning of the test (ΔM) is calculated as,

$$\Delta M = \frac{m - m_i}{A}, \tag{4.1}$$

where m is the mass of the test specimen measured at a specific time, m_i is the mass of the test specimen when the experiment started (i.e. the initial conditions) and A is the exposed surface area of the plywood. The bias uncertainty in ΔM is ± 0.4 g/m^2, but is not included in Figure 4.1 for clarity.

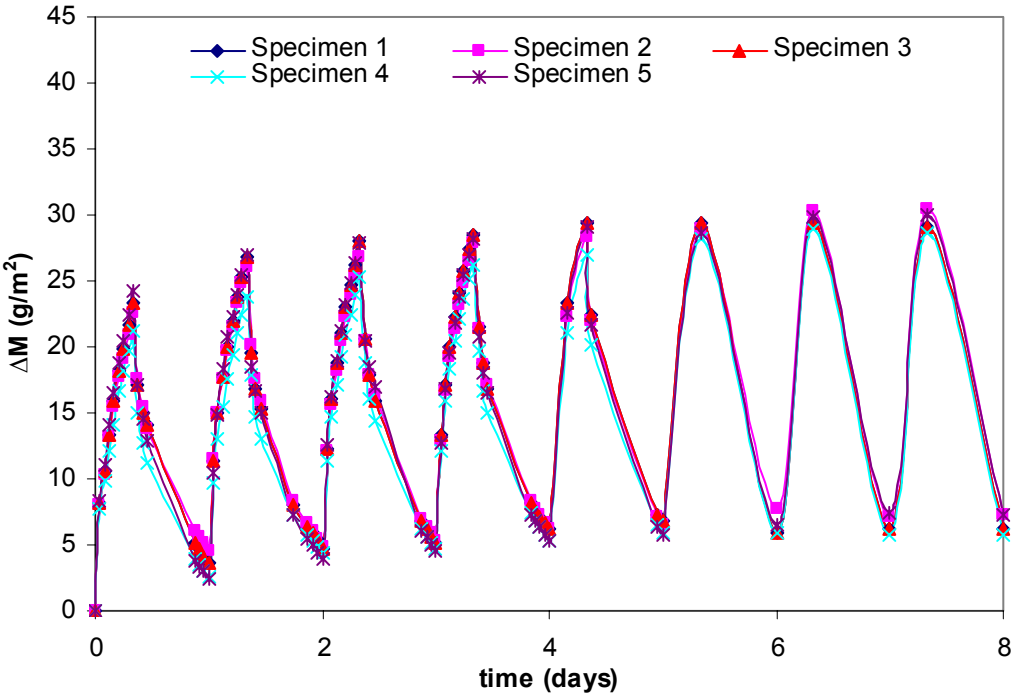

Figure 4.1. Change in mass of spruce plywood over eight 24-hour cycles measured using the glass jar facility for 5 different specimens.

It can be seen that the mass accumulation/loss in the spruce plywood for the five specimens follows a similar pattern of moisture adsorption and desorption. The maximum difference in ΔM for the five specimens is 0.8 g/m^2 with 95% of the data falling within ± 0.55 g/m^2 of the average. These demonstrate the excellent repeatability of the MBC test using the glass jar facility. Since the repeatability is very good, the average of the five measurements will be used for further calculation in this thesis. The total uncertainty (bias and precision) in the average value of ΔM determined using the glass jar facility is ± 0.7 g/m^2.

Figure 4.1 shows that in the first few days of the test, the moisture accumulated during the adsorption phase is slightly greater than the moisture desorbed during the desorption phase. After a few cycles, the plywood reaches a quasi-steady state condition where the moisture accumulation during the adsorption phase equals the moisture removal during the desorption phase. This is due to the initial moisture content of the plywood and will be investigated further in section 4.3.1. To determine when the spruce plywood has reached this quasi-steady state condition, the changes in mass during the adsorption and desorption phases of each cycle are compared. The change in mass for the phase (adsorption or desorption) of a given cycle of the test (Δm) is calculated as,

$$\Delta m = \frac{m_{final} - m_{start}}{A}, \tag{4.2}$$

where m_{final} is the mass of the test specimen measured at the end of an adsorption or desorption phase and m_{start} is the mass of the test specimen when the adsorption or desorption phase started. Quasi-steady state conditions are assumed when the percentage difference between Δm_{ads} and Δm_{des} is less than 0.1%. Mathematically, quasi-steady state exists when:

$$\frac{\Delta m_{ads} - \Delta m_{des}}{\Delta m_{ave}} < 0.1\%, \tag{4.3}$$

where

$$\Delta m_{ave} = \frac{\Delta m_{ads} + \Delta m_{des}}{2}. \tag{4.4}$$

It should be noted that Δm is also important as it will be used later in the calculation of the moisture buffering capacity (section 4.2).

Figure 4.2 presents the average value of Δm_{ads} and Δm_{des} for each cycle of the 5 test specimens conducted with the glass jar facility. It can be seen that the moisture accumulated during 8 absorption phases (Δm_{ads}) is fairly constant with a deviation of $\pm 0.1 g/m^2$. However, Δm_{des} changes significantly over the first 5 cycles, but is quite constant over the last 3 cycles. The fact that Δm_{ads} is consistent with time, but Δm_{des} increases with time is due to the initial conditions of the plywood specimen (55% RH) and the order of placing the plywood specimen in the jars (75% RH first, 33% RH second). The effect of the initial conditions and order of placement on Δm (and MBC) will be presented in later sections. The result presented in Figure 4.2 is consistent with the results of Salonvaara et al. (2004), which also show a similar pattern of fairly constant Δm_{ads} values for the first 4 cycles.

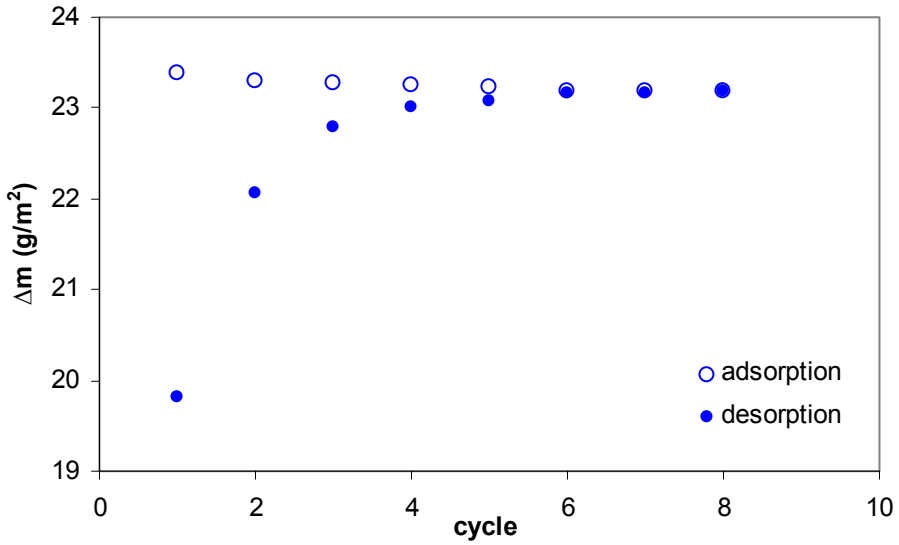

Figure 4.2. Measured change in mass (Δm) of spruce plywood during the adsorption and desorption phases of eight 24-hour cycles using the glass jar facility.

From Figure 4.2, it can also be seen that Δm for the adsorption and desorption phases is not changing significantly over the last few cycles. At the 6th cycle, the percentage difference between Δm_{ads} and Δm_{des} is less than 0.1%. Therefore, the spruce plywood can be considered to have reached quasi-steady state (i.e., when equation (4.3) is realized) at the 6th cycle. The individual values of Δm_{ads} and Δm_{des} are useful in determining when quasi-steady state conditions exist, but the uncertainty in the moisture accumulation/loss data can be reduced if the average of these two values is used. For the glass jar facility, the uncertainty in Δm_{ave} is $\pm$ 0.5 g/m^2 compared to $\pm$ 0.7 g/m^2 for Δm_{ads} and $\Delta m_{des.}$ As a result, Δm_{ave} will be used in future calculations.

Since 6 days is a reasonably long time to test, especially in the TMT facility, it is desirable to reduce the testing time. The testing time can be reduced if the test is stopped when Δm_{ave} is close to the quasi- steady state value (i.e., Δm_{ss}). Δm_{ss} is defined as the mass of moisture accumulation/loss during an adsorption /desorption cycle per exposed surface area when the plywood has reached quasi-steady state (i.e., when equation (4.3) is realized). It is also the value that Δm_{ave} will approach when the same adsorption and desorption cycle is repeated indefinitely. The percentage difference between Δm_{ave} and Δm_{ss}, defined as

$$\Delta m_{diff} = \left(\frac{\Delta m_{ss} - \Delta m_{ave}}{\Delta m_{ss}} \right) 100 , \qquad (4.5)$$

and is plotted for the 8 cycles in Figure 4.3. Figure 4.3 shows that Δm_{diff} is less than 1% after the third cycle. Since 1% is an acceptable difference from quasi-steady state, Δm_{ave} for the third cycle can be used as an estimation of Δm_{ss} for spruce plywood in the glass jar facility.

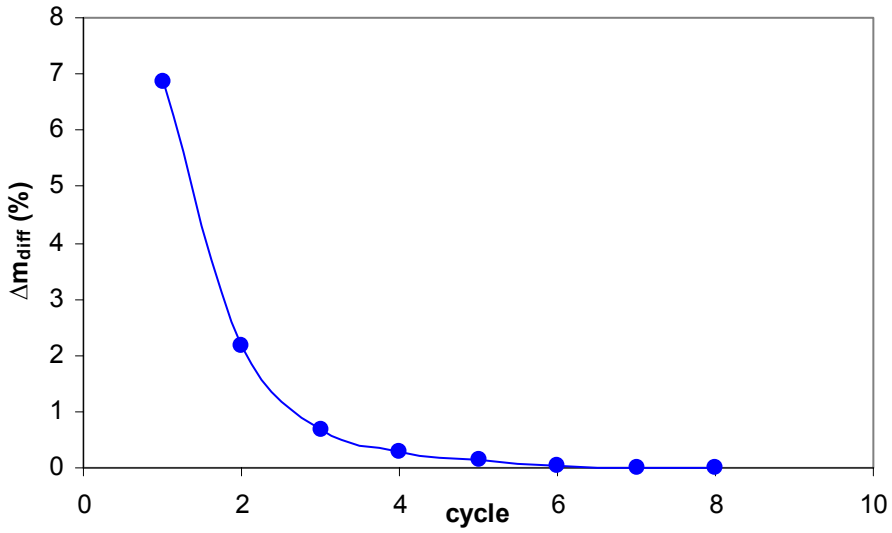

Figure 4.3. Percentage difference between Δm_{ave} for a given cycle and Δm_{ss} for the glass jar facility.

In this thesis, the moisture buffering capacity (MBC) will be defined as the value of Δm_{ave} for the cycle when the difference between Δm_{ave} and Δm_{ss} is less than 1%.

$$MBC = \Delta m_{ave}, \text{ when } \Delta m_{diff} < 1\% \tag{4.6}$$

As noted previously, the MBC can be determined using data from the third cycle, which is a significant reduction in the testing time with only a minor increase in uncertainty. The investigation using the TMT facility, presented in the next section, will take advantage of this finding and the change in mass will only be measured for 3 cycles (3 days).

4.1.2 Transient Moisture Transfer (TMT) Facility

The TMT facility is used to create fully developed air flow over a bed of spruce plywood. The plywood, which is initially conditioned to 48% RH, is first exposed to

75% RH air for 8 hours, followed by 33% RH air for 16 hours. Based on the results observed using the glass jar facility, this humidity cycle is repeated three times.

Figure 4.4 presents the measured and simulated values of ΔM for the three-day test. The total uncertainty in ΔM determined using the TMT facility is ± 1.2 g/m^2, which includes a bias uncertainty of ± 1.1 g/m^2 and an assumed precision uncertainty of ± 0.55 g/m^2 based on the repeatability measurements in Figure 4.1. Figure 4.4 shows the change in mass of spruce plywood using the TMT facility for Re = 1000, 2000 and 4000, which corresponds to convective heat transfer coefficients (h_a) of 2.5, 3.5 and 8.1 W/(m^2·K), respectively and convective mass transfer coefficients (h_m) of 0.0021, 0.0029 and 0.0067 m/s, respectively. It should be noted that the convective heat transfer coefficient is reported in this thesis since it is more familiar.

The agreement between the experimental and simulated values of ΔM is very good for all values of Re. The maximum error is 1.2 g/m^2 and 95% of the data agree within ± 0.9 g/m^2. A careful comparison of Figures 4.4(a), (b) and (c) shows that ΔM is the greatest for Re = 4000 and the smallest for Re = 1000. This effect of Re number is expected because the higher the Re, the higher the convection mass transfer coefficient and thus the higher the mass transfer. Both the experimental and numerical results show this same trend.

(a)

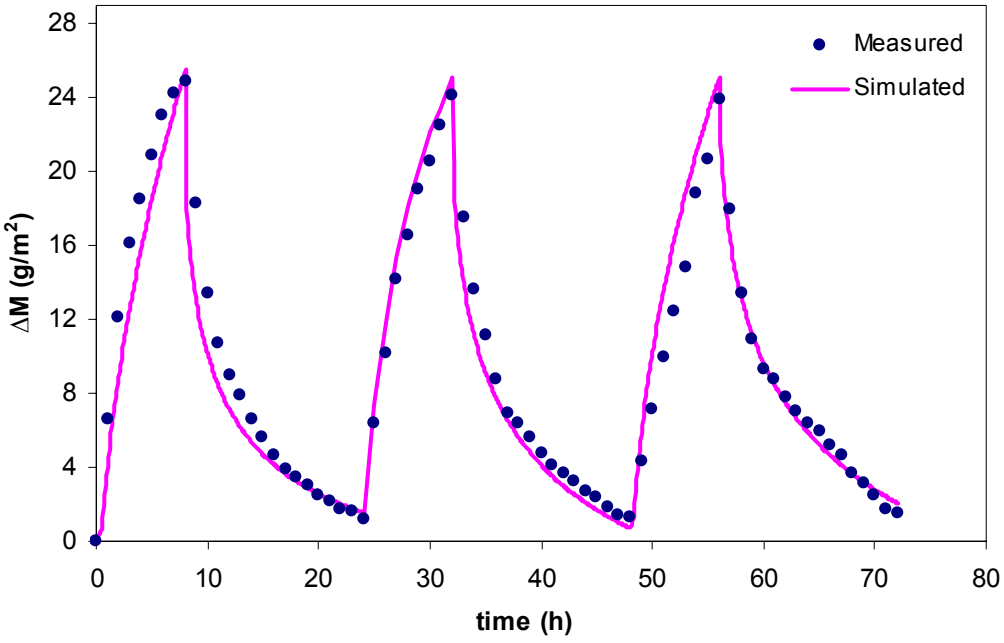
Measured
Simulated
ΔM (g/m²)
time (h)
0
4
8
12
16
20
24
28
0
10
20
30
40
50
60
70
80

(b)

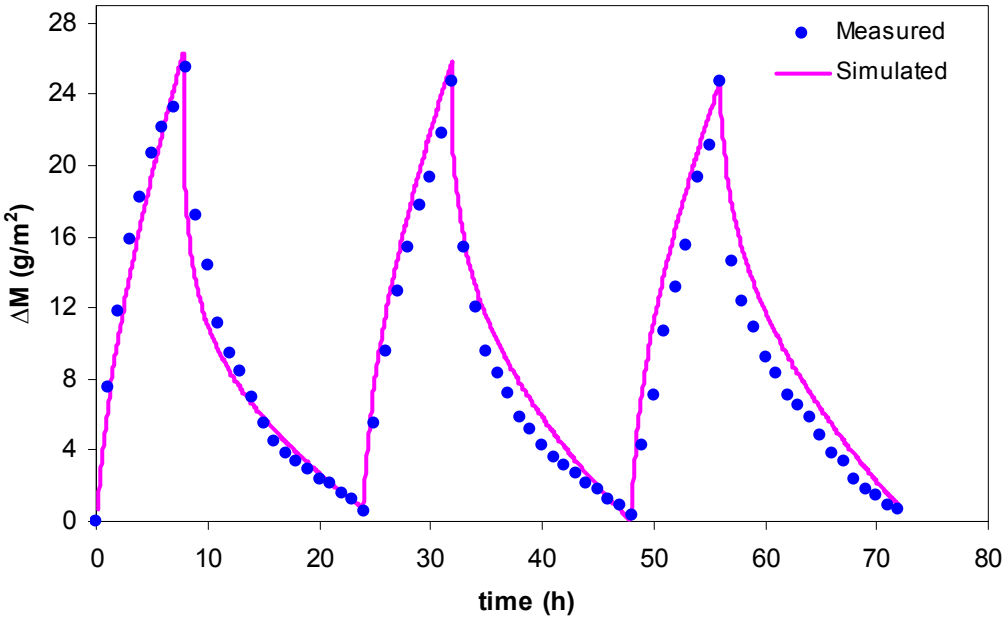
Measured
Simulated
ΔM (g/m²)
time (h)
0
4
8
12
16
20
24
28
0
10
20
30
40
50
60
70
80

(c)

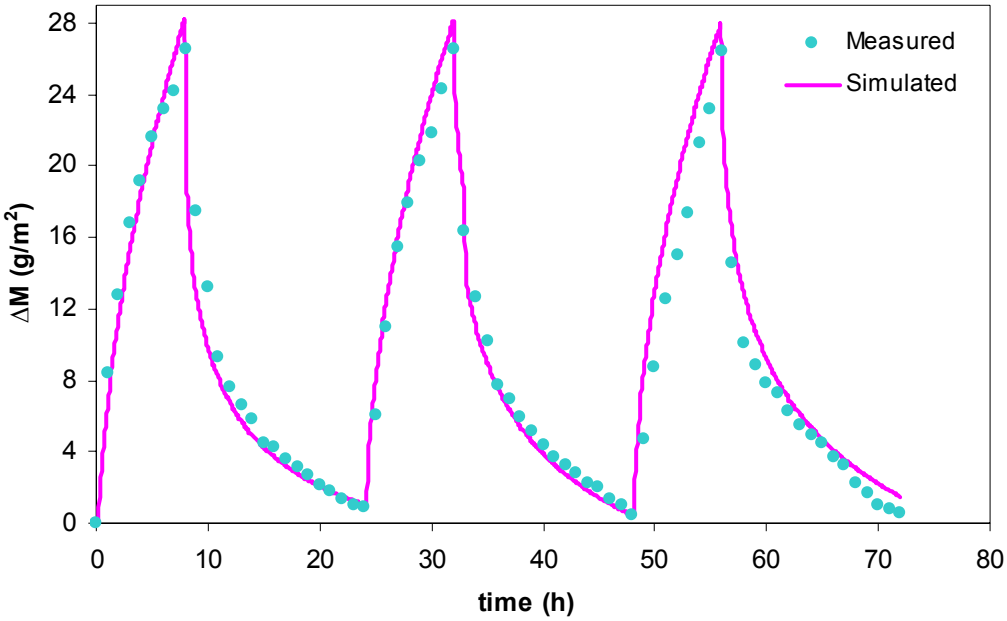

Figure 4.4. Comparison of the numerical and experimental data obtained from the TMT facility showing the change in mass of spruce plywood over three 24-hour cycles for air flow Reynolds number of (a) 1000, (b) 2000 and (c) 4000.

Using equation (4.2), the change in mass during the adsorption and desorption phase (Δm) of each cycle for the TMT facility is examined and the results are presented in Figure 4.5 for Re = 2000. The simulated values of Δm_{ads} and Δm_{des} for the same conditions (L = 45 mm and Re = 2000) as in the TMT facility, are also presented in Figure 4.5. The simulated and measured values of Δm agree very well. It can be seen from the simulated values in Figure 4.5 that Δm_{des} increases over the first 5 cycles, but is quite constant over the last 3 cycles. The figure also shows that both Δm_{ads} and Δm_{des} are not changing significantly over the last few cycles. Using the definition of quasi-steady state defined in equation (4.3) (i.e., the difference between Δm_{ads} and Δm_{des} is less than

0.1%), the simulated results indicate that quasi-steady state is reached on the 6th cycle, which is similar to the time to quasi-steady state in the glass jar facility.

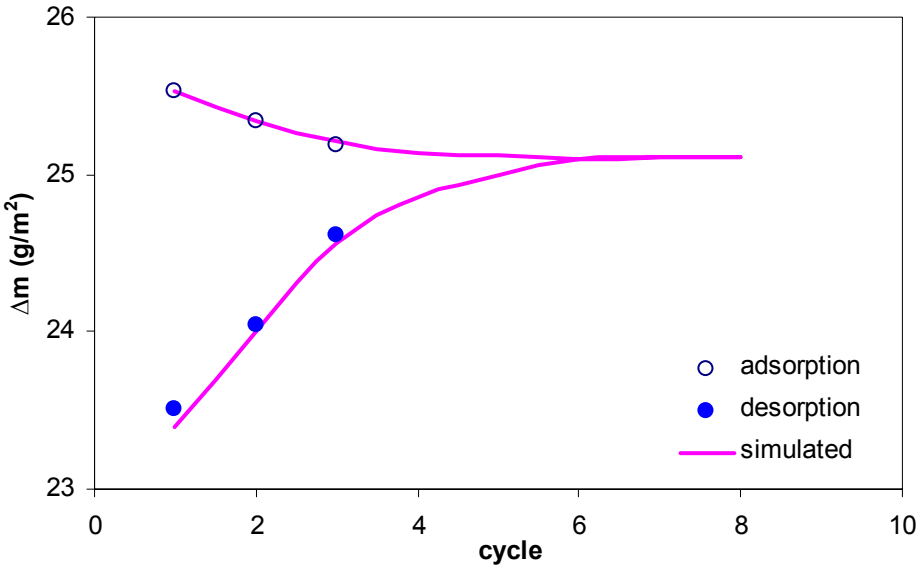

Figure 4.5. Measured change in mass (Δm) of spruce plywood during the adsorption and desorption phases of three 24-hour cycles from the TMT facility compared with simulated values for eight 24-hour cycles.

In order to see which cycle should be used to determine the MBC (see equation (4.6)), Δm_{diff} is presented in Figure 4.6 for the simulated and measured data. The data in Figure 4.6 show that Δm_{diff} is less than 1% on the 3rd cycle, therefore, Δm_{ave} for the third cycle can be used as the MBC for spruce plywood in the TMT facility. This shows that it is adequate to test for 3 cycles in order to determine the moisture buffering capacity of spruce plywood and confirms the choice of testing with 3 cycles in the TMT facility.

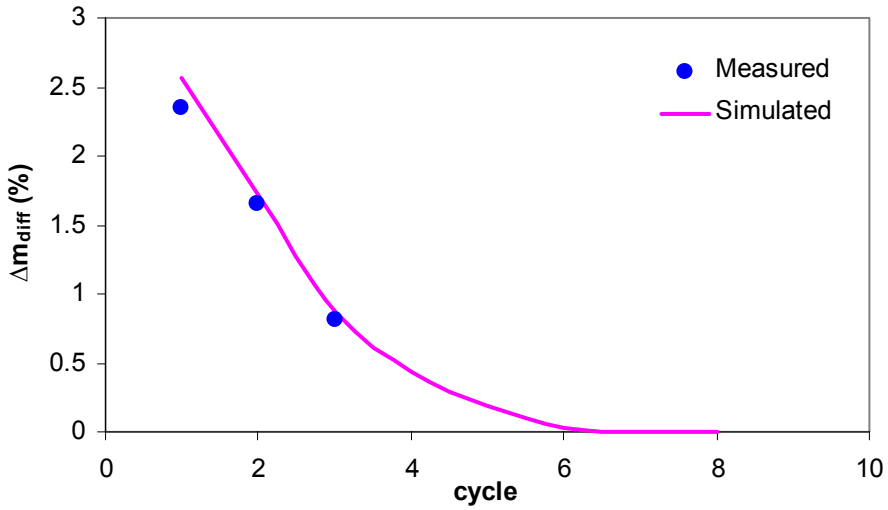

Figure 4.6. Percentage difference between Δm_{ave} for a given cycle and Δm_{ss} for the TMT facility.

4.2 Moisture Buffering Capacity (MBC) Data

The moisture buffering capacity (MBC) is an attempt to present one number to quantify the potential for hygroscopic materials to damp indoor humidity variations. The definition of MBC was defined in the previous section (see equations (4.6) and (4.3) to (4.5)) and this section will provide the measured and simulated MBC values from the data in the previous section.

Using the experimental data from both facilities and the definitions presented previously, the MBC of spruce plywood is calculated from the raw data. Figure 4.7 presents the MBC for different boundary conditions and thicknesses. The effective thickness is ten times greater in the TMT facility (L = 45 mm) than in the glass jar facility (L = 4.5 mm). Figure 4.7 clearly shows that increasing Re increases the MBC. The MBC values obtained from the TMT facility for Re of 1000, 2000, and 4000 are

22.5, 24.9, and 26.2 g/m^2 respectively with an uncertainty of ± 0.8 g/m^2. This uncertainty is lower than the uncertainty in ΔM (± 1.2 g/m^2), because it is based on the average of the adsorption and desorption phase. For the sealed glass jars, the average MBC is 22.3 g/m^2 with an uncertainty of ± 0.5 g/m^2. The largest percentage difference in MBC of spruce plywood for different boundary conditions (i.e. Reynolds numbers for forced convection) and thickness is about 18%. This means that different laboratories may produce MBC results that differ by as much as 20% even when they are testing the same material conditioned to the same initial humidity and reporting the MBC from the same humidity cycle. As will be shown in section 4.4, these differences may increase if the initial conditions are different and the MBC is reported from a different humidity cycle.

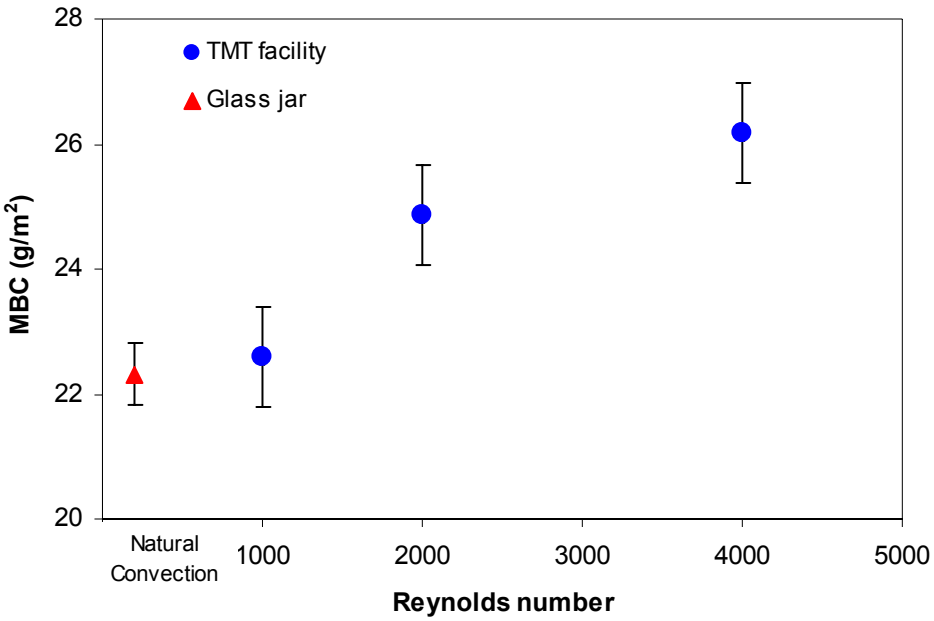

Figure 4.7. MBC of spruce plywood for two different facilities showing the effect of the convection conditions on MBC.

To compare the measured MBC from the two experimental facilities and compare the measured and simulated results, Figure 4.8 plots MBC as a function of the convection heat and mass transfer coefficients for the two tested thicknesses. This figure shows that as the convective transfer coefficients increase, the mass transfer rate and MBC increases.

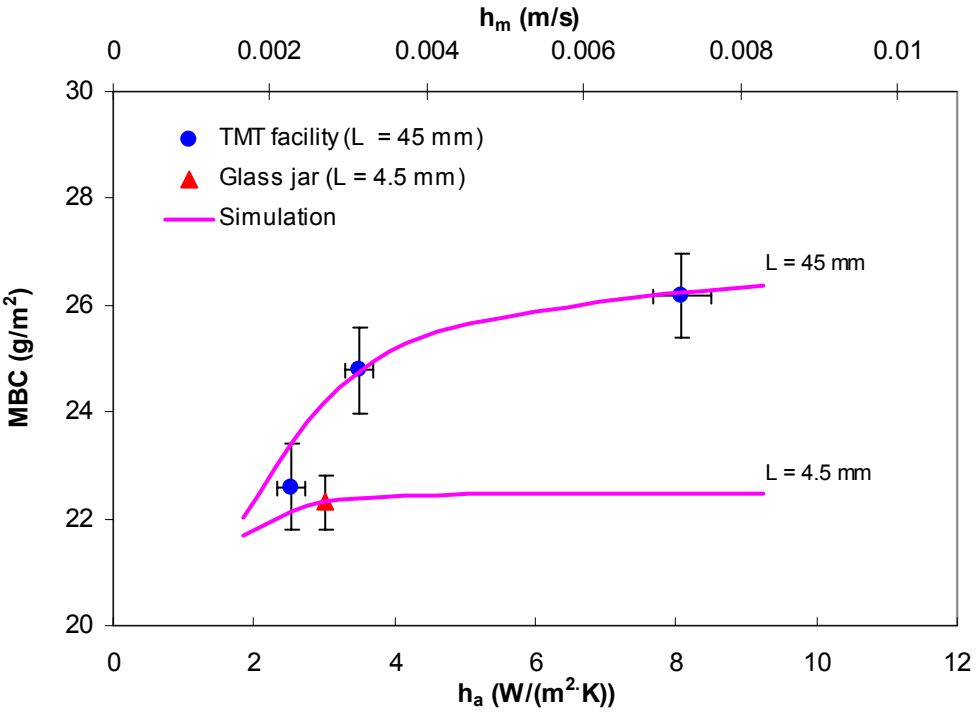

Figure 4.8. Comparison of the numerical and experimental results showing the effect of the convective heat (h_a) and mass (h_m) transfer coefficients and thickness (L) on the moisture buffering capacity (MBC) of spruce plywood. The error bars represent the 95% uncertainty bounds in the measured MBC and h.

This is in agreement with the experimental work of Tremblay et al. (2000), which showed that an increase in air velocity increased the convective transfer coefficients and consequently the moisture transfer between air and wood. Figure 4.8 also shows that as the thickness increases, the MBC increases. The measured results are in close agreement

with the numerical results (within ± 0.5 g/m^2) for the TMT facility. It should be noted that the convective transfer coefficients in the sealed glass jars are not known, however when compared to the MBC obtained using the numerical model, the best estimate for h_a is 3 W/(m^2·K) and h_m is 0.0025 m/s.

4.3 Numerical Investigations

Due to the difficulty or impossibility of carrying out some experimental conditions, a validated numerical model is a powerful tool that can be used to investigate the effect of the initial conditions, boundary conditions and thickness of spruce plywood on the MBC. For example, it is very time consuming to test a wide range of initial conditions and various RH step sizes in this experiment, but the validated numerical model can be used to quickly and accurately investigate different initial conditions and various RH step sizes. Similarly, not all thickness and convection boundary conditions can be investigated with the TMT facility, but the numerical model can be used to investigate these effects.

4.3.1 Effect of Initial Condition on MBC

The initial conditions will have no effect on the moisture absorbed/desorbed into/from the spruce plywood if the test is run for an infinitely long time. However, the initial conditions will affect Δm during the first few cycles and consequently must be considered for shorter tests. To reduce testing time and cost, MBC is defined as the value of Δm_{ave} for the cycle when the difference between Δm_{ave} and Δm_{ss} is less than 1% (i.e. equation (4.6)) and thus it is important to investigate the effect of different initial conditions on the measured MBC. Using the validated numerical model, the initial

relative humidity of the spruce plywood is varied (while keeping the temperature constant) to investigate the effect of initial conditions on the MBC of spruce plywood. For this simulation, the convective heat transfer coefficient employed is 3.5 W/(m^2·K) (Re = 2000) and the thickness of the plywood is 9 mm. Three different initial relative humidities (ϕ_i = 33%, 55% and 75% RH) are investigated under isothermal conditions (T = 23^{o}C) and the results are shown in Figure 4.9.

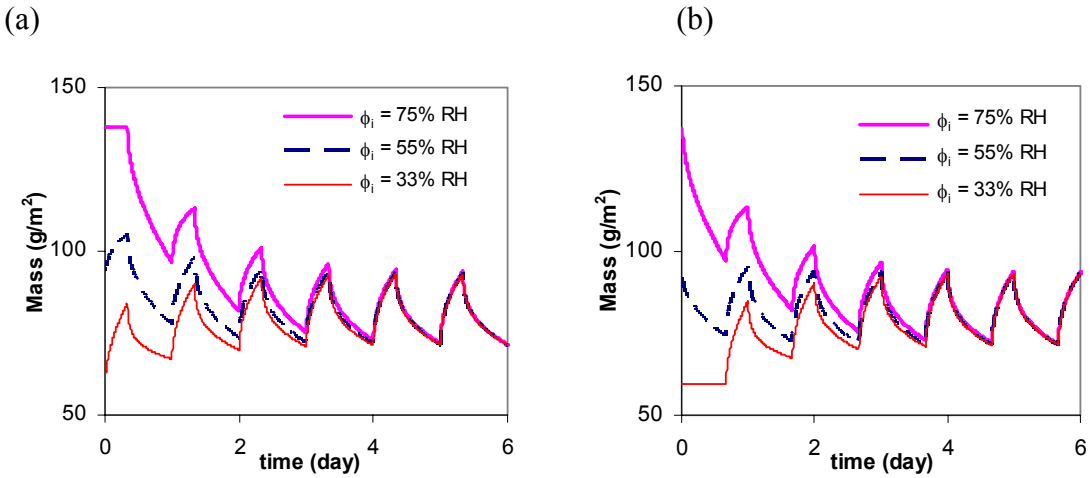

Figure 4.9. Numerical results showing the effect of initial conditions (ϕ_i) on the moisture buffering capacity of spruce plywood, when the first phase is (a) adsorption (ϕ_1 = 75% RH) and (b) desorption (ϕ_1 = 33% RH).

Figure 4.9 shows that the change in mass over the first 3 days depends on the initial conditions of the plywood and the humidity of the ambient air that the plywood is first exposed to. Figure 4.9(a) is for the case when the plywood is first placed in 75% RH ambient air (i.e., ϕ_1 = 75% RH) for 8 hours, while Figure 4.9(b) is for the case where the plywood is first placed in 33% RH ambient air (i.e., ϕ_1 = 33%) for 16 hours. In Figure 4.9, the effect of the initial conditions of the spruce plywood and the initial ambient humidity that it is exposed to appear to become negligible after three cycles. The time to

reach quasi-steady state for a given initial condition will depend on the rate of diffusion of water vapour into the material, the moisture storage capacity of the material as well as the period (24 hours in this case) and the magnitude of the step change in ambient air RH (42% RH in this case).

To clearly show when the sample has neared quasi-steady state (or when the MBC can be determined accurately), Figure 4.10 presents the percentage difference (Δm_{diff}) between the average moisture accumulated/loss (Δm_{ave}) for each cycle and the average moisture accumulated/loss at steady state (Δm_{ss}) for different initial conditions. As in Figure 4.9, the results in Figure 4.10 are presented for different initial conditions and different ambient humidities that the plywood is first placed in.

(a) (b)

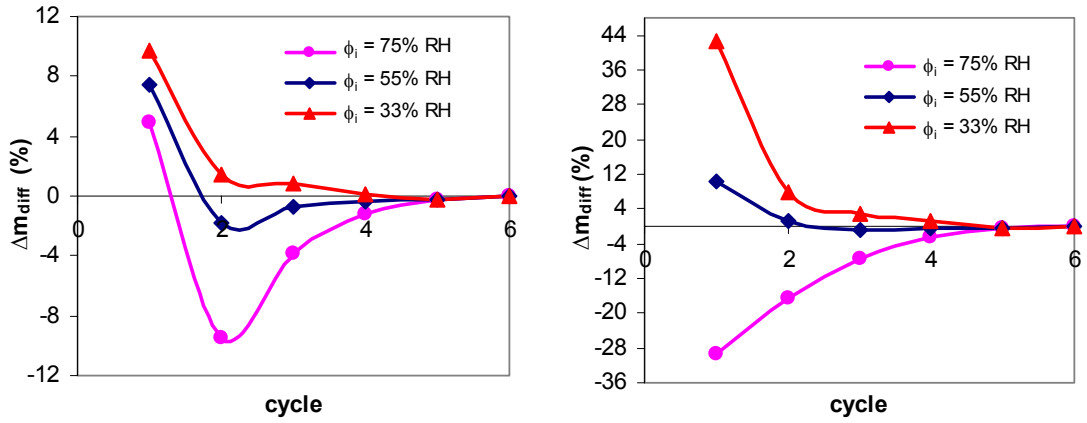

Figure 4.10. Percentage difference between Δm_{ave} for a given cycle and Δm_{ss} for six 24-hour cycles for the case when the first phase is (a) adsorption (ϕ_1 = 75% RH) and (b) desorption (ϕ_1 = 33% RH).

Figure 4.10 shows that Δm_{diff} is always the smallest when ϕ_i = 55% RH (i.e., mean the average of the two ambient humidity values). Therefore it is recommended that the specimen be conditioned to equilibrium with the average RH prior to testing.

With ϕ_i = 55% RH, the number of cycles to reduce $|\Delta m_{diff}|$ below 1% is 3 for both ϕ_1 = 75% RH and ϕ_1 = 33% RH, which confirms the choice of 3 cycles in the experiments presented previously where $\phi_i \approx$ 55% RH and ϕ_1 = 75% RH. The number of cycles required to reduce $|\Delta m_{diff}|$ below 1% is different for different values of ϕ_i and ϕ_1 (Table 4.2). This shows that care should be taken when selecting ϕ_i and ϕ_1 for a moisture buffering capacity test. If the values for the third cycle were arbitrarily used to determine the MBC, the MBC reported could be as much as 8% different than the quasi-steady state value of MBC (case of ϕ_i = 75% RH and ϕ_1 = 75% RH in Figure 4.10(a)).

Table 4.2. Number of cycles that need to be completed before the MBC value will be within 1% of the quasi-steady state value for different values of ϕ_i and ϕ_1.

ϕ_i	ϕ_1 = **75% RH**	ϕ_1 = **33% RH**
33% RH	3	5
55% RH	3	3
75% RH	5	5

As expected, Figures 4.9 and 4.10 show that the moisture accumulation/loss of the plywood reaches a steady state value after a certain number of cycles irrespective of the ϕ_i and ϕ_1. However, the rate of mass transfer in the plywood (which affects the time

required for steady state) has been shown in Figure 4.8 to be dependent on the convective transfer coefficients (h_a and h_m) and the plywood effective thickness (L). Therefore, the time (number of cycles) required for the spruce plywood to reach quasi-steady state as defined in equation (4.3) is expected to depend on h_a, h_m and L. To investigate this effect, the number of cycles required to reach quasi-steady state is calculated using the numerical model for effective thicknesses (L) of 4.5 mm, 9 mm, 18 mm, 27 mm, 36 mm and 45 mm (Figure 4.11). Since the results in Figure 4.11 are for discrete points, the number of cycles must be interpolated between these points. When this interpolation is uncertain (i.e., the exact thickness at which the number of cycles changes is not known), dashed lines are used in Figure 4.11. Figure 4.11 shows that as h_a increases, the number of cycles required for the plywood to reach quasi-steady state is decreased. As h_a increases, h_m and consequently, the rate of mass transfer increases and thus the plywood reaches quasi-steady state faster. It also shows that for a particular transfer coefficient, an increase in the material thickness increases the number of cycles required to reach quasi-steady state.

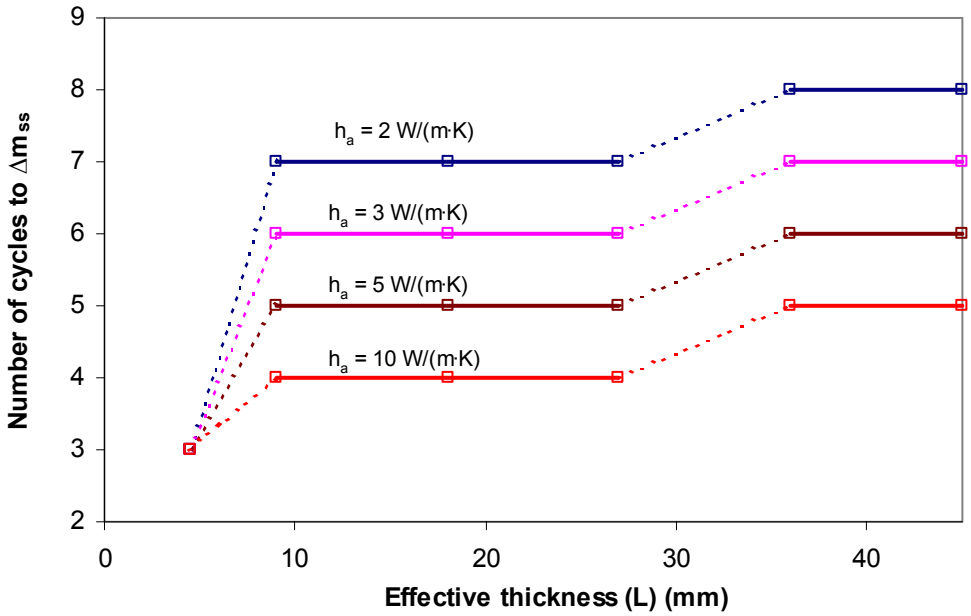

Figure 4.11. Numerical results showing the effect of the convective transfer coefficient and thickness on the number of cycles required for the spruce plywood to reach steady state.

Similar results are shown in Table 4.3, which presents the number of cycles required to reduce the difference between the MBC determined from a given cycle and the quasi-steady state MBC to less than 1%. Table 4.3 shows that for most of the conditions (convective transfer coefficient and thickness) investigated, testing for 3 cycles is sufficient to determine accurately (within 1%) the MBC of spruce plywood.

Table 4.3. Number of cycles that need to be completed before the MBC value will be within 1% of the quasi-steady state value for different values of h_a and L.

	Effective thickness (L) (mm)					
h_a (W/(m^2·K))	**4.5**	**9**	**18**	**27**	**36**	**45**
2	2	3	4	4	4	4
3	2	3	3	3	4	4
5	2	3	3	3	3	3
10	2	2	2	3	3	3

The results presented in Figure 4.11 and Table 4.3 can be used as a guide in designing an experiment since they help to determine the number of cycles to reach steady state and the number of cycles required to ensure Δm_{diff} is less than 1% respectively.

4.3.2 Effect of Boundary Conditions and Thickness on MBC

When measuring the MBC of hygroscopic materials, different facilities will create different convection transfer coefficients between the material and the ambient air. Also, different facilities may require different thicknesses for accurate testing. The purpose of this section is to (i) determine if these differences will have a large effect on the measured MBC, (ii) provide a method to compare results from different laboratories and (iii) allow measured experimental results to be extrapolated to actual applications.

Figure 4.12 shows that the MBC of spruce plywood is strongly influenced by the tested thickness (L) and the convection heat transfer coefficient (h_a). Increasing L and h_a, increases the MBC of spruce plywood. Therefore, care should be taken when comparing MBC values of spruce plywood from different facilities that create different boundary conditions and use different material thicknesses. For example, if one laboratory tested a 18 mm thick specimen using a facility providing h_a = 10 W/(m^2 ·K), the MBC would be 16% higher than that measured by another laboratory using the same thickness and h_a = 2 W/(m^2 ·K). In practice, the results of MBC experiments would be easier to compare between institutes, if the air flow was fully developed, well controlled and constant. If the air flow rate is high, the convection coefficient will be high and the results will approach the plain MBC of the material. Nevertheless, figures such as Figure 4.12 can be used to compare the results from different laboratories testing with different transfer coefficients and thicknesses.

The MBC for practical applications should consider the convection coefficients and thickness in practice and graphs such as the one in Figure 4.12 can be used as a "performance graph" to estimate the MBC in application with different values of h_a and L. When the MBC is measured at a specific thickness and convection coefficient, this result can be extrapolated to other test conditions and applications using Figure 4.12 (e.g., h_a in a building may vary between 5 and 10 W/(m^2 ·K). In this way, a designer can determine the MBC of a material for their application thickness and convection coefficient.

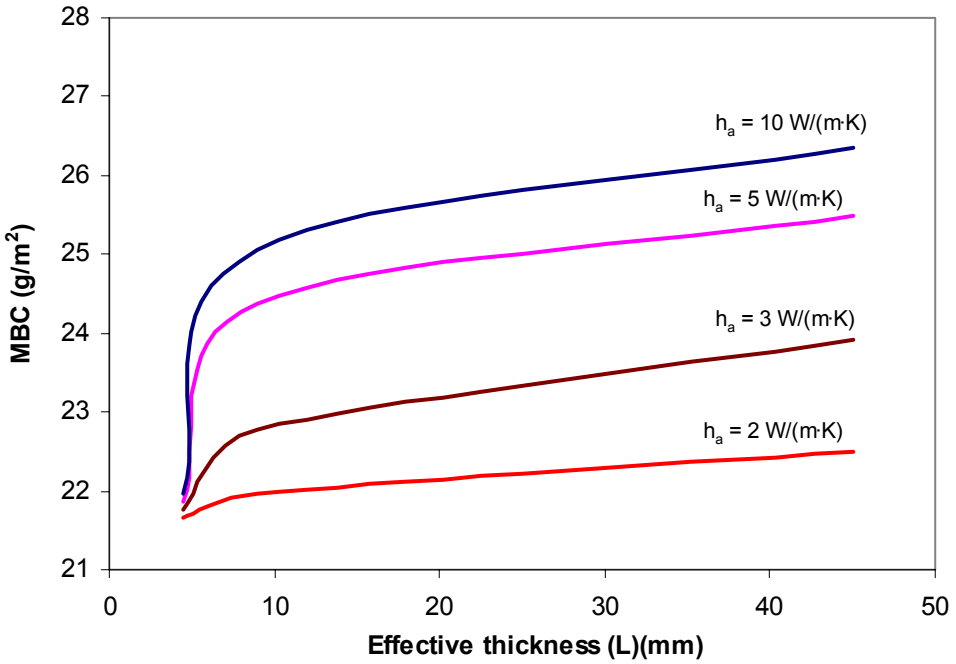

Figure 4.12. Numerical results showing the effect of the convective heat transfer coefficient (h_a) and thickness (L) on the moisture buffering capacity of spruce plywood.

4.3.3 Effect of RH Step Size on MBV

It is expected that testing with different ambient air humidities will give different MBC results. One method of reducing the impact of the selected humidity cycle is to normalize the amount of moisture uptake or release with the size of the relative humidity change (Rode et al., 2005). The resulting parameter is termed the moisture buffer value (MBV) and has units of g/(m^2·% RH). MBV can be related to MBC as,

$$MBV = \frac{MBC}{(\Delta RH)100} \quad . \tag{4.7}$$

where ΔRH is the daily RH variation. In the previous results, the daily RH variation (75% and 33%) is constant and therefore, the MBV can be determined by dividing the

MBC by 42. The purpose of this section is to investigate the effect of the RH step size on MBV.

Using the validated numerical model, the RH step size (ΔRH) is varied while the average of the high and low humidities (RH_{mean}) is kept constant. For these simulations, h_a = 3.5 W/(m^2·K) (Re = 2000) and L = 9 mm. The MBV for eight different ΔRH values (10% to 80%) with RH_{mean} = 50% are shown in Figure 4.13. The data point at ΔRH = 10 corresponds to a moderate humidity cycle of 55% RH for 8 hours and 45% RH for 16 hours. Similarly, ΔRH = 80 corresponds to an extreme humidity cycle of 90% RH for 8 hours and 10% RH for 16 hours.

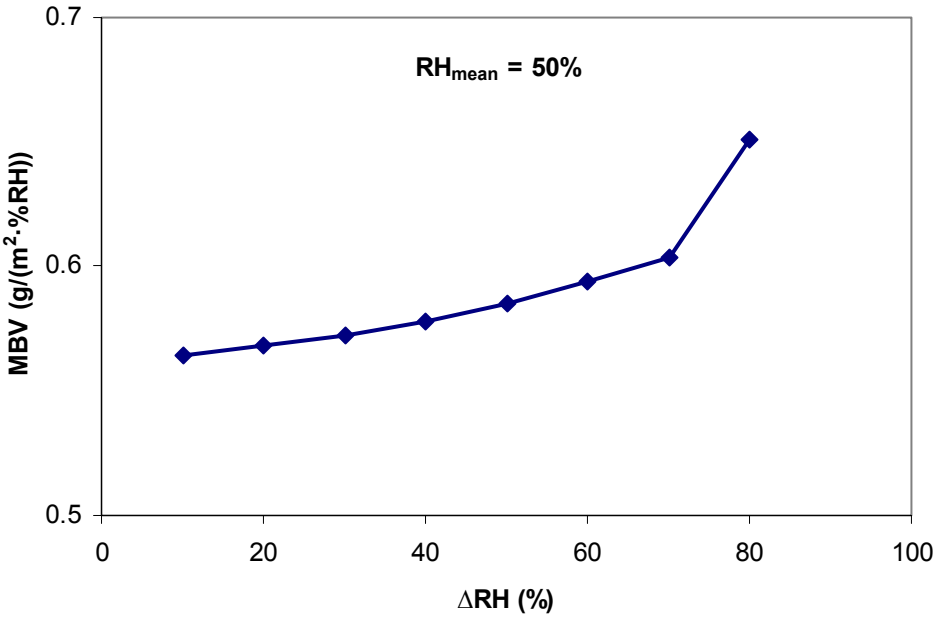

Figure 4.13. Numerical results of the moisture buffering value (MBV) of spruce plywood showing the effect of different values of ΔRH (for RH_{mean} = 50% RH).

Figure 4.13 shows that the MBV increases gradually as ΔRH increases from 10% to 80% RH. The greatest difference between the MBVs in Figure 4.13 is 15%. The small change in MBV is due to the fact that the slope of the sorption isotherm for spruce plywood, which indicates that the moisture capacity of the material, is nearly constant for RH_{mean} = 50% and different values of ΔRH. However, if RH_{mean} is changed, the MBV will also change as shown in Figure 4.14. For a particular ΔRH, the MBV increases as much as 19% as RH_{mean} increases from 30% to 70% RH.

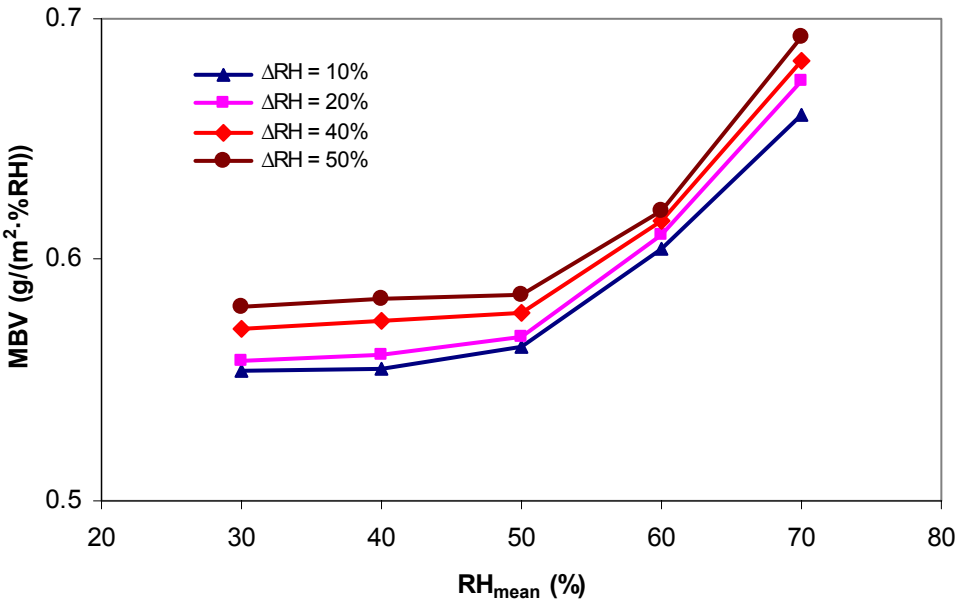

Figure 4.14. Numerical results of the moisture buffering value (MBV) of 9mm spruce plywood showing the effect of different values of ΔRH and RH_{mean}.

4.4 Comparison of Test Results with Results from Other Institutions

The moisture buffering value (MBV) of spruce plywood measured at four different institutions (University of Saskatchewan (U of S), Technical Research Centre of Finland, Finland (VTT), Technical University of Denmark (DTU), and Norwegian Building Research Institute (NBI)) using five different test facilities are compared and

presented in Figure 4.15. It can be seen that the MBV measured at VTT is the lowest, while the NBI facility gives the highest MBV. The largest percentage difference in the MBV determined from the different institutions is as much as 17% different. This difference in the MBVs can be attributed to the use of different experimental facilities, which provide different convective transfer coefficients and thus different mass transfer rates. As noted in Section 4.2, different laboratories with different facilities may produce MBC results that differ as much as 18% for the same initial conditions and humidity cycle. The results presented in Figure 4.15 further confirm the need for a standard test method.

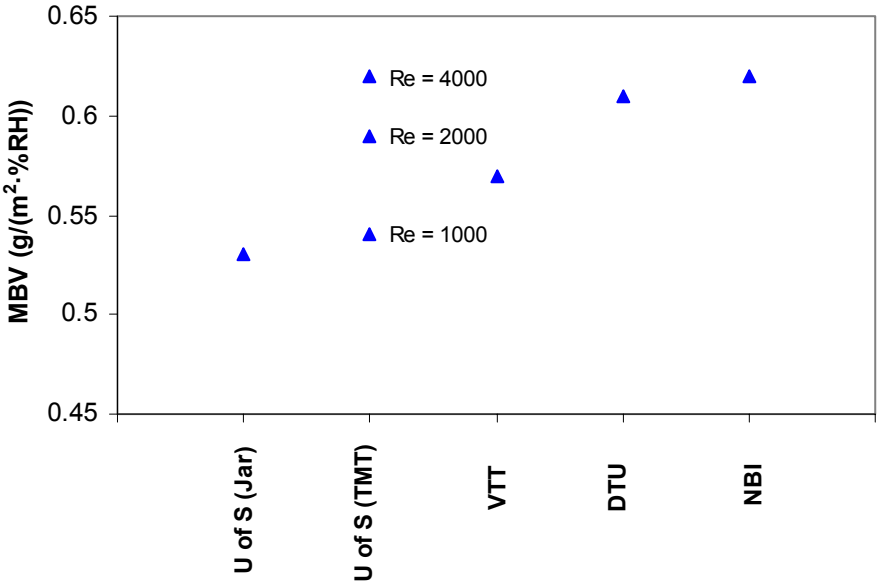

Figure 4.15. Measured results of the moisture buffering value (MBV) of spruce plywood determined by different institutions using different test facilities.

4.5 Sensitivity Studies

Sensitivity studies help to quantify how the numerical results are influenced by the uncertainties in material properties and also show which properties have the most important impact on the results. The sensitivity of the MBC to ± 10% changes in the

sorption isotherm, effective vapour diffusion coefficient, effective thermal conductivity, heat of sorption, density and specific heat capacity are presented in this section. The sensitivity studies are for a typical MBC test conditions of three 24-hour cycles: 75% RH for 8 hours and 33% RH for 16 hours. The results of the sensitivity studies are for L = 9 mm, h_a = 3.5 W/($m^2 \cdot K$), ϕ_i = 55% RH and T_i = 23°C.

4.5.1 Sorption Isotherm

The sorption isotherm used in the numerical simulation is a curve fit of the experimental data and the equation for this curve fit is given in equation (2.6). All the experimental data points fall within ± 10% of the curve fit as shown in Figure 2.15. The effect of changing the sorption curve (i.e., moisture content (u)) by 10% on the simulated moisture content of the spruce plywood (ΔM) is shown in Figure 4.16.

The data in Figure 4.16 show that changing the sorption isotherm by 10% has a noticeable effect on the moisture content (ΔM) variation with time. Since the difference between the numerical and experimental data, presented previously in Figure 4.4, is much smaller than the difference between the different curves in Figure 4.16, these results help confirm the sorption isotherm used in the model. Neglecting hysteresis between the adsorption and desorption isotherm is an adequate assumption for spruce plywood. The results in Figure 4.16 also help confirm the validity of the numerical model because the numerical data correctly show that increasing the sorption curve (which increases the moisture capacity of the material), increases the moisture accumulated/loss as expected.

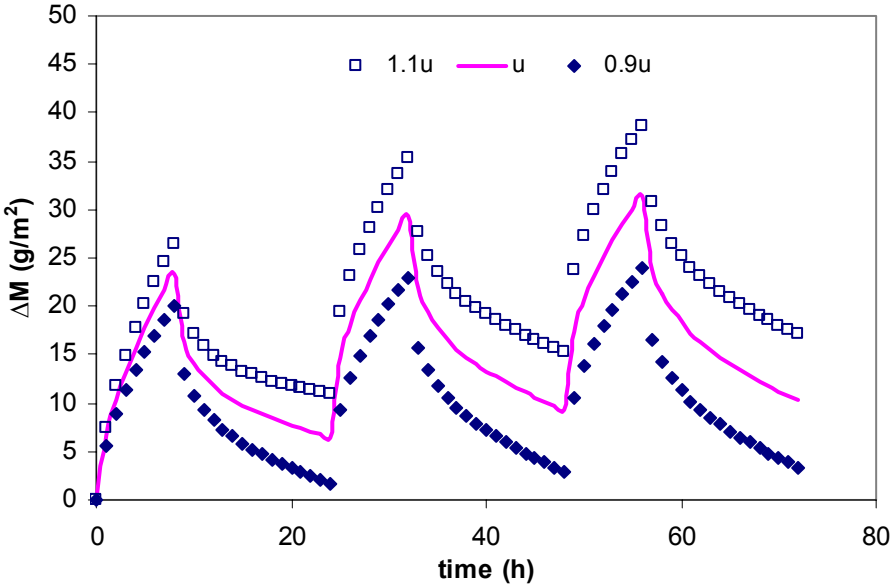

Figure 4.16. Sensitivity study showing the effect of changing the moisture content (u) calculated by the adsorption isotherm (equation (2.6) and Figure 2.15) by ± 10% on the simulated moisture content for a typical MBC test.

4.5.2 Effective Vapour Diffusion Coefficient

The effective vapour diffusion coefficient (D_{eff}) used in the model is given by equation (3.15) and is based on the water vapour permeability data in Chapter 2 (equation (2.12) and Figure 2.21). Figure 4.17 shows that effect of changing D_{eff} by ± 10% on the simulated moisture content of the spruce plywood. These results help validate the numerical model because increasing D_{eff} increases the moisture accumulation during adsorption and the moisture loss during desorption as expected. Comparing Figures 4.16 and 4.17 shows that the moisture content is much more sensitive to changes in the sorption isotherm than to changes in $D_{eff.}$

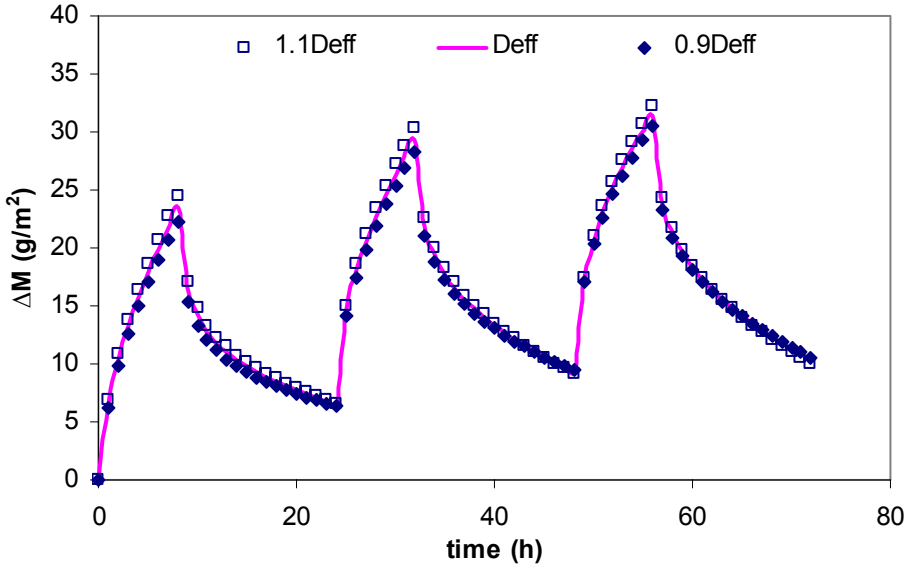

Figure 4.17. Sensitivity study showing the effect of changing D_{eff} by ± 10% on the simulated moisture content for a typical MBC test.

4.5.3 All Sensitivity Properties

To directly compare the sensitivity of different properties, Table 4.4 presents the MBC calculated by the model for ± 10% change in the most important properties in the model. Table 4.4 shows that the simulated MBC of spruce plywood is most sensitive to the change in moisture content (u) calculated by the sorption isotherm and moderately sensitive to the effective vapour diffusion coefficient (D_{eff}). The simulated MBC of spruce plywood changes by ± 7% and ± 3% for ± 10% changes in u and D_{eff} respectively, while ± 0.5% changes in MBC are noticed with ± 10% changes in k_{eff} and $h_{ad.}$ Changing ρ_o and Cp by ± 10% results in a negligible change in the MBC.

Table 4.4. Summary of the sensitivity studies on the MBC calculated using the model.

Property	S = 0.9		S = 1.0	S = 1.1	
	MBC (g/m^2)	% diff	MBC(g/m^2)	MBC (g/m^2)	% diff
Sorption isotherm (u)	20.1	- 7	21.6 g/m^2	23.1	+ 7
Effective vapour diffusion coefficient (D_{eff})	21.0	- 3	21.6 g/m^2	22.2	+ 3
Effective thermal conductivity (k_{eff})	21.5	- 0.5	21.6 g/m^2	21.7	+ 0.5
Heat of sorption (h_{ad})	21.7	+ 0.5	21.6 g/m^2	21.5	- 0.5
Dry density (ρ_o)	21.6	0	21.6 g/m^2	21.6	0
Specific capacity (Cp)	21.6	0	21.6 g/m^2	21.6	0

4.6 Summary

The moisture buffering capacity (MBC) determined from the different facilities vary by as much as 18% different because the thickness of plywood tested and the convection transfer coefficients between the plywood and the humid air are not the same in each test facility. The experimental results are in close agreement with results from the numerical model. The difference between the MBC calculated from the experimental and numerical data is less than the experimental uncertainty and typically less than ± 2%.

The numerical and experimental data are applied to show how the moisture buffering capacity of spruce plywood depends on thickness and the convection transfer

coefficients. As expected, the moisture buffering capacity increases as the thickness and convection coefficients increase. The numerical and experimental data are also used to determine the number of humidity cycles that are required for plywood to reach quasi-steady state where the moisture accumulation/change does not change with further cycles. These results are useful in experimental design and show that the number of cycles required in experimental testing depends on the initial conditions, boundary conditions and the effective thickness. The MBC can be determined with fewer repeated cycles when the plywood is initially in equilibrium with the average of the high and low RH. If the test duration is not increased for other initial conditions, errors as large as 8% may result.

Sensitivity studies are carried out to further verify the numerical model and the material properties used. The results from the sensitivity studies confirm the validity of the numerical results and the property data used in the model. These studies also show that the MBC is significantly affected by changes in the sorption isotherm and moderately affected by changes in the effective vapour diffusion coefficient, while the other properties have a negligible effect on MBC.

CHAPTER 5

THERMAL AND VAPOUR BOUNDARY LAYER RESULTS

In this chapter, the measured and simulated relative humidity, temperature and moisture accumulation within a bed of spruce plywood are presented to further quantify the transient heat and moisture transfer in spruce plywood and verify the numerical model. The experimental and numerical data are also used to verify the moisture diffusivity property developed by Olutimayin and Simonson (2005).

The experimental data in this chapter are measured using the TMT facility with three pieces of plywood in the test section (Figure 2.7). Most of the tests are conducted for two days following a single step increase in the humidity of the air flowing above the plywood. One multi-step test consisting of a series of six step changes in humidity over a 12-day period is conducted. The single, step-change tests investigate the effect of the size of the humidity step and the air flow rate (Re) on the transient temperature and humidity fields within the bed of plywood. All tests are for isothermal test conditions, where the initial temperature of the plywood and the temperature of the air passing over the plywood are the same (or nearly the same).

5.1 Tests with Different Humidity Changes

Two tests are performed with a single-step change increase in humidity. In one test, the plywood is initially conditioned to equilibrium with air at 22% RH (ϕ_i = 22% RH) and the humidity of the air passing over the top of the spruce plywood is 70% RH (ϕ_∞ = 70% RH), giving a nominal humidity change of 50% RH (ΔRH = 50%). The other test has ϕ_i = 50% RH, ϕ_∞ = 85% RH and ΔRH = 35%. Both tests are for laminar air flow above the spruce plywood (Re = 2000). The test conditions are summarized in Table 5.1.

Table 5.1. Summary of the test conditions for the tests with different humidity changes.

Test	Initial condition	Condition of air flow	Test duration
ΔRH = 50%	ϕ_i = 22% RH T_i = 23°C	ϕ_∞ = 70% RH T_∞ = 23.2°C Re = 2000	2 days single step
ΔRH = 35%	ϕ_i = 50% RH T_i = 23°C	ϕ_∞ = 85% RH T_∞ = 23.1°C Re = 2000	2 days single step

5.1.1 50% RH Change

Figure 5.1 shows the measured and simulated relative humidity in the plywood at depths of 9 mm and 18 mm in the plywood bed. The results presented for the 9-mm depth are the averages of the five sets of data from the five sensors at that depth. It can be seen that it takes about 20 hours for the humidity sensor at a depth of 18 mm to begin to record a change in relative humidity. The maximum and average differences between the experimental and numerical data are 0.3% RH and 0.2% RH respectively. This agreement is excellent and well within the ± 1% RH experimental uncertainty. Relative

to the size of the step change in humidity (50%), the measured and simulated data agree within ± 0.6%.

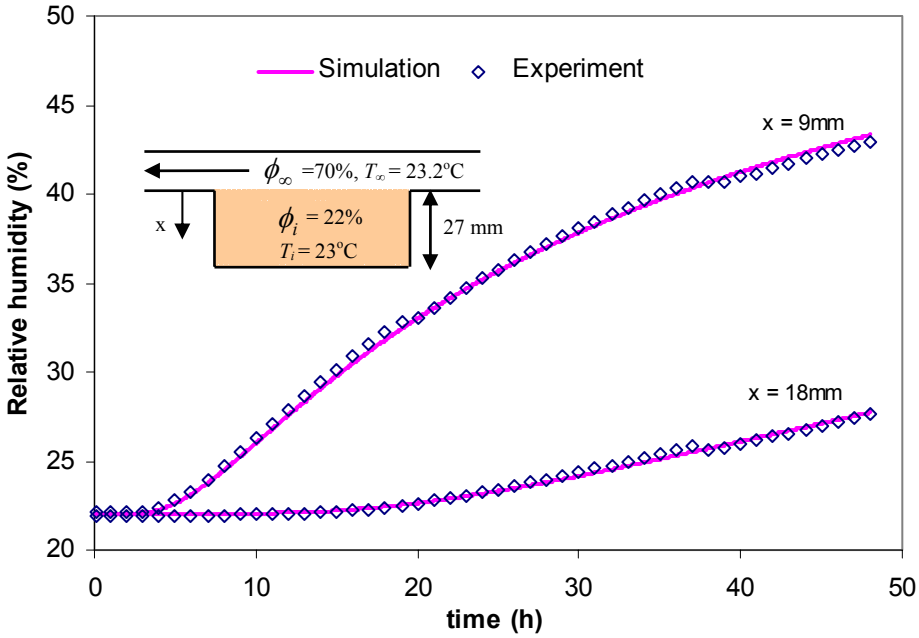

Figure 5.1. Measured and simulated relative humidity within the plywood bed following a 50% RH step change. The measured data presented for x = 9 mm are averages of the 5 sensors located at 9 mm, while data for x = 18 mm are from a single sensor at 18 mm.

The measured and simulated temperatures at depths of 9 mm and 18 mm are shown in Figure 5.2. In Figure 5.1 (and all temperature and relative humidity plots in this chapter), the measured value at x = 9 mm is the average of the five sensors located at a depth of 9 mm and the value at x = 18 mm is from a single sensor at a depth of 18 mm. The agreement between the measured and simulated results is very good, but the maximum change in temperature is very small. Relative to the maximum temperature change during the test (0.3°C), the experimental and numerical data agree within ± 3%. Figure 5.2 shows that the temperature in the spruce plywood increases up to 23.2°C at a depth of 9 mm within the first 5 hours, which is due to a combination of convection of heat

transfer from the flowing air and the heat of phase change. After about 20 hours, the temperature of the plywood at x = 18 mm exceeds the temperature at x = 9 mm due to the diffusion of heat into the plywood and convection heat transfer to the air above the plywood. The thermal boundary layer grows faster than the vapour boundary layer as can be seen by comparing Figures 5.1 and 5.2. The thermal boundary layer penetrates to a depth of 18 mm after the first hour, while the water vapour boundary layer does not penetrate to a depth of 18 mm until after 20 hours.

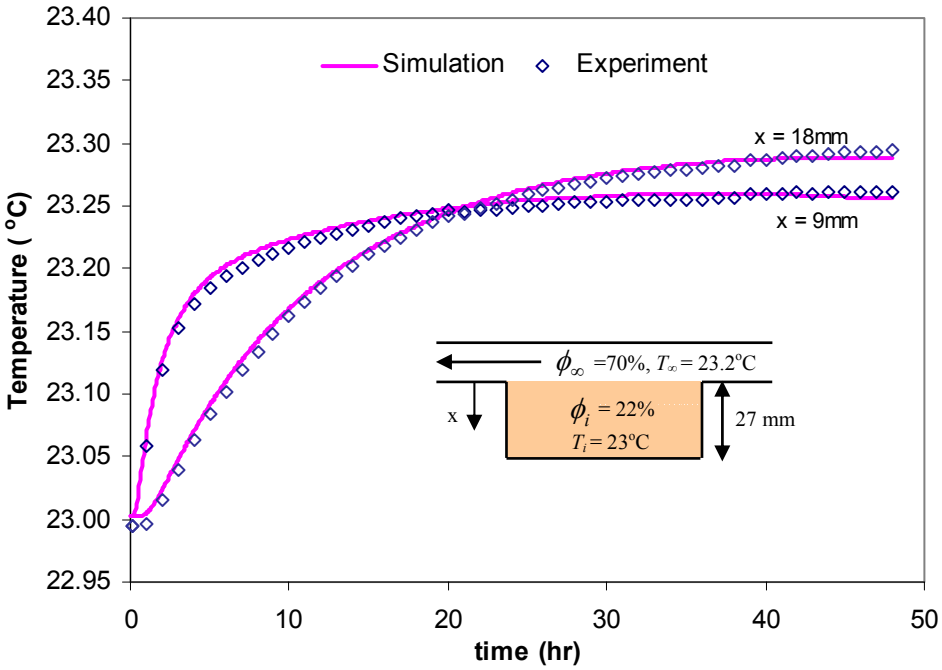

Figure 5.2. Measured and simulated temperature within the plywood bed following a 50% RH step change. The measured data presented for x = 9 mm are averages of the 5 sensors located at 9 mm, while data for x = 18 mm are from a single sensor at 18 mm.

Figure 5.3 presents a comparison between the moisture accumulation calculated with the numerical model and that measured using load sensors and the relative humidity sensors in the air stream. All moisture accumulation data follow the same trend with time. The

rate of moisture accumulation decreases with time and is consistent with boundary layer growth theory.

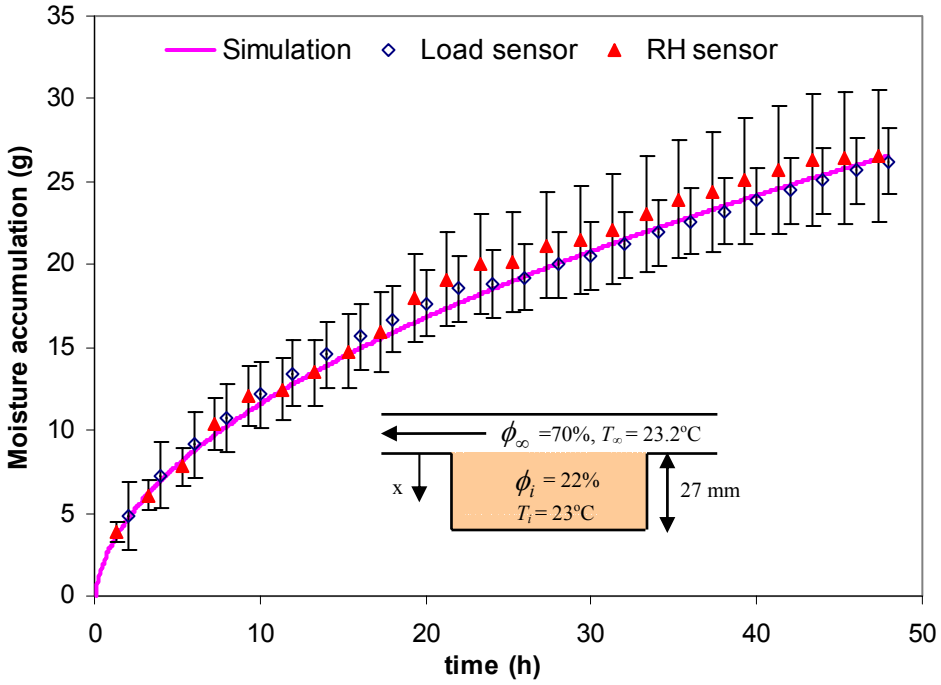

Figure 5.3. Measured and simulated moisture accumulation within the plywood bed following a 50% RH step change. The error bars represent the 95% uncertainty bounds in the measured data.

The moisture accumulation measured using the load sensors shows a better agreement with the simulated results than the data measured with the relative humidity sensors. The maximum and the average differences between the measured and simulated moisture accumulation is 1.5 g and 0.6 g for the load sensors and 2.8 g and 1.6 g for the relative humidity sensors, respectively. When normalized by the maximum moisture accumulation at the end of the test (26.2 g), the average differences between the measured and simulated data are 2% for the load sensors and 6% for the RH sensors. Even though the differences between the simulated and the measured data using the relative humidity sensors are higher than the difference between the simulated and

measured data from the load sensors, the results are well within the experimental uncertainty bounds as shown in Figure 5.3.

5.1.2 35% RH Change

The measured and simulated humidity, temperature and moisture accumulation data for the 35% RH change test are in Figures 5.4, 5.5 and 5.6 respectively. The agreement between the experiment and model is very good in all cases. The maximum differences between the measured and simulated data are 1% for relative humidity, 4% for temperature and 6% (load sensors) and 9% (relative humidity sensors) for moisture accumulation when normalized by the step change in humidity (35% RH), the maximum measured temperature change (0.25°C) and the maximum moisture accumulation (21.6 g) respectively.

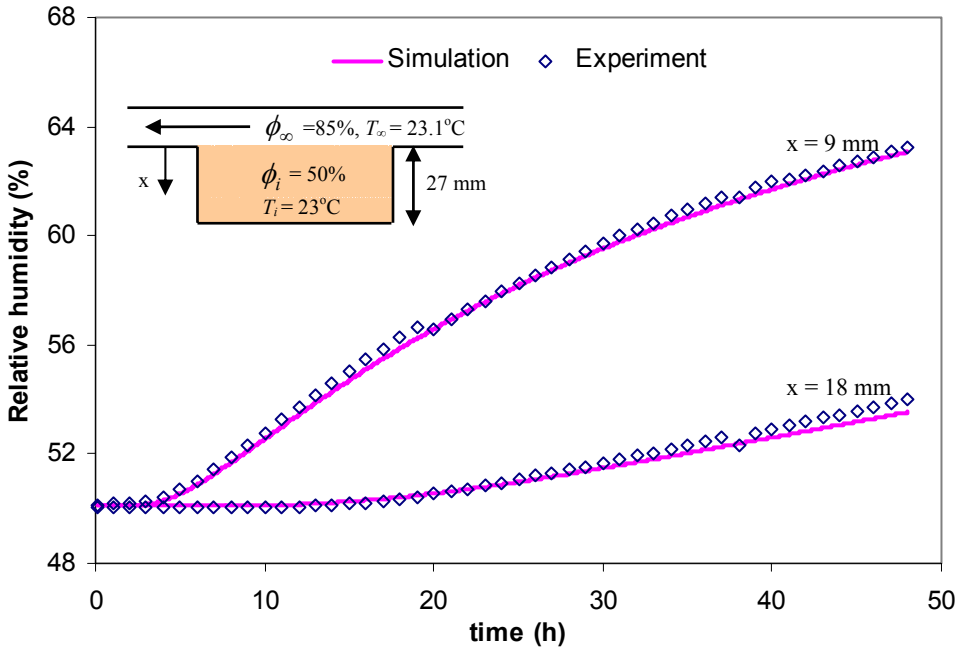

Figure 5.4. Measured and simulated relative humidity within the plywood bed following a 35% RH step change. The measured data presented for x = 9 mm are averages of the 5 sensors located at 9 mm, while data for x = 18 mm are from a single sensor at 18 mm.

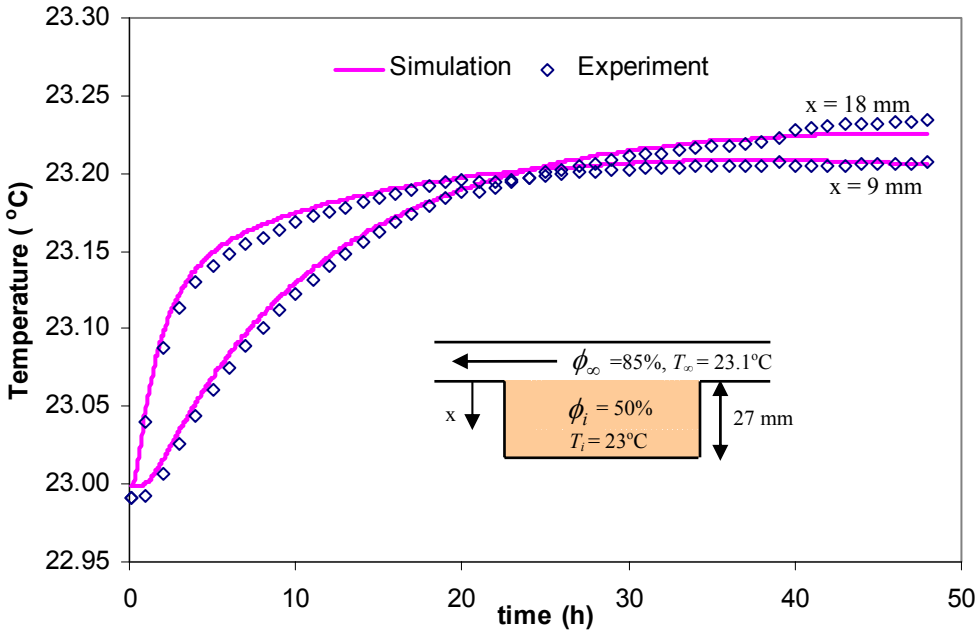

Figure 5.5. Measured and simulated temperature within the plywood bed following a 35% RH step change. The measured data presented for x = 9 mm are averages of the 5 sensors located at 9 mm, while data for x = 18 mm are from a single sensor at 18 mm.

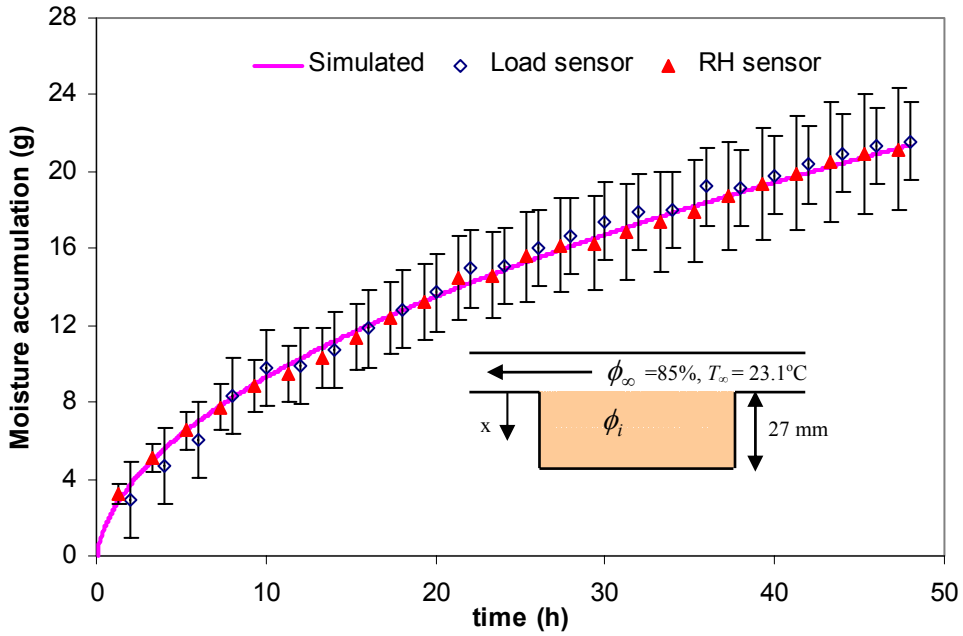

Figure 5.6. Measured and simulated moisture accumulation within the plywood bed following a 35% RH step change. The error bars represent the 95% uncertainty bounds for the measured data.

Comparing the data from the 35% RH test (Figures 5.4 to 5.6) with the data from the 50% RH changes test (Figures 5.1 to 5.3) shows that, the increase in relative humidity, temperature and moisture content is lower for the 35% RH test. This is expected because the vapour pressure difference (which is responsible for moisture transfer) in the 35% RH test is less than the one in the 50% RH test. The ratio of the RH step change size for the two tests (ΔRH = 50% and 35%) is 1.4 and when compared to the ratio of the maximum increase in the relative humidity and moisture accumulation for the two tests, which are 1.6 and 1.2 respectively, a difference of ±14% is noticed instead of 0% difference that would be expected in theory.

5.2 Tests with Different Airflow Rates

This section presents results of tests using four different airflow rates, which correspond to Reynolds numbers of 1000, 2000, 4000 and 7600. Since the Reynolds number used throughout the previous experiments is 2000, the purpose of this experiment is to investigate the effect of different airflow rates on the convection heat and mass transfer coefficients and consequently, the temperature and relative humidity fields. The test conditions for the different flow rate tests are summarized in Table 5.2.

To directly compare the results at different airflow rates, the measured and simulated relative humidity and temperature at $x = 9$ mm from the top of the plywood are presented in Figures 5.7 and 5.8 respectively. The moisture accumulation after 2 days of test is also presented in Figure 5.9. The measured results presented in Figures 5.7 and 5.8 are the averages of five relative humidity sensor and thermocouple readings. The maximum differences between the measured and simulated relative humidity, temperature and moisture accumulation using the load sensors are 0.7%, 4% and 6% for

Re = 1000 and 2000, and 1.1%, 5% and 10% for Re = 4000 and 7600, when normalized by the maximum change in the measured relative humidity, temperature and moisture accumulation respectively.

Table 5.2. Summary of the test conditions for the tests with different airflow rates.

Test	Initial condition	Condition of air flow	Test duration
Re = 1000	ϕ_i = 22% RH T_i = 22.9°C	ϕ_∞ = 70% RH T_∞ = 23.1°C	2 days single step
Re = 2000	ϕ_i = 22% RH T_i = 23°C	ϕ_∞ = 70% RH T_∞ = 23.1°C	2 days single step
Re = 4000	ϕ_i = 22% RH T_i = 24°C	ϕ_∞ = 70% RH T_∞ = 24.2°C	2 days single step
Re = 7600	ϕ_i = 22% RH T_i = 24.3°C	ϕ_∞ = 70% RH T_∞ = 24.4°C	2 days single step

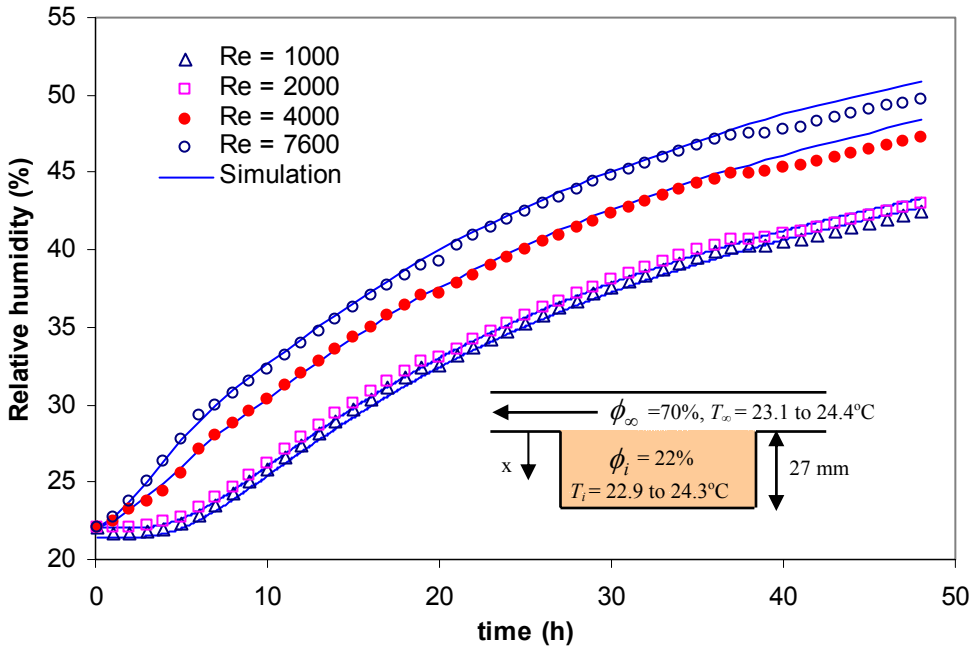

Figure 5.7. Measured and simulated relative humidity within the plywood at a depth of 9 mm following a 50% RH step change with different airflow rates. The measured data presented are averages of the 5 sensors located at 9 mm.

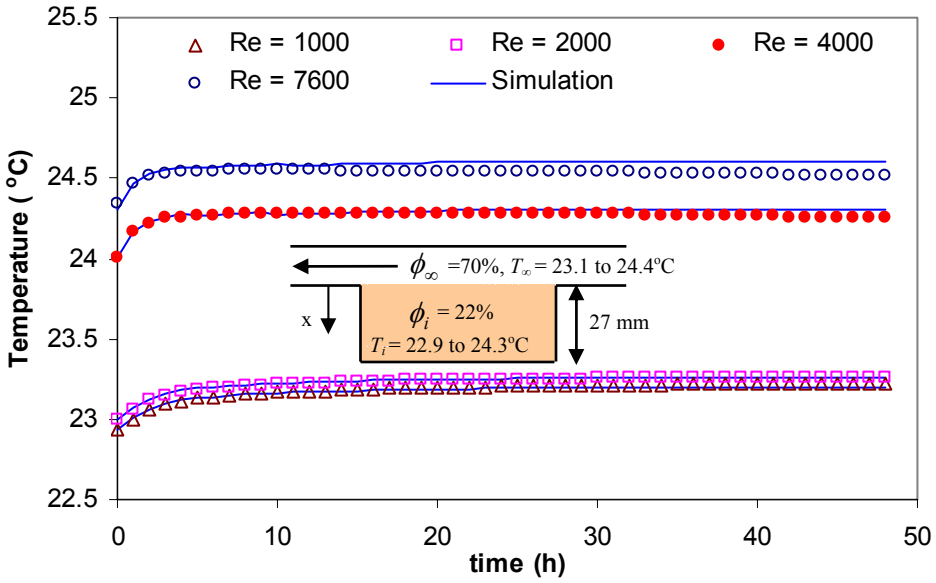

Figure 5.8. Measured and simulated temperature within the plywood at a depth of 9 mm following a 50% RH step change with different airflow rates. The measured data presented are averages of the 5 sensors located at 9 mm.

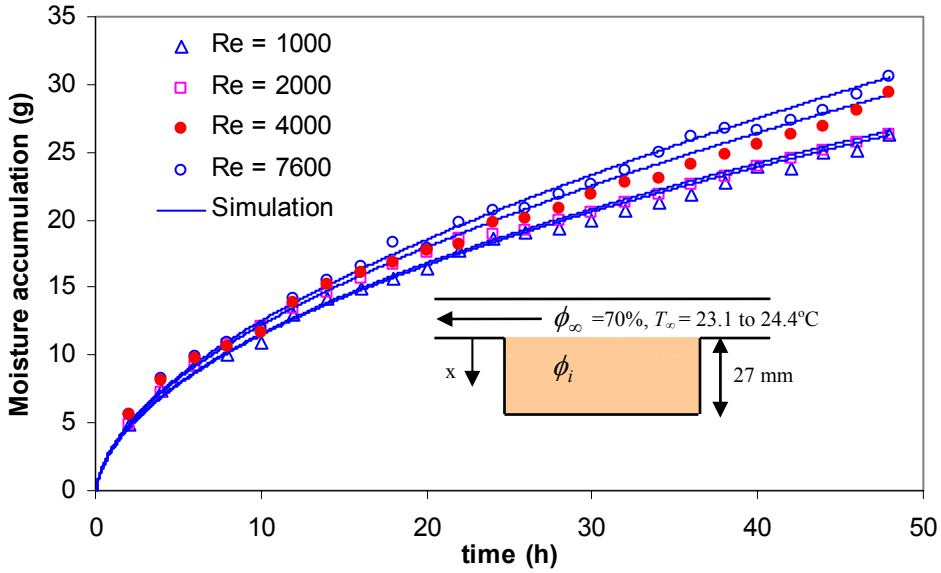

Figure 5.9. Measured and simulated moisture accumulation within the plywood following a 50% RH step change with different airflow rates.

Figures 5.7 and 5.9 shows that the relative humidity and moisture accumulation increases as Re increases, which is expected because as Re increases, the convective heat and mass transfer coefficients are increased and thus moisture accumulated and relative humidity within the plywood increases. The measured temperatures at Re = 4000 and 7600 are significantly different than the values at Re = 1000 and 2000 as shown in Figure 5.8. This is because of the different ambient temperature (T_∞) used for the higher flow rates as shown in Table 5.2.

5.3 Cyclical Adsorption-Desorption Test

In this test, the plywood, initially at equilibrium with air at 22% RH and 23^{o}C is tested for 12 days in the TMT facility with Re = 2000. During this time, the plywood is subjected to six step changes in humidity each two days apart. The average conditions of the air flowing over the plywood are 75% RH and 23.6^{o}C during the adsorption phase of the humidity cycle and 33% RH and 22.8^{o}C during the desorption phase.

The measured and simulated relative humidity, temperature and moisture accumulation within the spruce plywood for the adsorption-desorption cycles test are shown in Figures 5.10, 5.11 and 5.12, respectively. The maximum differences between the measured and simulated data are 0.7% for relative humidity and 5% for temperature, when normalized by the maximum change in relative humidity and temperature, respectively. For moisture accumulation, the average differences are 6% with load sensors and 11% with relative humidity sensors, when normalized by the maximum change in moisture accumulation.

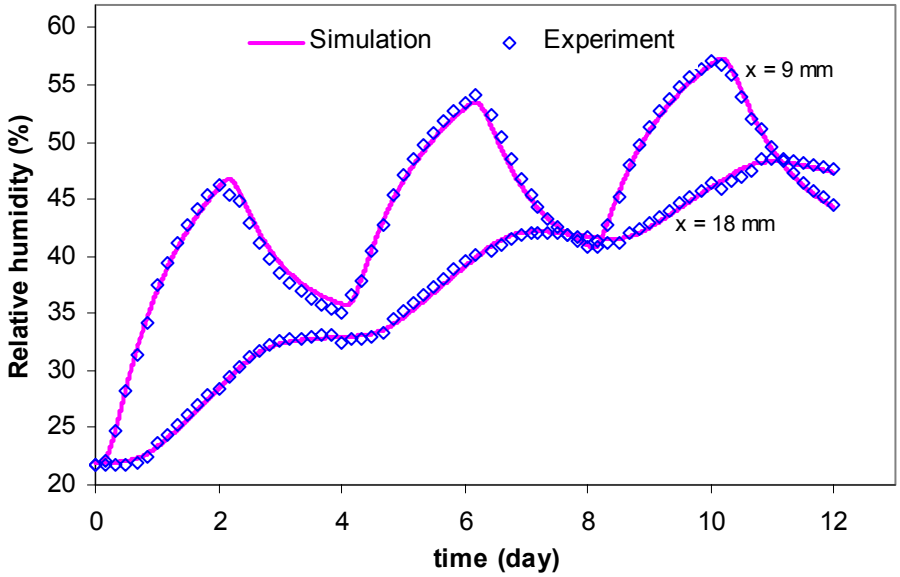

Figure 5.10. Measured and simulated relative humidity within the plywood during the cyclical adsorption-desorption test. The measured data presented for x = 9 mm are averages of the 5 sensors located at 9 mm, while data for x = 18 mm are from a single sensor at 18 mm.

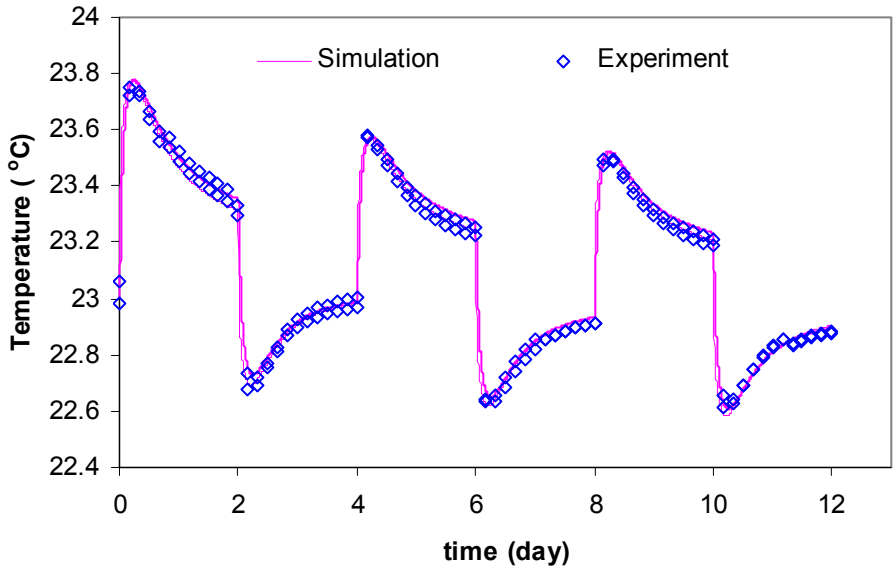

Figure 5.11. Measured and simulated temperature within the plywood during the cyclical adsorption-desorption test. The measured data presented for x = 9 mm are averages of the 5 sensors located at 9 mm, while data for x = 18 mm are from a single sensor at 18 mm.

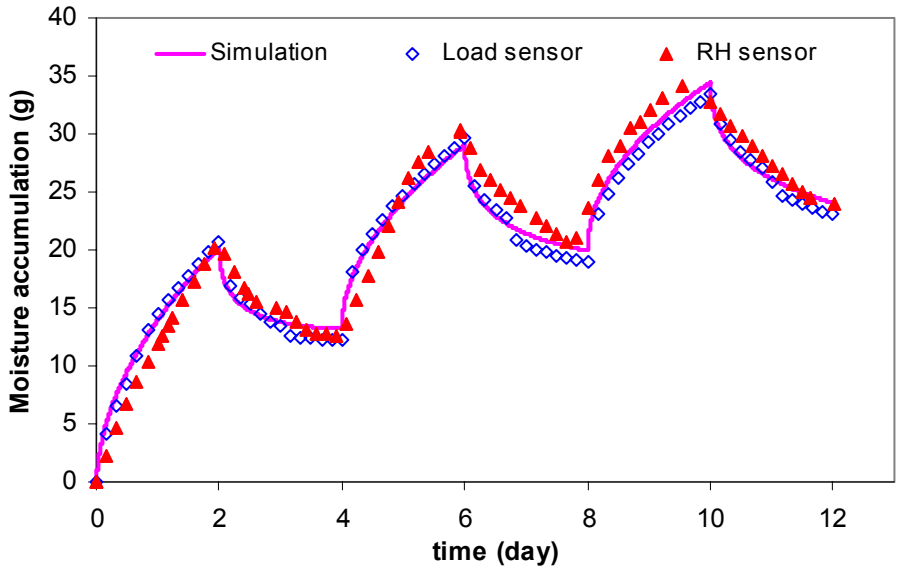

Figure 5.12. Measured and simulated moisture accumulation within the plywood during the cyclical adsorption-desorption test.

5.4 Verification of Moisture Diffusivity (α_m) Property

Many engineering textbooks (e.g. Incropera and Dewitt, 2002) contain solutions for transient conduction heat transfer problems and suggest that these solutions can be used for mass transfer as well, when analogous or equivalent moisture transfer properties are used in place of the heat transfer properties. As shown in Table 5.3, the vapour diffusion coefficient (D_{eff}) is typically assumed to be the equivalent moisture property for both thermal conductivity (k) and thermal diffusivity (α). The fact that the diffusion coefficient is typically used as the equivalent moisture property for thermal diffusivity implies that moisture storage is negligible. Since moisture storage is not negligible for hygroscopic materials, Olutimayin and Simonson (2005) developed a moisture diffusivity property (α_m) that is analogous to the thermal diffusivity property and includes moisture storage, as shown in Table 5.3.

Table 5.3. Summary of the thermal-moisture property analogy for solving transient moisture transfer.

Thermal Property	**Equivalent Moisture Property (Previous)**	**Equivalent Moisture Property (Olutimayin and Simonson, 2005)**
h_a	h_m	h_m
k	D_{eff}	D_{eff}
$\alpha = \frac{k}{\rho c_p}$	D_{eff}	$\alpha_{m,eff} = \frac{D_{eff}}{C_m}$

The equation for the effective moisture diffusivity of a porous medium is,

$$\alpha_{m,eff} = \frac{D_{eff}}{C_m} \tag{5.1}$$

where

$$C_m = \left(\varepsilon_g + \frac{\rho_o R_v T}{P_{vsat}} \frac{\partial u}{\partial \phi} \right). \tag{5.2}$$

The term $\frac{\partial u}{\partial \phi}$ is the slope of the sorption curve and the value of C_m for spruce plywood operating between 22% and 70% RH is 122. As can be seen in Figure 2.14, the slope of the sorption curve is nearly linear between these two humidity values.

Olutimayin and Simonson (2005) verified that $\alpha_{m,eff}$ can be used to accurately solve moisture transfer in cellulose insulation. The purpose of this section is to determine if $\alpha_{m,eff}$ can be applied to accurately model moisture transfer in spruce plywood. The experimental data and numerical model presented in the previous sections will be used for this.

To verify the moisture diffusivity property, the moisture penetration depth of spruce plywood is calculated analytically using both the previous analogy and analogy of Olutimayin and Simonson (2005). The analytical solution to the vapour transport equation for a semi-infinite porous medium with convective boundary conditions is (Incropera and Dewitt, 2002):

$$\frac{\rho_v-\rho_{vi}}{\rho_\infty-\rho_{vi}}=erfc\left(\frac{x}{2\sqrt{\alpha_{m,eff}t}}\right)-\left[exp\left(\frac{h_m x}{D_{eff}}+\frac{h_m{}^2\alpha_{m,eff}t}{D_{eff}{}^2}\right)\right]\left[erfc\left(\frac{x}{2\sqrt{\alpha_{m,eff}t}}+\frac{h_m\sqrt{\alpha_{m,eff}t}}{D_{eff}}\right)\right]. \quad (5.3)$$

The moisture penetration depth (δ_m) is defined as the position in the porous medium where,

$$\frac{\rho_{v,\delta_m}-\rho_{v,i}}{\rho_\infty-\rho_{v,i}}=0.01. \quad (5.4)$$

The moisture penetration depth (δ_m) can be calculated from the analytical, numerical and experimental data and these are presented in Figure 5.13 for the case of $h_{ad} = 2.5 \times 10^6$ J/kg. Figure 5.13 shows very close agreement (within ± 1.8%) between the simulated, experimental and analytical values of δ_m obtained using equations (5.3) and (5.4) when using $\alpha_{m,eff}$ as defined in equation (5.1) (i.e., including moisture storage). On the other hand, δ_m determined from the analytical solution using the previous moisture property, D_{eff} (i.e. neglecting moisture storage), is significantly greater than the simulated values. This shows that the moisture diffusivity term developed by Olutimayin and Simonson (2005) can be used together with the analytical model to determine the moisture penetration depth for spruce plywood.

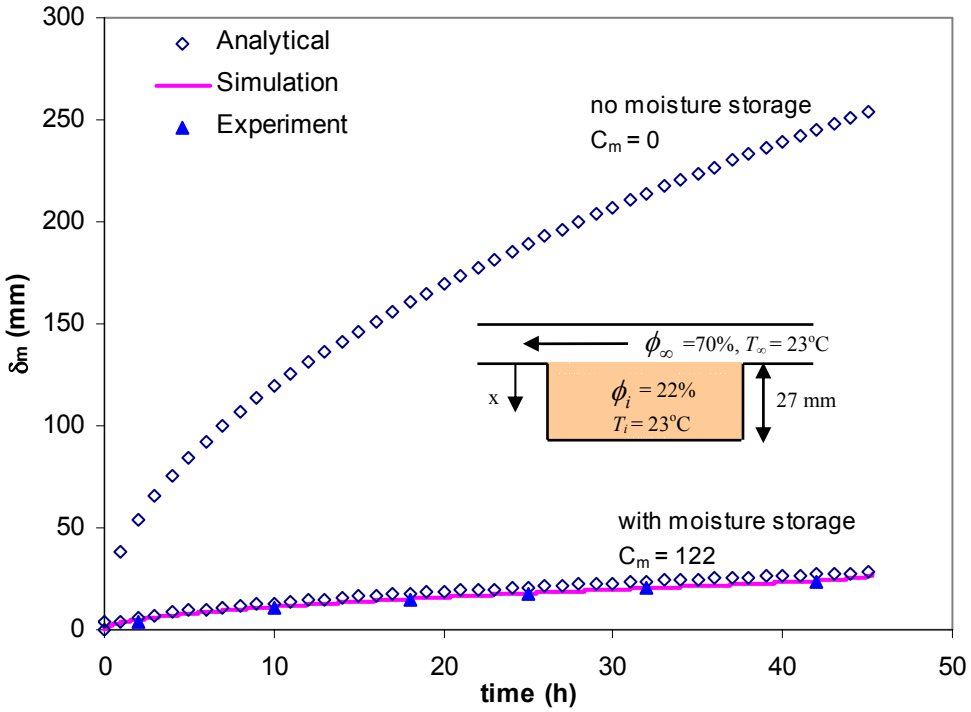

Figure 5.13. Vapour boundary layer thickness in spruce plywood calculated using the analytical solution (with and without moisture storage) compared to that obtained from the numerical model and experimental data for Re = 2000.

The results obtained from the analytical solution show the importance of moisture storage for spruce plywood. If moisture storage is neglected, the moisture will penetrate out of the 27-mm thick bed of spruce plywood after two hours; whereas, the simulation and experimental data indicate that it would take about 45 hours for moisture to penetrate through the spruce plywood. After 10 hours, δ_m = 120 mm when moisture storage is neglected and δ_m = 12 mm when moisture storage is included. These results show that excluding the moisture storage term overestimates the moisture penetration depth as much as ten times.

Moisture diffusivity is further verified by calculating the vapour density within the porous medium using equation (5.2) and comparing the results with simulated values.

These results are presented in Figure 5.14 and show excellent agreement (within ± 2%) between the simulated and the analytical data when moisture storage is included.

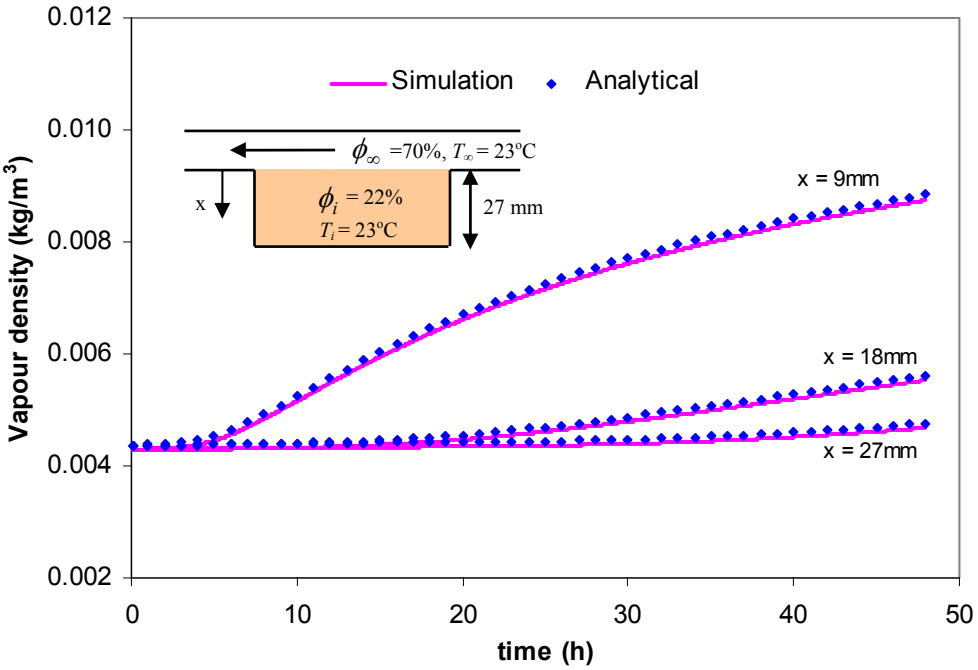

Figure 5.14. Vapour density distribution in spruce plywood calculated using the analytical solution (with moisture storage) compared to that obtained using numerical model for Re = 2000.

5.5 Sensitivity Studies

The sensitivity of the numerical results to changes in the sorption isotherm, effective thermal conductivity, heat of sorption and effective diffusion coefficient are presented in this section. All the sensitivity studies are performed for using the 50% RH single-step change test conditions at Re = 2000. The results of the sensitivity studies are concentrated on the locations in the spruce plywood where the numerical results were verified with experimental data; these locations are 9 mm and 18 mm for the relative humidity data and only 9 mm for the temperature (for clarity). The sensitivity of the

moisture accumulation to these properties can be found in Chapter 4 (Section 4.5) and is not repeated here.

5.5.1 Sorption Isotherm

In the numerical simulation, a curve fit of the experimental sorption isotherm data is used and the equation for this curve fit was given in equation (2.6). Figures 5.15 and 5.16 show the effect of changing the sorption curve (i.e., moisture content (u)) by 10%, on the simulated relative humidity and temperature, respectively.

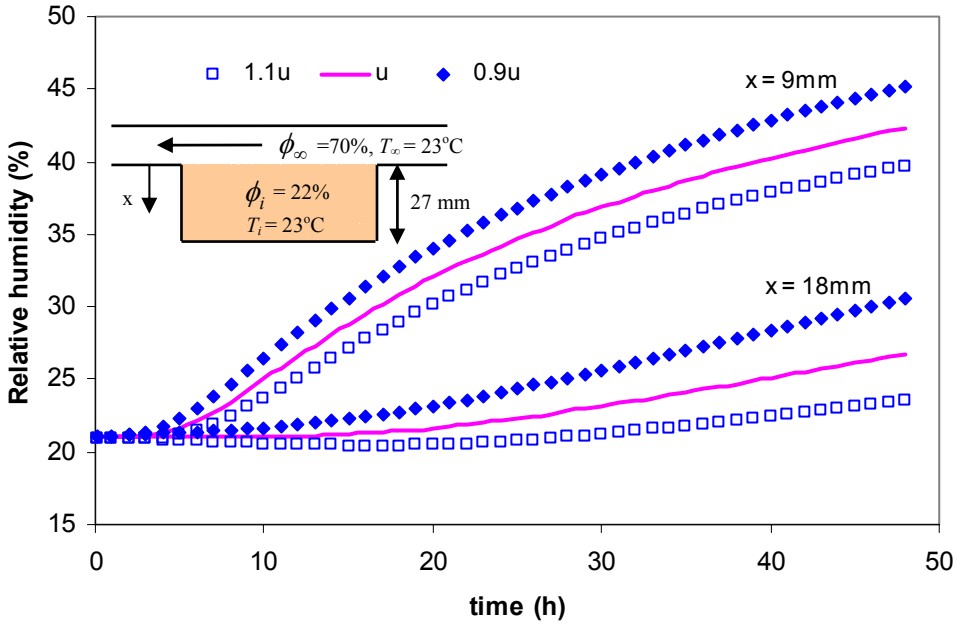

Figure 5.15. Sensitivity study showing the effect of changing the moisture content (u) calculated by the sorption isotherm (equation (2.6) and Figure 2.15) by ± 10% on the simulated relative humidity field within plywood following a 50% RH step change.

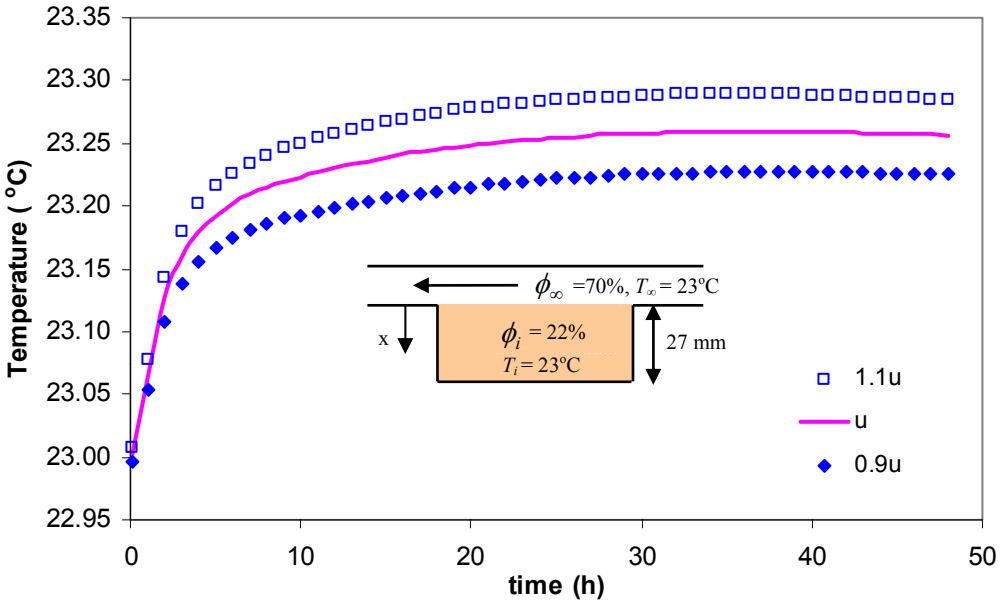

Figure 5.16. Sensitivity study showing the effect of changing the moisture content (u) calculated by the sorption isotherm (equation (2.6) and Figure 2.15) by ± 10% on the simulated temperature field within plywood at a depth of 9mm following a 50% RH step change.

Figure 5.15 shows that increasing the sorption curve by 10% results in a maximum of 6% reduction in the humidity relative to the size of the step change in humidity (50%) (at x = 9 mm and t = 48 hours) within the spruce plywood, whereas, a 10% reduction in the sorption curve increases the relative humidity by a maximum of 6% (at x = 9 mm and t = 48 hours). For the simulated temperature presented in Figure 5.16, a 10% increase of the sorption curve increases the temperature by up to 10%, while a 10% reduction in the sorption curve results in a maximum of 10% reduction in the temperature. These results make physical sense because an increase in the sorption isotherm will mean more moisture accumulation, which will reduce the water vapour diffusion within the vapour phase and also increase the temperature due to the phase change. These results also indicate that the sorption curve used in the model is correct

because the difference between the measured and simulated relative humidity is smaller than the fluctuations in Figure 5.15. Also, the difference between the measured and simulated temperature is less than the fluctuations accounted for by a 10% change in the sorption curve.

5.5.2 Heat of Sorption

In the numerical simulation, the heat of sorption (h_{ad}) is assumed constant and equal to the latent heat of vapourization of water obtained from the literature, as shown in Table 3.1. It is therefore important to investigate the effect of changes in h_{ad} on the simulated temperature. Increasing or decreasing h_{ad} by 10% in the numerical simulation results in a 8% maximum increase or decrease of the temperature respectively as shown in Figure 5.17. The resulting increase or decrease in temperature gives a 0.1% decrease or increase in the humidity relative to the size of the step change in humidity (50%) (not presented graphically), respectively. This confirms the numerical model because increasing h_{ad} increases the temperature field and thus decreases the relative humidity field, which demonstrates the coupling between the heat and moisture transport equations.

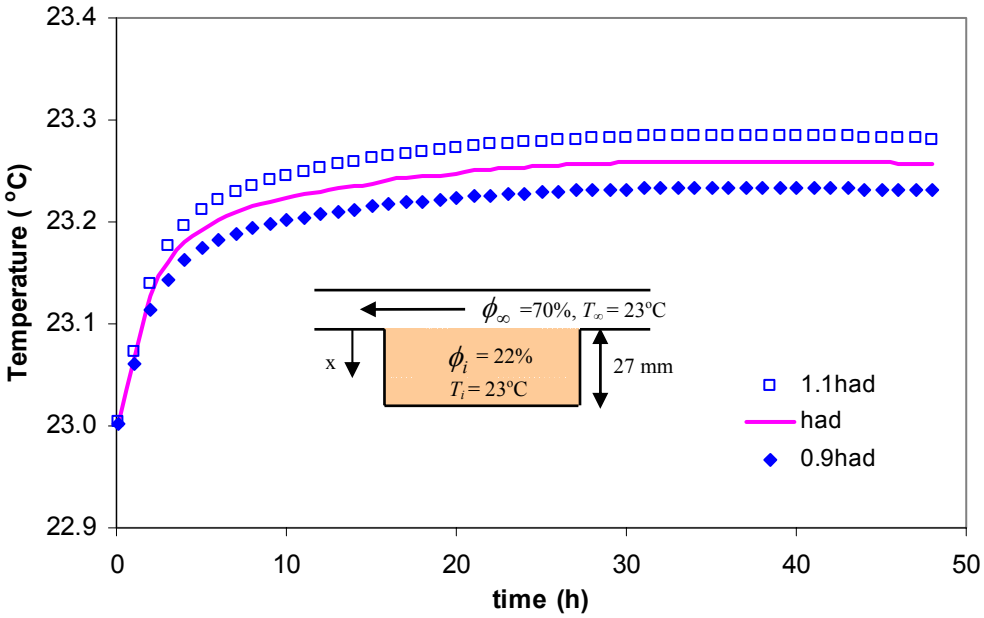

Figure 5.17. Sensitivity study showing the effect of changing h_{ad} by ± 10% on the simulated temperature field of plywood at a depth of 9 mm following a 50% RH step change.

5.5.3 Effective Vapour Diffusion Coefficient

Equation (3.15), presented in Chapter 3, gives the effective vapour diffusion coefficient (D_{eff}), which is used in the model. The D_{eff} is based on the water vapour permeability data presented in Chapter 2 (equation (2.12) and Figure 2.21). Increasing or decreasing D_{eff} by 10% results in a maximum of 2% increase or decrease in the humidity relative to the size of the step change in humidity (50%) as shown in Figure 5.18. The numerical results show that increasing D_{eff} increases the relative humidity at all depths as expected. Changing D_{eff} by ± 10% results in a ± 4% change in the temperature (not presented graphically).

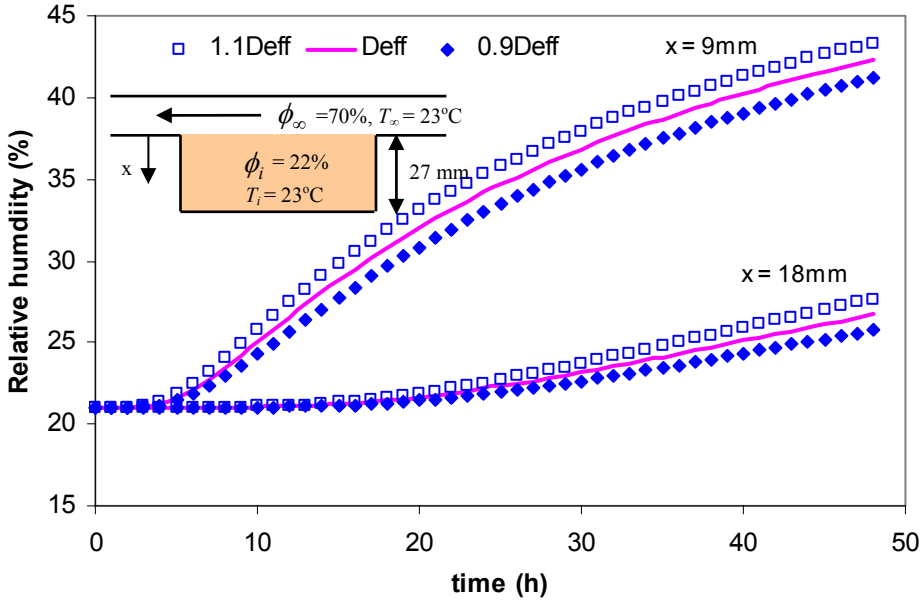

Figure 5.18. Sensitivity study showing the effect of changing D_{eff} by ± 10% on the simulated relative humidity field of plywood following a 50% RH step change.

5.5.4 Effective Thermal Conductivity

The effective thermal conductivity used in the numerical simulation is a curve fit of the experimental data and the equation for this curve fit was given in equation (2.10). Changing the effective thermal conductivity by ± 10% has a small effect on the temperature field as shown in Figure 5.19. A change of ± 10% in k_{eff} results in a maximum change of ± 3% in the temperature field. Figure 5.19 shows that increasing k_{eff} tends to decrease the temperature in the spruce plywood. Increasing k_{eff} decreases the temperature within the spruce plywood because a higher value of k_{eff} results in more of the heat released during adsorption being conducted deeper into the plywood or upward through the plywood into the air stream. These results indicate that the model is correctly predicting the coupled heat and moisture transfer. They also confirm that the plywood is losing heat to the ambient air during the test. The ± 10% change in k_{eff} also

gives a ± 0.04% change in the humidity relative to the size of the step change in humidity (50%) (not presented graphically).

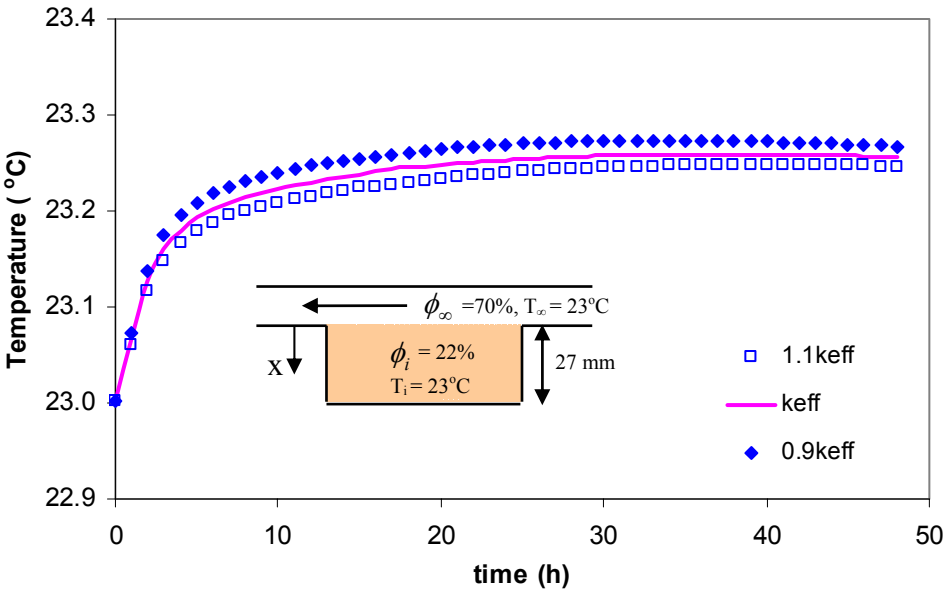

Figure 5.19. Sensitivity study showing the effect of changing k_{eff} (defined in equation (2.11) and Figure 2.18) by ± 10% on the simulated temperature field of plywood at a depth of 9mm following a 50% RH step change.

5.6 Summary

The experimental and numerical results presented in this chapter quantify transient heat and moisture transfer in spruce plywood. The experimental data are in close agreement with numerical data. The maximum differences between the measured and simulated data presented in this chapter all fall within 1.1% of the maximum ΔRH for relative humidity, 5% of the maximum ΔT for temperature and 6% and 11% of the maximum Δu for moisture accumulation using load sensors and relative humidity respectively. These differences are summarized in Table 5.4 and are within the uncertainty values in the relative humidity, temperature and moisture accumulation measurements. The experimental results show that the results from the numerical model are reliable.

Table 5.4. Summary of the maximum differences between the measured and simulated data for relative humidity, temperature and moisture accumulation normalized by the maximum changes during each test.

		Relative humidity	Temperature	Moisture Accumulation
Tests with different humidity changes	**ΔRH = 50%**	± 0.6%	± 3%	**Load sensors:** ± 6%
				RH sensors: ± 11%
	ΔRH = 35%	± 1.0%	± 4%	**Load sensors:** ± 6%
				RH sensors: ± 9%
Tests with different flow rates	**Re = 1000 Re = 2000**	± 0.7%	± 4%	**Load sensors:** ± 6%
	Re = 4000 Re = 7600	± 1.1 %	± 5%	**Load sensors:** ± 10%
Cyclical adsorption-desorption test		± 0.7%	± 5%	**Load sensors:** ± 6%
				RH sensors: ± 11%

The moisture diffusivity property developed by Olutimayin and Simonson (2005) is shown to apply for spruce plywood. The moisture penetration depth strongly depends on moisture storage and neglecting moisture storage over-predicts the boundary layer thickness by an order of magnitude for spruce plywood.

To further verify the numerical model presented in this thesis and determine the sensitivity of the simulated temperature and relative humidity to changes in the material properties used in the model, sensitivity studies are carried out. The results from the sensitivity studies further confirmed the validity of the numerical results. The sorption isotherm has the greatest effect in the numerical simulation of the relative humidity profile within plywood, while the effective thermal conductivity has the least effect. For the numerical simulation of the temperature profiles within plywood, the sorption isotherm and the heat of phase change have the greatest effect, while the effective vapour diffusion coefficient has the least effect.

CHAPTER 6

CONCLUSIONS AND FUTURE WORK

The goal of this thesis is to quantify the moisture buffering capacity (MBC) of spruce plywood during transient humidity changes using both experimental and numerical data, thereby providing support towards the development of a standard test method and validation data for numerical models. In support of this goal, the moisture buffering capacity, transient temperature and humidity profiles and the material properties of spruce plywood are measured. These measurements provide data that are used to validate a numerical model for one-dimensional transient heat and moisture transfer in spruce plywood. Also, the measured data as well as results from the numerical model are used to verify the moisture diffusivity (α_m) property, developed by Olutimayin and Simonson (2005), for spruce plywood. The validated numerical model is also used to investigate the effect of initial conditions, boundary conditions, thickness and RH step change size on the MBC of spruce plywood.

6.1 Research Summary and Conclusions

The moisture buffering capacity (MBC) of spruce plywood has been determined from moisture accumulation data measured using the glass jar facility and the TMT facility. These facilities measure moisture accumulation with an uncertainty of ± 0.7 g/m^2 and ± 1.2 g/m^2, respectively. The average MBC value obtained from the glass jar is

22.3 g/m^2 with an uncertainty of ± 0.5 g/m^2. For the TMT facility, the MBC is measured for Re of 1000, 2000, and 4000 and the MBC values are 22.5, 24.9, and 26.2 g/m^2 respectively with an uncertainty of ± 0.8 g/m^2. The measured results are used to validate a numerical model for one-dimensional heat and moisture transfer in spruce plywood. The differences between experimental and numerical data are typically less than ± 2%, which is less than the experimental uncertainty.

The effect of thickness and the convection transfer coefficients on the MBC of spruce plywood has been investigated using the numerical and experimental data. As expected, the MBC increases as the thickness and convection coefficients increase. The MBC determined from testing with different thickness of plywood and different convection transfer coefficients between the plywood and the humid air, is as much as 18% different. The numerical data are also used to show that the MBC of plywood depends on the initial conditions for short tests, but tend to be insignificant for infinitely long tests. The number of humidity cycles that are required for the plywood to reach quasi-steady state (where the moisture accumulation/change does not change with further cycles) is also determined using the numerical and experimental data. The MBC can be determined with fewer repeated cycles when the plywood is initially in equilibrium with the average of the high and low RH. If the test duration is not increased for other initial conditions, errors as large as 8% may result.

The MBC results obtained has been shown to be dependent on the initial conditions, boundary conditions and the effective thickness. These results are useful in experimental design and also confirm that the moisture storage capacity of hygroscopic materials

during transient changes in ambient air relative humidity (moisture buffering capacity) is an important parameter that requires a standard test method and facility that can quantify it accurately and repeatably. The research in this thesis has provided both experimental and numerical data in support of such standard.

The temperature and humidity profiles as well as the moisture accumulation within spruce plywood are measured using the TMT facility. In this facility, the temperature and humidity profiles within the spruce plywood are measured with an uncertainty of $0.1^{o}C$ and ± 1% RH respectively. The mass accumulation is measured with an uncertainty of ± 8% and ± 15%, using the load sensors and the relative humidity respectively. The data in this thesis are measured for single step-change in humidity with different humidity changes and different airflow rates at the top boundary. A cyclical adsorption-desorption test is also performed.

For the tests with different humidity changes, relative humidity and temperature (measured at a depth of 9 mm from the top surface of the spruce plywood) as well as moisture accumulation increased by as much as 21% RH, $0.3^{o}C$ and 26.2 g respectively after a 2-day test, depending on the vapour pressure difference between the air at the top boundary and the plywood. The results for the tests with different airflow rates show that at higher flow rate (when Re = 4000 and 7600), there is a very significant increase in moisture accumulation in the spruce plywood compared to the low airflow rates (when Re = 1000 and 2000). This increase in moisture accumulation within the medium is due to an increase in the convective heat and mass transfer coefficients at the top surface of the medium at the higher Re. The results for the cyclical adsorption-desorption test show

that after 12 days, the relative humidity measured at a depth of 9 mm and moisture accumulation, increased by 23% RH and 23.8 g, respectively. The temperature in the plywood varied by only ± 0.1^{o}C during the 12 day isothermal test. These measured data are also used to validate the numerical model. The measured and numerical data are in close agreement. For all the tests performed, the maximum difference between the measured and simulated data normalized by the maximum changes during each test is ± 1% for relative humidity, ± 4% for temperature, and ± 6% and ± 11% for moisture accumulation using the load sensors and relative humidity respectively. This shows the reliability of the numerical model.

The moisture diffusivity property developed by Olutimayin and Simonson (2005) has been shown to apply for spruce plywood and that the moisture penetration depth strongly depends on moisture storage. Therefore, neglecting moisture storage over predicts the boundary layer thickness by an order of magnitude for spruce plywood.

The numerical model and the material properties used in the model are further verified with sensitivity studies. These studies show that the simulated MBC of spruce plywood changes by ± 7% and ± 3% for ± 10% changes in the moisture content calculated by the sorption isotherm and effective vapour diffusion coefficient respectively, while ± 0.5% changes in MBC are noticed with ± 10% changes in effective thermal conductivity and heat of phase change. Changing the dry density and specific heat by ± 10% results in a negligible change in the MBC. The studies also show for ± 10% changes in the moisture content calculated by the sorption isotherm and effective vapour diffusion coefficient, the simulated humidity profile changes by ± 6% and ± 2%, respectively. While ± 10%

changes in effective thermal conductivity and heat of phase change, changes the simulated temperature profile by ± 8% and ± 3%, respectively.

6.2 Future work

This numerical and experimental investigation into transient heat and moisture transfer in spruce plywood has resulted in the identification of several areas for future work, which are listed below.

1. Further experimental and numerical works are required to investigate the moisture buffering capacity of other building materials. More experiments using the method presented in this thesis are required to cover a wider range of building materials and the data from these experiments will help to compare the moisture buffering capacity of different materials under different test conditions. These results can be used to determine the material that is best suited to buffer the humidity in a building by extrapolating these results to real life conditions.

2. There is a need to incorporate the moisture buffering capacity data for different materials in to a new or existing building energy simulation tools. This could be done by accounting for the storage capacity of the material in the simulation tools. This will enable a modeler to simulate the moisture buffering effect of a material on the indoor humidity, perceived indoor air quality and the energy consumption of a building.

3. Research has shown that the drying conditions have a very significant effect on the measured sorption isotherm data, which are used in the numerical model. This is because during drying it is desired that all hygroscopically bound water is removed, without

removing the chemically bound water. In this thesis, a vented-oven (at 50^{o}C and ≈ 2% RH) is used to dry the plywood samples to determine the dry mass. However, research has shown that when gypsum board is dried using a vented oven at 50^{o}C, all the hygroscopically bound water is not removed. This means that there can be an off-set in the dry weight (intended starting point of the sorption isotherm) of the sample. Therefore, it is recommended that the drying conditions of the plywood should be changed to observe if the dry weight of the plywood sample will exhibit similar offset.

4. Using the moisture diffusivity property (α_m) developed by Olutimayin and Simonson (2005), an analytical solution should be developed to calculate the moisture buffering capacity (MBC) from the calculated vapour density in the boundary layer. This analytical solution could be used to determine the MBC instead of the numerical solution, thereby saving time and may even increase the accuracy of the solution.

REFERENCES

ASHRAE, 2005. *Fundamentals Handbook*, Atlanta, GA, USA.

ASME PTC 19.1, 1998. *Test Uncertainty*, ASME National Standard, NY, USA.

ASTM E104, 1985. *Maintaining Constant Relative Humidity by Means of Aqueous Solutions*, ASTM, Philadelphia.

ASTM C518, 2003. *Standard Test Method for Steady-State Heat Flux Measurements and Thermal Transmission Properties by Means of The Heat Flow Meter Apparatus*, Annual Book of Standards, 04.06, 153-164, ASTM, Philadelphia.

ASTM E96, 1996. *Standard Test Methods for Water Vapour Transmission of Materials*, Annual Book of Standards, ASTM, Philadelphia.

Avramidis, S., Englezos, P., and Papathanasiou, T., 1992. Dynamic Nonisothermal Transport in Hygroscopic Porous Media: Moisture Diffusion in Wood, *AIChE Journal*, **38** (8), 1279-1287.

Carmeliet, J., Gaublomme, J. and Janssen, H., 2005. Influence of Hysteresis on Moisture Buffering of Wood, Report Annex 41, IEA ECBCS.

Cunningham, M. J., 1990. Modeling of Moisture Transfer in Structure-2. A Comparison of a Numerical Model, an Analytical Model and Some Experiment Results, *Building and Environment*, **23** (2), 85-94.

Dedic, A., 2000. Convective Heat and Mass Transfer in Moisture Desorption of Oak Wood by Introducing Characteristics Transfer Coefficients, *Drying Technology*, **18** (7), 1617-1627.

Dinwoodie, J. M., 1981. *Timber: Its Structure, Properties and Utilization*, 6th edition. MacMillan Press Ltd., London. 410.

Fang, L., Clausen, G. and Fanger, P.O., 1998. Impact of Temperature and Humidity on the Perception of Indoor Air Quality, *Indoor Air*, **8**, 80–90.

Gardner, D. J., 2004. The Relevance of Surface Properties & Wood Finishes to the Wood Science & Technology Research Community, *The 2nd SWST Annual Fundamental Disciplines Session*, http://www.swst.org/meetings/AM04/Gardner.pdf.

Gaur, R. C. and Bansal, N. K., 2002. Effect of Moisture Transfer across Building Components on Room Temperature, *Building and Environment*, **37** (1), 11-17.

Geving, S., 2000. Hygrothermal analysis of building structures using computer models, *Journal of Thermal Envelope and Building Science*, **23** (3), 224-243.

Håkansson H., 1998. *Retarded Sorption in Wood*. Department of Building Science, Lund Institute of Technology, PhD Dissertation, Lund University. Lund, Sweden.

Hameury, S., 2005. Moisture Buffering Capacity of Heavy Timber Structures Directly Exposed to an Indoor Climate: A Numerical Study, *Buildings and Environment*, **40**, 1400-1412.

Holm, A., Künzel, H. M. & Sedlbauer, K., 2003. The Hygrothermal Behaviour of Rooms: Combining Thermal Building Simulation and Hygrothermal Envelope Calculation: *IBPSA Proceedings Building Simulation*, Einhoven, Netherlands.

Incropera, F. P. and Dewitt, D. P., 2002. *Fundamentals of Heat and Mass Transfer*, J. Wiley, New York.

ISO 12571, 1996. *Building Materials- Determination of Hygroscopic Sorption Curves*, ISO, Brussels, Belgium.

ISO 5176-1, 1991. *Measurement of Fluid Flow by Means of Pressure Differential Devices*, ISO, Switzerland.

Kaviany, M., 1991. *Principles of Heat Transfer in Porous Media*, Springer-Verlag, New York.

Kellog, R. M. and Wangaard, F. F., 1969. Variation in the Cell-Wall Density of Wood, *Wood and Fiber*, **1**, 180-204.

Kunzel, H.M., Holm, A., Zirkelbach, D. and Karagiozis, A.N., 2005. Simulation of Indoor Temperature and Humidity Conditions Including Hygrothermal Interactions with the Building Envelope, *Solar Energy*, **78**, 554-561.

Lucas, F., Adelard, L., Garde, F. and Boyer, H., 2002. Study of Moisture in Buildings for Hot Humid Climates, *Energy and Buildings*, **34**, 345-355.

Luikov, A. V., 1966. *Heat and Mass Transfer in Capillary-Porous Bodies*, Pergamon Press, Oxford.

Mendes, N., Ridley, I., Lamberts, R., Phillipi, P. C. and Budag, K., 1999. UMIDUS: A PC Program for the Prediction of Heat and Mass Transfer in Porous Building Elements, *Building Simulation Conference – IBPSA 99*, 277-283.

Mendes, N., Philippi, P.C., and Lamberts, R., 2002. A New Mathematical Method To Solve Highly Coupled Equations of Heat and Mass Transfer in Porous Media, *International Journal of Heat and Mass Transfer*, **45**, 509-518.

Mendes, N., Winkelmann, F.C., Lamberts, R. and Philippi, P. C., 2003. Moisture Effects on Conduction Loads, *Energy and Buildings*, **35**, 631-644.

Mualem, Y., 1974. *A Conceptual Model of Hysteresis,* Water Resources Research, **10** (3).

Mukhopadhyaya, P., Kumaran, K., Tariku, F. and van Reenen, D., 2003. Final Report from Task 7 of the MEWS Project, Long-Term performance: Predict the Moisture Management Performance of Wall Systems as a Function of Climate, Material Properties, etc. Through Mathematical Modeling, IRC-RR-132, Ottawa, Canada, http://irc.nrc-cnrc.gc.ca/fulltext/rr132/rr132.pdf.

New Zealand Forest Insight, 2004. *Products and Processes: Veneer Products- Plywood Manufacturing Process*. http://www.insights.co.nz/products_processes_vp.aspx.

Ojanen, T. and Ahonen, J., 2005. *Moisture Performance Properties of Exterior Sheathing Products made of Spruce Plywood or OSB*, ESPOO 2005, VTT Working Papers 22, 52 pp + app. 12pp.

Olutimayin, S. and Simonson, C. J., 2005. Measuring and Modelling Vapour Boundary Layer Growth during Transient Diffusion Heat and Moisture Transfer in Cellulose Insulation, *International Journal of Heat and Mass Transfer*, **48**, 3319-3330.

Padfield, T., 1998. *The Role of Absorbent Building Materials in Moderating Changes of Relative Humidity*, Ph.D. thesis in the Department of Structural Engineering and Materials, Technical University of Denmark.

Pedersen, C.R., 1990. *Combined Heat and Moisture Transfer in Building Constructions*, PhD Thesis, Technical University of Denmark, Denmark.

Peukhuri, R., Rode, C. and Hansen, K.K., 2004. Moisture Buffering Capacity of Different Insulation Materials, in; *Proceedings (CD) of the Performance of Exterior Envelopes of Whole Buildings IX International Conference*, Clearwater Beach, Florida, USA, 14 pages.

Plumb, O. A., Spolek, G. A., and Olmstead, B. A., 1985. Heat and Mass Transfer in Wood during Drying, *International Journal of Heat and Mass Transfer*, **28** (9), 1669-1678.

Prigogine, I., 1961. *Introduction to Thermodynamics of Irreversible Processes*, Interscience Publishers.

Rode, C., Grau, K. and Mitamura, T., 2001. Hygrothermal Conditions in the Envelope and Indoor Air of Buildings, in: *Proceedings (CD) of Performance of Exterior Envelopes of Whole Buildings VIII: Integration of Building Envelopes*, Clearwater Beach, Florida, ASHRAE.

Rode, C., Mitamura, T., Shultz, J. and Padfield, T., 2002. Test Cell Measurements of Moisture Buffer Effects, in: *Proceedings of the 6th Nordic Building Physics Symposium*, Trondheim, Norway, pp.619-626.

Rode, C., Holm, A. and Padfield, T., 2004. A Review of Humidity Buffering in the Interior Spaces, *Journal of Thermal Envelope and Building Science*, **27** (3), 221-226.

Rode, C., Peuhkuri, R., Hansen, K. K., Time, B., Svennberg, K., Arfvidsson, J. and Ojanen, T., 2005. Moisture Buffer Value of Materials in Buildings, in: *Proceedings of the Nordic Building Physics Conference*, Reykjavík, Iceland, June 13-15, 8 pages.

Salin, J., 1996. Mass Transfer from Wooden Surfaces and Internal Moisture Non-Equilibrium, *Drying Technology*, **14** (10), 2213-2224.

Salonvaara, M. and Karagiozis, A., 1994. Moisture Transport in Building Envelopes Using an Approximate Factorization Solution Method, in: Gottlieb, J. and Ethier, C. (eds), in: *Proceedings of the Second Annual Conference of the CFD Society of Canada*, pp. 317–326, Toronto, Canada.

Salonvaara, M., Ojanen, T., Holm, A., Kunzel, H.M. and Karagiozis, A.N., 2004. Moisture Buffering Effects on Indoor Air Quality – Experimental and Simulation Results, in: *Proceedings (CD) of the Performance of Exterior Envelopes of Whole Buildings IX International Conference*, Clearwater Beach, Florida, 11 pages.

Samuleson, I., 1998. Hygrothermal Performance of Attics, *Journal of Thermal Envelope and Building Science*, **22,** 132-145.

Simonson, C. J., Salonvaara, M. and Ojanen, T., 2004a. Heat and Mass Transfer between Indoor Air and a Permeable and Hygroscopic Building Envelope, Part II – Verification and Numerical Studies, *Journal of Thermal Envelope and Building Science*, **28** (2), 161-185.

Simonson, C. J., Olutimayin, S., Salonvaara, M., Ojanen, T., and O'Connor, J., 2004b. Potential for Hygroscopic Building Materials to Improve Indoor Comfort and Air Quality in the Canadian Climate, in: *Proceedings (CD) of Performance of the Exterior Envelopes of Whole Buildings IX International Conference*, Clearwater Beach, Florida, December 5-10, 15 pages.

Simonson, C.J., 2005. Energy Consumption and Ventilation Performance of a Naturally Ventilated Ecological House in a Cold Climate, *Energy and Buildings,* **37** (1), 23-35.

Svennberg, K., Hedegaard, L. and Rode, C., 2004. Moisture Buffer Performance of a Fully Furnished Room, in: *Proceedings (CD) of the Performance of Exterior Envelopes of Whole Buildings IX International Conference*, Clearwater Beach, Florida, 11 pages.

TenWolde, A., 1987. A Mathematical Model for Indoor Humidity in Homes During Winter, in: *Proceedings of the Symposium on Air Infiltration, Ventilation and Moisture Transfer*, Fort Worth, Texas, Building Envelope Coordinating Council, Washington DC.

Toftum, J., Jorgensen, A. S. and Fanger, P. O., 1998a. Upper Limits of Air Humidity for Preventing Warm Respiratory Discomfort, *Energy and Buildings*, **28**, 15-23.

Toftum, J., Jorgensen, A. S. and Fanger, P. O., 1998b. Upper Limits for Indoor Air Humidity to Avoid Uncomfortably Humid Skin, *Energy and Buildings*, **28**, 1-13.

Tong L., 1986. *Moisture Transport in Wood*. Swedish Institute for Wood Technology Research, Report P 8609056. Stockholm, Sweden.

Tremblay, C., Cloutier, A. and Fortin, Y., 2000. Experimental Determination of the Convective Heat and Mass Transfer Coefficients for Wood Drying, *Wood Science and Technology*, **34**, 253-276.

Wadsö L., 1993. *Studies of Water Vapour Transport and Sorption in Wood*. Doctoral Dissertation. Report TVBM-1013. Dept. of Building Materials, Lund University, Lund, Sweden.

Wadsö L., 1994. Describing Non-Fickian Water-Vapour Sorption in Wood, *Journal of Materials Science*, **29**, 2367-2372

Wadsö, L., Svennberg, K. and Dueck, A., 2004. An Experimentally Simple Method for Measuring Sorption Isotherms, *Drying Technology*, **22** (10), 2427-2440.

Whitaker, S., 1977. Simultaneous Heat, Mass and Momentum Transfer in Porous Media: A Theory of Drying, *Advances in Heat Transfer*, 13, Academic Press, New York.

Yu, D., Klein, S.A. and Reindl, D. T., 2001. An Evaluation of Silica Gel for Humidity Control in Display Cases, *WAAC Newsletter*, **23** (2).

APPENDIX A

UNCERTAINTY ANALYSIS

The uncertainty analysis used to determine the uncertainties in the results presented in this thesis are presented in this appendix. This analysis helps to estimate the accuracy of a measurement and/or calculation and thus gives a level of confidence in the results obtained from such measurements and/or calculations.

Uncertainty analysis is used to quantify the errors associated with measured data and calculated results using a quantitative standard method. The precision and bias uncertainties form the main components of an uncertainty analysis and are calculated independently (ASME PTC 19.1-1998). The ASME standard defines the total uncertainty as the root-sum-square uncertainty (U_{RSS}) by combining the total bias (B) with the total precision (P).

This uncertainty is expressed as:

$$U_{RSS} = \left[U_B{}^2 + U_P{}^2 \right]^{1/2}, \tag{A.1}$$

where U_B is the bias uncertainty and U_P is the precision uncertainty. The confidence level of this uncertainty is 95%.

The bias error is a fixed or steady error which remains constants for all measurements. Bias errors are often more difficult to quantify because they come from various sources like: calibration errors, scale reading errors, data acquisition, etc. The precision error is a

result of random error caused by the data spread about the mean. This error will change based on the repeatability and accuracy of the measurements.

$$U_p = t\, S_{\bar{x}}, \tag{A.2}$$

where t is the student t for the 95% confidence level and $S_{\bar{x}}$, the precision index is calculated as the sample standard deviation for N samples of the measured data as shown:

$$S_{\bar{x}} = \left[\frac{\sum_{k=1}^{N} \left(X_k - \overline{X} \right)^2}{N-1} \right]^{1/2}, \tag{A.3}$$

where X_k is the parameter which is measured and $\overline{X}$ is the average value of measured data. For example, the uncertainty in the relative humidity measurement (using the Honeywell humidity sensor) is based on the bias uncertainty of ± 1.1% RH obtained from calibrating the humidity sensor and a precision uncertainty of ± 0.7% RH, obtained from the repeatability of the humidity sensor. The total uncertainty of the humidity sensor is therefore ± 1.3% RH (root-sum square of the bias and the precision uncertainties).

For calculated results, uncertainty is analyzed using the uncertainties from measured properties that were used in obtaining the new result. For example in the calculation of moisture accumulation using the measured relative humidity and mass flow rate, the moisture accumulation is determined using,

$$\Delta m = \dot{m}_a \left(W_{inlet} - W_{outlet}\right)\Delta t \,. \tag{A.4}$$

The total uncertainty is the root-sum-square uncertainty (U_{RSS}), which includes the individual uncertainties of the measured data as shown below:

$$\frac{U\Delta m}{\Delta m} = \left[\left(\frac{U\dot{m}_a}{\dot{m}_a}\right)^2 + \left(\frac{U\left(W_{inlet} - W_{outlet}\right)}{\left(W_{inlet} - W_{outlet}\right)}\right)^2 + \left(\frac{U\Delta t}{\Delta t}\right)^2\right]^{1/2} \tag{A.5}$$

where $U\Delta m$ is the uncertainty in the calculated moisture accumulation, $U\dot{m}_a$ is the uncertainty in the measured mass flow rate, $U\left(W_{inlet} - W_{outlet}\right)$ is the uncertainty in the calculated humidity ratio (using the measured relative humidity) and $U\Delta t$ is the uncertainty in the time.

APPENDIX B

PROPERTIES USED IN THE NUMERICAL MODEL

The material and thermodynamic properties used in the numerical model are presented in this appendix. These properties are measured, obtained from the literature or calculated from other properties. All the properties obtained from the literature are taken at 300K. The properties and the appropriate references are given below.

Dry Spruce Plywood Properties

$\rho_o = 445 \pm 0.3$ kg/m^3	(Measured)
$k_{eff} = 0.082 \pm 0.00082$ W/(m·K)	(Measured)
$D_{eff} = 4.10 \pm 0.5 \times 10^{-7}$ m^2/s	(Measured)
$\varepsilon_g = 0.7 \pm 0.01$	(Calculated)

Solid Properties

$Cp_s = 1880$ J/(kg·K)	(Incropera and Dewitt, 2002)
$\rho_s = 1530$ kg/m^3	(Dinwoodie, 1981)
$\varepsilon_s = 0.3$	(Calculated)

Air

$Cp_a = 1007$ J/(kg·K)	(Incropera and Dewitt, 2002)
$R_a = 287$ J/(kg·K)	(Incropera and Dewitt, 2002)

Water Vapour

$Cp_v = 1872$ J/(kg·K) (Incropera and Dewitt, 2002)

$R_v = 462$ J/(kg·K) (Calculated)

Adsorbed Properties

$\rho_\ell = 997$ kg/m^3 (Incropera and Dewitt, 2002)

$Cp_\ell = 4181$ J/(kg·K) (Incropera and Dewitt, 2002)

Others

$h_{ad} = 2.5 \times 10^6$ J/kg (Incropera and Dewitt, 2002)

APPENDIX C

DISCRETIZED EQUATIONS AND THE COMPUTER SIMULATION PROGRAM

This appendix presents the discretized equations of the numerical model presented in Chapter 3 and the computer simulation program to solve these equations. The computer simulation program is written in FORTRAN 77.

C.1 Discretized Equations

The discretized equations used in the numerical model and boundary conditions are shown below (note that m refers to the current node (spatial location) while n refers to the current time step.).

The continuity for the adsorbed phase is,

$$\frac{\varepsilon_\ell(m,n)-\varepsilon_\ell(m,n-1)}{\Delta t}+\frac{\dot{m}(m,n)}{\rho_\ell}=0\,. \tag{C.1}$$

The gas diffusion of water vapour is,

$$\rho_v(m,n)\left(\frac{\varepsilon_g(m,n)-\varepsilon_g(m,n-1)}{\Delta t}\right)+\varepsilon_g(m,n)\left(\frac{\rho_v(m,n)-\rho_v(m,n-1)}{\Delta t}\right)-\dot{m}(m,n)\;=$$

$$\left(\frac{D_{eff}(m+1,n)-D_{eff}(m-1,n)}{2\Delta x}\right)\left(\frac{\rho_v(m+1,n)-\rho_v(m-1,n)}{2\Delta x}\right)+$$

$$D_{eff}(m,n)\left(\frac{\rho_v(m-1,n)-2\rho_v(m,n)+\rho_v(m-1,n)}{\Delta x^2}\right) \tag{C.2}$$

Energy transport equation is given by,

$$\rho_v(m,n)c_p(m,n)\left(\frac{T(m,n)-T(m,n-1)}{\Delta t}\right)+\dot{m}(m,n)h_{ad} = \left(\frac{k_{eff}(m+1,n)-k_{eff}(m-1,n)}{2\Delta x}\right)\left(\frac{T(m+1,n)-T(m-1,n)}{2\Delta x}\right)+ k_{eff}(m,n)\left(\frac{T(m-1,n)-2T(m,n)+T(m-1,n)}{\Delta x^2}\right) \quad \text{(C.3)}$$

The rate of phase change is,

$$\dot{m}(m,n) = \rho(m,n)\left(\frac{u(m,n-1)-u(m,n)}{\Delta t}\right). \quad \text{(C.4)}$$

The volume constraint is,

$$\varepsilon_s(m,n)+\varepsilon_\ell(m,n)+\varepsilon_g(m,n)=1. \quad \text{(C.5)}$$

The thermodynamic relationships are,

$$\phi(m,n)=\frac{p_v(m,n)}{P_{vsat}(m,n)}, \quad \text{(C.6)}$$

$$P_v(m,n)=\rho_v(m,n)R_vT(m,n), \quad \text{(C.7)}$$

$$P_g=P_v(m,n)+P_a(m,n), \quad \text{(C.8)}$$

$$P_a(m,n)=\rho_a(m,n)R_aT(m,n), \quad \text{(C.9)}$$

$$\rho_g=\rho_v(m,n)+\rho_a(m,n). \quad \text{(C.10)}$$

The properties of the medium are,

$$D_{eff} = \delta R_v T(m,n), \tag{C.11}$$

$$\rho(m,n) = \varepsilon_s(m,n)\rho_s(m,n) + \varepsilon_\ell(m,n)\rho_\ell(m,n) + \varepsilon_g(m,n)\rho_g(m,n), \tag{C.12}$$

$$Cp(m,n) = \frac{\varepsilon_s(m,n)\rho_s(m,n)Cp_s + \varepsilon_\ell(m,n)\rho_\ell(m,n)Cp_\ell + \varepsilon_g(m,n)(\rho_a(m,n)Cp_a + \rho_v(m,n)Cp_v)}{\rho(m,n)}, \tag{C.13}$$

$$k_{eff} = a + b\phi(m,n) + c(\phi(m,n))^2 + d(\phi(m,n))^3, \tag{C.14}$$

The boundary conditions are,

Convection @ x = 0

$$h_a\left(T(0,n) - T_\infty\right) = k_{eff}\left(\frac{4T(1,n) - T(2,n) - 3T(0,n)}{2\Delta x}\right). \tag{C.15}$$

Adiabatic @ x = L

$$4T(M-1,n) - T(M-2,n) - 3T(M,n) = 0. \tag{C.16}$$

Where M is the last node @ x = L

Convection @ x = 0

$$h_m\left(\rho_v(0,n) - \rho_{v,\infty}\right) = D_{eff}\left(\frac{4\rho_v(1,n) - \rho_v(2,n) - 3\rho_v(0,n)}{2\Delta x}\right). \tag{C.17}$$

Impermeable @ x = L

$$4\rho_v(M-1,n) - \rho_v(M-2,n) - 3\rho_v(M,n) = 0. \tag{C.18}$$

Where M is the last node @ x = L

C.2 Computer Simulation Program

The computer simulation program presented below is written in FORTRAN 77. The program presented in this appendix is the general program used by the author and has been modified depending on the specific results required.

```
------------------------------------------------------------------------------------------------------
THIS PROGRAM MODELS A ONE-DIMENSIONAL HEAT AND MOISTURE TRANSFER IN SPRUCE PLYWOOD BY OLALEKAN OSANYINTOLA, APRIL 2005
------------------------------------------------------------------------------------------------------

DECLARE ALL VARIABLES AND CONSTANT
INTEGER  NGRID, NTSTEP, NITER
PARAMETER (NTSTEP=5761)
PARAMETER (NGRID= 450)
REAL  DELT, DELX
DOUBLE PRECISION KV, RV, WD, CPW, KW, KS, HM, HA, HAD, CPV, TI
DOUBLE PRECISION CPA, POROS, DA, KA, RA, EGI, CPS, SD, ES, VDI
DOUBLE PRECISION ELI, PATM, RELAX, TOLT, TOLV, TOLL, TAMB, C2
DOUBLE PRECISION VDAMB, C1, C8, C9, C10, C11, C12, C13, MOIST (NTSTEP)
DOUBLE PRECISION T (NTSTEP, NGRID), EL (NTSTEP, NGRID)
DOUBLE PRECISION U (NTSTEP, NGRID), PCR (NTSTEP, NGRID), SUMVD
DOUBLE PRECISION TOLD (NTSTEP, NGRID), RH (NTSTEP, NGRID), TEST2
DOUBLE PRECISION VDOLD (NTSTEP, NGRID), PCROLD (NTSTEP, NGRID)
DOUBLE PRECISION SVP (NTSTEP, NGRID), VP (NTSTEP, NGRID), VDMIN
DOUBLE PRECISION UM (NTSTEP, NGRID), UA (NTSTEP, NGRID), VDMAX
DOUBLE PRECISION AD (NTSTEP, NGRID), GD (NTSTEP, NGRID)
DOUBLE PRECISION VD (NTSTEP, NGRID), KD (NTSTEP, NGRID)
DOUBLE PRECISION DENI (NTSTEP, NGRID), KEFF (NTSTEP, NGRID)
DOUBLE PRECISION CPEFF (NTSTEP, NGRID), KG (NTSTEP, NGRID)
DOUBLE PRECISION DEFF (NTSTEP, NGRID), CPG (NTSTEP, NGRID)
DOUBLE PRECISION TMAX, A, PA (NTSTEP, NGRID), CPDEN,
DOUBLE PRECISION TMIN, SUMT, TEST1, MS (NTSTEP, NGRID)
DOUBLE PRECISION EGOLD (NTSTEP, NGRID), EG (NTSTEP, NGRID)
------------------------------------------------------------------------------------------------------
OPEN (UNIT=1, FILE="TEMPFIELD.TXT", STATUS="REPLACE")
OPEN (UNIT=2, FILE="VAPDFIELD.TXT", STATUS="REPLACE")
OPEN (UNIT=3, FILE="BOUNDVAP.TXT", STATUS="REPLACE")
OPEN (UNIT=4, FILE="MC.TXT", STATUS="REPLACE")
OPEN (UNIT=5, FILE="RHFIELD.TXT", STATUS="REPLACE")
OPEN (UNIT=6, FILE="PCRFIELD.TXT", STATUS="REPLACE")
OPEN (UNIT=7, FILE="MOISSTORAGE.TXT", STATUS="REPLACE")
```

ASSIGN VALUES TO CONTANTS AND SET INITIAL VALUE

GRID PARAMETERS

DELT = 30 ! TIME STEP (SECONDS)
DELX = 0.0001 ! SPATIAL STEP (METRES)
NITER = 2000 ! NO OF ITERATION

SPRUCE PLYWOOD PROPERTIES

POROS = 0.69 ! POROSITY OF SPRUCE PLYWOOD

AIR PROPERTIES

CPA = 1007 ! CP OF AIR
DA = 0.000026 ! DIFFUSIVITY COEFF OF AIR
RA = 287 ! GAS CONSTANT FOR AIR
EGI = 0.6879 ! INITIAL GAS VOL
HM = 0.002904667 ! CONV. COEFF OF MASS OF AIR
HA = 3.51 ! CONV. COEFF OF HEAT OF AIR
HAD = 2500000 ! HEAT OF ADSORPTION

VAPOUR PROPERTIES

CPV = 1872 ! CP OF VAPOUR
RV = 462 ! GAS CONSTANT FOR VAPOUR

WATER PROPERTIES

WD = 997 ! DENSITY OF WATER
CPW = 4181 ! CP OF WATER

SOLID PROPERTIES

CPS = 1880 ! CP OF SOLID
SD = 1530 ! DENSITY OF SOLID
ES = 0.31 ! VOL OF SOLID

INITIAL PROPERTIES

TI = 296 ! INITIAL TEMP
VDI = 0.004521303 INITIAL VAPOUR DENSITY
EGI = 0.6879 ! INITIAL GAS VOL FRACTION
ELI = 0.0001 ! INITIAL LIQUID VOL FRACTION
PATM = 101325 ! ATM. PRESSURE
RELAXT = 0.05 ! RELAXATION FACTOR FOR TEMP
RELAXV = 0.05 ! RELAXATION FACTOR FOR VAPOUR DENSITY
TOLT = 0.000001 ! TOLERANCE FOR TEMP
TOLV = 0.00001 ! TOLERANCE FOR VAPOUR DENSITY.
TAMB = 296 ! AMBIENT TEMPERATURE
VDAMB = 0.014385964! AMBIENT VAPOUR DENSITY

INITIALIZE VALUES FOR TIME t=0 (I=1)

```
DO 10 J= 1, NGRID
T (1, J) = TI  ! INITIAL TEMP
EG (1, J) = EGI    ! INITIAL GAS FRACTION
EL (1, J) = ELI    ! INITIAL LIQUID FRACTION
VD (1, J) = VDI   ! INITIAL VAPOUR DENSITY
DENI (1, J) = 445     ! INITIAL DENSITY OF PLYWOOD
U (1, J) = 0.013   ! INITIAL MOISTURE CONTENT
PCR (1, J) = 0.0       ! INITIAL PHASE CHANGE RATE

10   CONTINUE
```

START OF TIME LOOP

```
DO 20 I = 2, NTSTEP
```

ASSIGN OLD TIME STEP TO THE NEW ONE FOR FIRST ITERATION

```
DO 30 M = 1, NGRID
T (I, M) = T (I-1, M)
VD (I, M) = VD (I-1, M)
U (I, M) = U (I-1, M)
EL (I, M) = EL (I-1, M)
EG (I, M) = EG (I-1, M)
PCR (I, M) = PCR (I-1, M)
DENI (I, M) = DENI (I-1, M)

30   CONTINUE
```

START OF ITERATION LOOP

```
DO 40 N = 1, NITER
```

START OF POSITION LOOP

```
DO 50 J=1, NGRID
```

SET OLD VALUES TO VARIABLES TO CHECK CONVERGENCE

```
TOLD (I, J) = T (I, J)
VDOLD (I, J) = VD (I, J)
PCROLD (I, J) = PCR (I, J)
EGOLD (I, J) = EG (I, J)
```

CONSTANTS FOR EVALUATING SAT VAPOUR PRESSURE

```
C8 = -5800.2206
C9 = 1.3914993
C10 = -0.048640239
```

C11 = 0.000041764768
C12 = -0.000000014452093
C13 = 6.5459673

CALCULATE SAT VAPOUR PRESSURE, VAPOUR PRESSURE, RH AND PCR

C1 = ((C12*T (I, J)**3) + (C13*DLOG(T(I,J))))
SVP(I,J) = EXP((C8/T(I,J))+C9+(C10*T(I,J))+(C11*T(I,J)**2)+ C1)
VP (I, J) = VD (I, J)*RV*T (I, J)
RH (I, J) = VP (I, J)/SVP (I, J)
U (I, J) = 1.0147E-04 + 0.06754*RH (I, J) + (-0.06574*RH (I, J)**2)/ (1 +
0.2339*RH (I, J) + (-2.3603*RH (I, J)**2) + 1.1329*RH (I, J)**3)
PCR (I, J) = ((U (I-1, J)-U (I, J))*DENI (I, J))/DELT

CALCULATE LIQUID VOLUME FRACTION

EL (I, J) = EL (I-1, J)-((PCR (I, J)*DELT)/WD)

CALCULATE GAS FRACTION, DEFF, AND VAPOUR DENSITY

EG (I, J) = 1.0 - (ES + EL (I, J))
KD (I, J) = -2.3573E-25 + ((-8.1601E-24*RH (I, J))/DLOG (RH (I, J)))
DEFF (I, J) = KD (I, J)*RV*T (I, J)

FOR TOP NODE
IF (J.EQ.1) THEN
VD (I, 1) = (HM*VDAMB + DEFF (I, 1)*(4.0*VD (I, 2)-VD (I, 3))/ (2*DELX))/
(HM+ 1.50*DEFF (I, 1)/DELX)

ENDIF

FOR BOTTOM NODE
IF (J.EQ.NGRID) THEN
VD (I, NGRID) = (4*VD (I, NGRID-1) - VD (I, NGRID-2))/3

ENDIF

FOR INTERNAL NODES
IF (J.GT.1 .AND. J.LT.NGRID) THEN
VD(I,J) = (EG(I,J)*VD(I-1,J)/DELT + PCR(I,J) + (DEFF(I,J+1)-
DEFF (I, J-1))*(VD (I, J+1)-VD (I, J-1))/ (4.0*DELX**2) + DEFF (I, J)*
(VD (I, J-1) +VD (I, J+1))/DELX**2)/ ((2.0*EG (I, J)-EG (I-1, J))/DELT+ 2.0*DEFF
(I, J)/DELX**2)
VD(I,J) = VDOLD(I,J) + RELAXV*(VD(I,J)-VDOLD(I,J)) ! RELAX THE VALUE

ENDIF

```
------------------------------------------------------------------------------------------------------
CALCULATE DENSITY, CP, KEFF AND TEMPERATURE
------------------------------------------------------------------------------------------------------
PA (I, J) = PATM-VP (I, J)
AD(I,J) = PA(I,J)/(RA*T(I,J)) ! AIR DENSITY
GD (I, J) = AD (I, J) +VD (I, J)   ! GAS DENSITY
DENI(I,J) = ES*SD+EL(I,J)*WD+EG(I,J)*GD(I,J)  ! WOOD DENSITY
CPG (I, J) = (AD (I, J)*CPA + VD (I, J)*CPV)
CPEFF(I,J) = (ES*SD*CPS+EL(I,J)*WD*CPW+EG(I,J)*CPG(I,J))/DENI(I,J)
KG (I, J) = AD (I, J)*KA+VD (I, J)*KV
KEFF (I, J) = 0.08185 + 0.02212*RH (I, J) + (-0.02313*RH (I, J)**2) +
0.01291*RH (I, J)**3

FOR TOP NODE
IF (J.EQ.1) THEN
T (I, 1) = (HA*TAMB + KEFF (I, 1)*(4.0*T (I, 2)-T (I, 3))/ (2*DELX))/
(HA+ 1.50*KEFF (I, 1)/DELX)

ENDIF

FOR BOTTOM NODE
IF (J.EQ.NGRID) THEN
T (I, NGRID) = (4*T (I, NGRID-1) - T (I, NGRID-2))/3

ENDIF

FOR INTERNAL NODES
IF (J.GT.1 .AND. J.LT.NGRID) THEN
CPDEN= DENI (I, J)*CPEFF (I, J)
T (I, J) = (CPDEN*T (I-1, J)/DELT - PCR (I, J)*HAD + (KEFF (I, J+1)-
KEFF (I, J-1))*(T (I, J+1)-T (I, J-1))/ (4.0*DELX**2) + KEFF (I, J)*
(T (I, J-1) +T (I, J+1))/DELX**2)/ (CPDEN/DELT + 2.0*KEFF (I, J)/DELX**2)
T(I,J) = TOLD(I,J) + RELAXT*(T(I,J)-TOLD(I,J)) ! RELAX THE VALUE

ENDIF

50   CONTINUE

40   CONTINUE

END OF A TIME STEP
     20    CONTINUE
```

```
------------------------------------------------------------------------------------------------------------
TEST FOR CONVERGENCE OF TEMPERATURE
------------------------------------------------------------------------------------------------------------
DO 150 I = 2, NTSTEP
TMAX=0.0
TMIN= 1000000.00
SUMT = 0.0

DO 60 M= 1, NGRID
IF (T (I, M) > TMAX) THEN
TMAX= T (I, M)
ELSE
GOTO 70
ENDIF

70      IF (T (I, M) < TMIN) THEN
TMIN = T (I, M)
ELSE
GOTO 80
ENDIF

80      SUMT = SUMT + ABS (T (I, M)-TOLD (I, M))
60      CONTINUE

IF (SUMT/ (NGRID*(TMAX-TMIN)) <= TOLT) THEN
PRINT *,"TEMPCONVERGENCE", I
ELSE
PINT *, "TEMP-NONCONVERGENCE", I

ENDIF

150   CONTINUE
------------------------------------------------------------------------------------------------------------
TEST FOR CONVERGENCE OF VAPOUR DENSITY
------------------------------------------------------------------------------------------------------------
DO 160 I = 2, NTSTEP
VDMAX=0.0
VDMIN= 1000000.00
SUMVD = 0.0

DO 600 M= 1, NGRID
IF (VD (I, M) > VDMAX) THEN
VDMAX= VD (I, M)
ELSE
GOTO 170
ENDIF
```

```
170       IF (VD (I, M) < VDMIN) THEN
VDMIN = VD (I, M)
ELSE
GOTO 180
ENDIF

180       SUMVD = SUMVD + ABS (VD (I, M)-VDOLD (I, M))
600       CONTINUE

IF (SUMVD/ (NGRID*(VDMAX-VDMIN)) <= TOLT) THEN
PRINT *,"VDCONVERGENCE", I
ELSE
PRINT *, "VD-NONCONVERGENCE", I

END IF

160      CONTINUE

DO 300 I = 11, NTSTEP, 10
WRITE(1,800) I,T(I,20),T(I,180),T(I,360),T(I,NGRID)
800 FORMAT (I5, 1X, 7(F12.3, 1X))
WRITE(2,900) I,VD(I,20),VD(I,180),VD(I,360),VD(I,NGRID)
900 FORMAT (I5, 1X, 7(F12.6, 1X))
WRITE(4,1100) I,U(I,20),U(I,180),U(I,360),U(I,NGRID)
1100 FORMAT (I5, 1X, 7(F12.6, 1X))
WRITE(5,1200) I,RH(I,20),RH(I,180),RH(I,360),RH(I,NGRID)
1200 FORMAT (I5, 1X, 7(F12.4, 1X))

300 CONTINUE
-------------------------------------------------------------------------------------------------
LOOP TO DETERMINE THE DEPTH OF THE VAPOUR BOUNDARY LAYER
-------------------------------------------------------------------------------------------------
DO 240 I = 2, NTSTEP
DO 250 J = 2, NGRID

IF (VD (I, J).LE.0.006878546) THEN
WRITE (4,*) I, J, VD (I, J), DEFF (I, J)
GOTO 240

ELSE
GOTO 250
ENDIF

250   CONTINUE
240   CONTINUE
```

```
------------------------------------------------------------------------------------------------------------
LOOP TO CALCULATE MOISTURE STORAGE
------------------------------------------------------------------------------------------------------------
DO 1500 I = 11, NTSTEP, 10
MOIST (I) = 0.0
DO 1600 J = 1, NGRID
UM (I, J) = U (I, J)*0.673
UA (I, J) = UM (I, J)-UM (I-1, J)
MOIST (I) = MOIST (I) +UA (I, J)

1600 CONTINUE
1500 CONTINUE

DO 3000 I = 11, NTSTEP, 10

WRITE (7, 3500) I, MOIST (I)
3500 FORMAT (I5, 1X, F12.6)

3000 CONTINUE

END
```